

REFLECTOR ANTENNAS

The most commonly used high gain antenna is a reflector antenna. This is so because it is the most economical large aperture antenna. The only other large aperture antenna is an array. An array requires at least four elements per square wavelength and all the associated circuitry to feed the elements. We can get a very large aperture in terms of wavelengths without making thousands of elements. It is difficult to achieve low sidelobes and high efficiency because the aperture illumination cannot be controlled exactly, but the cost outweighs these disadvantages in most applications.

GEOMETRIC OPTICS

Geometric optics is a means of approximating the field by assuming that the wavelength is very small (or the frequency is very high) compared to the dimensions of the antenna. It is the zero wavelength approximation. As the size of the reflector becomes larger and larger in terms of wavelengths, the solution approaches the exact solution. To solve a problem we must trace rays from the source antenna through reflections off the reflector to the field point. The reflections off reflectors follow simple rules and in free space the rays travel in straight lines. We need to consider conservation of energy relations to find the amplitude levels along the rays. Finally we trace all possible rays and add the electric fields using superposition.

The electric field in a source free, isotropic, homogeneous, non-conducting medium can be expanded in an asymptotic series in descending powers of ω called the Luneburg-Kline expansion.

$$E(x,y,z,\omega) = e^{-jk L(x,y,z)} \sum_{m=0}^{\infty} \frac{E_m(x,y,z)}{(j\omega)^m}$$

$L(x,y,z) = \text{Constant}$ is an equation which defines equal phase surfaces of the field and k is the free space propagation constant. The function $L(x,y,z)$ is called the eikonal. Maxwell's equations can be reduced to a vector Helmholtz equation in free space for the electric field.

$$\nabla^2 E + k^2 E = 0$$

When we substitute the asymptotic expansion into this equation and consider the lowest order term, we get an equation for L ; the eikonal equation.

$$|\nabla L|^2 = n^2$$

n is the refractive index (assuming $\mu_r = 1$). The equation for the electric field becomes

$$E = E_0(x,y,z) e^{-jk L(x,y,z)}$$

when we use only the first order term of the asymptotic expansion. These are the wavefronts of geometric optics. The waves will travel in the direction of

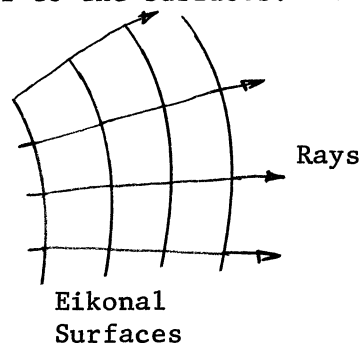
the gradient of the constant phase surfaces.

$$\nabla L/n = \bar{S}$$

\bar{S} is the direction of the ray in space.

We only have a first order solution for the waves in space. If we take a parabolic reflector with a feed at the focus, then the first order field predicts a pattern only on the axis of the parabola and zero everywhere else. There are three methods which will predict the field off the axis of the reflector. The first is the aperture field method. Geometric optics is used to predict the fields at an aperture plane in front of the reflector which is a constant phase (eikonal) surface. The Huygens source approximation is applied to this aperture to find the fields off axis. The second method uses geometric optics to predict the fields at the surface of the reflector. The boundary conditions are applied to find the induced currents. From these currents we can find the fields using the magnetic vector potential. This is the physical optics method. The third method is GTD (geometric theory of diffraction). This method patches the geometric optics solution with diffraction coefficients for diffracted fields from the edges of the reflector. We will apply each one of these methods to reflector problems.

The geometric optics solutions assume that the energy flows in flux tubes in the direction of the rays between equal phase surfaces (eikonal). These rays are identical to the far fields of an antenna. The electric and magnetic fields are orthogonal to the ray direction, \bar{S} , and form a right hand vector triad. Since the ray direction is found from the gradient of the eikonal surfaces, the rays are orthogonal to the surfaces. They form an orthogonal set.



The energy flows in flux tubes whose edges are rays. If the index of refraction is constant throughout a region of space, then the rays will travel in straight lines.

ASTIGMATIC RAY

The power flow per unit area along the ray does not stay constant because the wavefront (eikonal) has curvature, in general. Only the special case of a plane wave does the power flow per unit area remain constant along the ray tube. Consider a ray and the eikonal which is a surface that is orthogonal to the ray. The vector direction of the ray defines a plane. We can define an X-Y coordinate system locally around the ray which is contained in the plane defined by the ray. The Z axis is coincident with the ray. For now the direction of the X axis is arbitrary. Since locally the eikonal or wavefront surface is a plane, the first derivatives with respect to the X and

Y axes are zero. Locally the surface can be approximated by a quadratic surface which is the first three terms of a two dimensional Taylor series expansion of $L(x,y,z)$. In the neighborhood of the ray the Z axis dimension is given by the expression:

$$z = \frac{1}{2} \left(\frac{\partial^2 L}{\partial x^2} x^2 + 2 \frac{\partial^2 L}{\partial x \partial y} xy + \frac{\partial^2 L}{\partial y^2} y^2 \right)$$

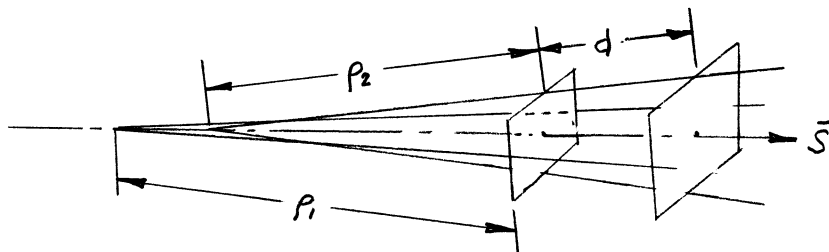
Since the direction of the X axis is arbitrary, we can rotate the coordinate system until

$$\frac{\partial^2 L}{\partial x \partial y} = 0$$

In this coordinate system the Z axis equation becomes

$$z = \frac{1}{2} \left(\frac{x^2}{\rho_1^2} + \frac{y^2}{\rho_2^2} \right) \quad \rho_1^2 = \frac{1}{\partial^2 L / \partial x^2} \quad \rho_2^2 = \frac{1}{\partial^2 L / \partial y^2}$$

ρ_1 and ρ_2 are the principle radii of curvature of the eikonal at the point of the ray. In general $\rho_1 \neq \rho_2$. It appears that the ray is spreading from ρ_1 in one plane and ρ_2 in the other orthogonal plane.



When the two principle plane radii of curvature are not equal, then it is called an astigmatic ray,

Suppose in the figure above the areas shown are differential areas. The distance between the differential planes is d . The ratio of the two areas is given by

$$\frac{dA_1}{dA_2} = \frac{\rho_1 \rho_2}{(\rho_1 + d)(\rho_2 + d)}$$

This is also the ratio of the power densities since no power leaves the sides of the ray tubes. Given the power density at one point along the ray, we can find the power density at another point of the ray. Keep in mind that these are differential areas around the ray and they have no real area in the limit. The points where $d = -\rho_1$ or $d = -\rho_2$, the power density is mathematically infinite. They are called caustics.

SPECIAL RAY TYPES

Spherical Waves - On page 29 we discussed spherical waves. A single antenna radiates spherical waves in the far field. The geometric optics field of the spherical wave is given by

$$\frac{e^{-jkr}}{r}$$

r is the distance from the source and $k (2\pi/\lambda)$ is the propagation constant. The eikonals are spheres and the rays are radials.

Cylindrical Waves An infinite line source will radiate cylindrical waves. They are physically impossible but it is a handy approximation when the problem can be reduced to a two dimensional problem. One such problem is a parabolic cylinder. The cylindrical wave is given by $\frac{e^{-jkr}}{\sqrt{r}}$

The eikonals are cylinders and the rays are radials of the cylindrical coordinates. The field decreases as the square root of the radius because the power in cylindrical waves decreases by $1/R$.

Plane Waves The plane wave is of constant amplitude but has the same phase factor as the spherical and cylindrical waves. The eikonal wavefront surfaces are planes.

$$e^{-jkx}$$

The field of an astigmatic ray will have the variation given by

$$E_0 e^{-jkd} \sqrt{\frac{\rho_1 \rho_2}{(\rho_1 + d)(\rho_2 + d)}}$$

where E_0 is the field at the reference point. These rays arise when spherical waves are reflected off surfaces and from antennas whose phase centers are not coincident in the principle planes.

FERMAT'S PRINCIPLE

The optical path length between two points is defined as the following line integral,

$$\int_C n ds$$

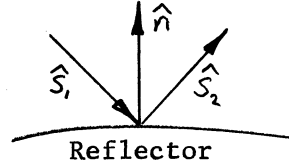
where C is some prescribed path in space and n is the index of refraction, $n = \sqrt{\epsilon_r}$. This is also the phase change of the wave when multiplied by the propagation constant of free space since the index of refraction is a measure of the slowing of the wave in the dielectric. The path of the ray is not arbitrary between two points.

Fermat's Principle states that the optical path length of a ray is stationary. To be stationary means that the first derivatives are zero, that is, the optical path length is a minimum (or maximum). Since we are not dealing with lenses, we will take n to be a constant everywhere. The shortest distance between two points is a straight line which means rays travel in straight lines through a homogeneous medium. More important is that Fermat's principle also holds through reflections (refractions also). We can use this to trace rays through reflections by searching for the minimum optical path length.

It is possible to use Fermat's principle to find the laws of reflection and refraction (or Snell's laws). The two laws of reflection are given as:

- (1) The incident ray, the reflected ray, and the normal to the reflecting surface all lie in a plane.
- (2) The incident and reflected rays make equal angles with the normal.

Implicit in Snell's laws of reflection is the idea that locally the wavefront behaves like a plane wave and that the reflector can be treated as a plane.



If the three vectors in the figure above are unit vectors, we can express the reflection laws by the vector relations given below.

$$(1) \quad \hat{n} \times (\hat{S}_2 - \hat{S}_1) = 0$$

This expresses the law that the three vectors lie in a plane. The vector cross product of two vectors defines the normal of the plane. The equation states that the normals which are defined by the two vector cross products are coincident. If two planes have the same normal, then they are the same. This is also part of the pair of relations which states that the angle of the incident ray with respect to the normal vector is the same as the angle of the reflected ray with respect to the normal. The second vector relation which defines the angle to be equal is

$$(2) \quad \hat{n} \cdot (\hat{S}_2 + \hat{S}_1) = 0$$

We can use these expressions to find the reflected ray unit vector in terms of the incident ray and the normal.

$$\hat{S}_2 = \hat{S}_1 - 2(\hat{S}_1 \cdot \hat{n})\hat{n}$$

By symmetry we can find the incident ray from the normal and the reflected ray.

$$\hat{S}_1 = \hat{S}_2 - 2(\hat{S}_2 \cdot \hat{n})\hat{n}$$

These last two equations state that it does not matter which direction the rays are traced through a set of reflections. We can also get there by considering reciprocity.

Snell's law of refraction can be expressed in a similar vector relation as the reflection law:

$$\hat{n} \times (n_1 \hat{S}_1 - n_2 \hat{S}_2) = 0$$

$$\text{or} \quad n_1 \sin \theta_1 = n_2 \sin \theta_2$$

with the same condition that the three vectors lie in a plane. n_1 and n_2 are the index of refractions of the two mediums.

RAY TRACING

Tracing rays through a reflector system is conceptually straight forward. Where a ray strikes a reflector we must find the normal to the surface. Using the equation above, we can find the reflected ray direction from the incident ray unit vector and the unit normal of the surface. The problem comes when we have specified the location of the source and the field measurement point and must find the location of the reflection on the reflector. For the general problem we cannot find an analytical expression which will give the location of the reflection. The usual computer technique uses Fermat's principle to search for the minimum optical path length. We also may find that there are more than one ray that will reflect off the reflector which will satisfy the reflection conditions and locally satisfy Fermat's principle. The field at a point is the sum of the rays which can reach the field point. This process can become a difficult geometry problem.

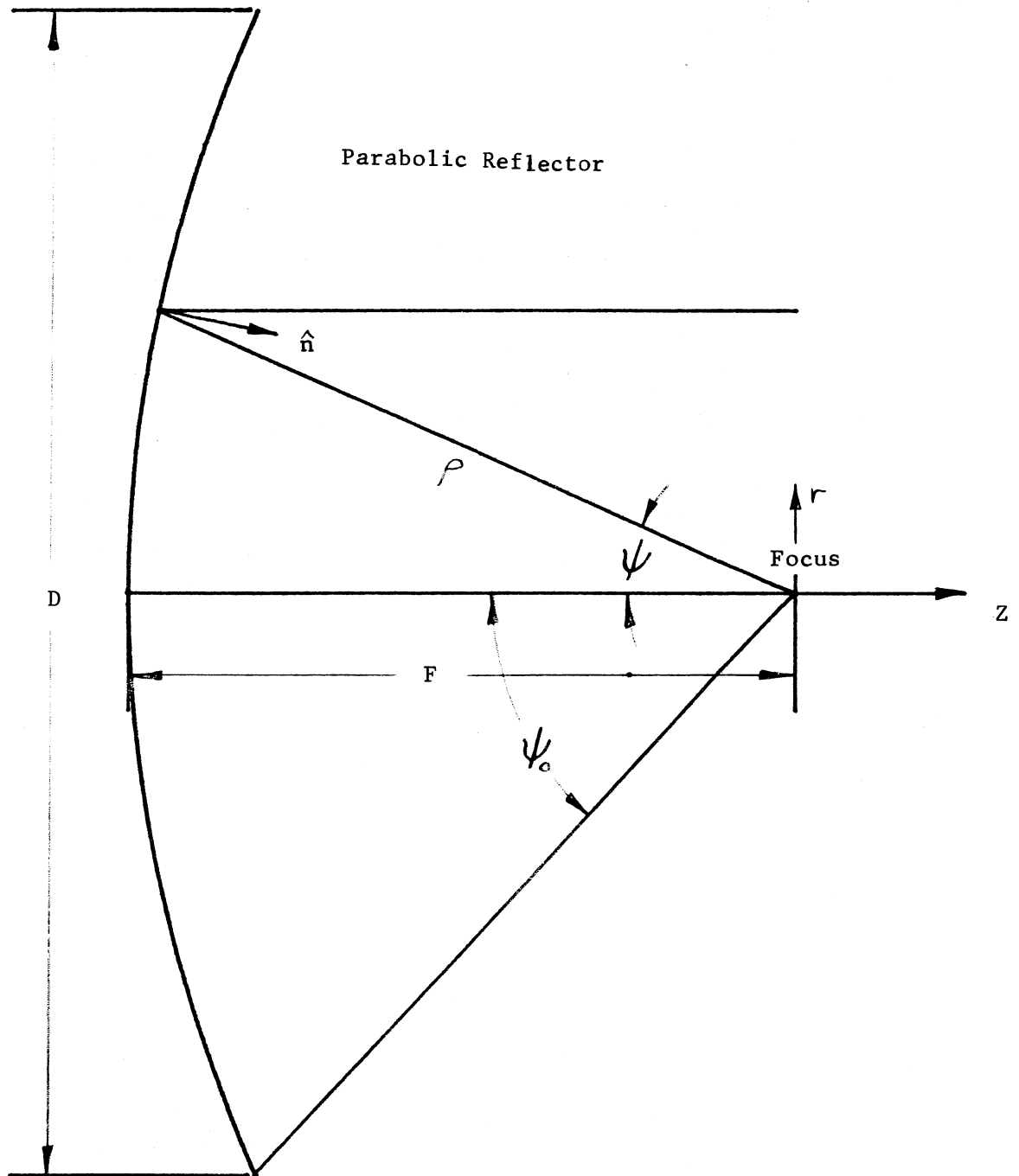
Once we have found the ray paths, we must determine the amplitude variation along the ray. Keep in mind that even though we discuss the spreading factor of the ray differential area, the area of the ray remains a differential area and has no real area. Rays remain rays and do not become surfaces. The type of source will determine the variation of the amplitude of the rays radiating from it (spherical, astigmatic, cylindrical, etc.). Knowing the type of ray radiated from the source, we can find the amplitude of the ray at the point of reflection. If the reflector surface has curvature, then the ray curvature will change after reflection. It is necessary to use the amplitude of the ray at the reflector and the new radii of curvature to find the amplitude along the reflected ray. The radii of curvature of the reflected wave can be found as a function of the incident ray curvature, the angle of incidence, and the radii of curvature of the reflector. For most of the cases we will consider, we can find the curvature of the reflected rays from simple geometric considerations.

PARABOLIC REFLECTOR

The parabolic reflector surface is formed by rotating a parabola about an axis through the center of the parabola and the focus. This surface will transform the curvature of a spherical wave centered on the focus into that of a plane wave. We say that the reflector surface has collimated or focused the wave. In a similar fashion the parabolic cylinder reflector converts a cylindrical wave from the focus into a plane wave. Not only is the ray curvature changed, but all rays from a plane with its normal coincident with the axis of the reflector to the reflector and to the focus have the same phase length. This plane is called the aperture plane and is an eikonal for sources at the focus.

On page 586 is a diagram of the parameters of the parabola. Since the antenna is symmetrical about the Z axis, the problem can be reduced to a two dimensional problem if we ignore polarization. The equation of the parabola can be given in both rectangular coordinates and spherical coordinates.

$$r^2 = 4F(F - z) \qquad \rho = \frac{F}{\cos^2 \frac{\psi}{2}}$$



F is the focal length, D is the diameter, ρ is the distance from the focus to the reflector, and ψ is the angle from the negative Z axis.

When considering the feed antenna which is placed at the focus, we want to reduce the problem to a dimensionless one. To do this we will find the subtended angle of the reflector seen from the focus which is $2\psi_o$ versus the dimensionless parameter: F/D.

$$D/2 = \sin \psi_o \rho(\psi_o) = \frac{\sin \psi_o F}{\cos^2 \psi_o / 2}$$

We can use the following trigonometric identity to reduce the equation.

$$\sin \psi_o = 2 \sin \psi_o / 2 \cos \psi_o / 2$$

$$D/2 = 2 \tan \psi_o / 2 F$$

$$\psi_o = 2 \tan^{-1}(1/(4 F/D))$$

The subtended angle is twice this. An alignment chart of the subtended angle versus F/D is given on page 588.

Let us find the unit normal vector, \hat{n} , of the reflector. The vector can be found from the gradient of the curve equation.

$$\hat{n} = \nabla(F - \rho \cos^2 \psi / 2) = -\cos^2 \psi / 2 \bar{a}_\rho + \sin \psi / 2 \bar{a}_\psi$$

Normalizing this expression it becomes

$$\hat{n} = -\cos \psi / 2 \bar{a}_\rho + \sin \psi / 2 \bar{a}_\psi$$

We can use this to find the direction of the reflected ray which is incident from the focus.

$$\hat{s}_1 = \bar{a}_\rho$$

The reflected wave is found the equation:

$$\hat{s}_2 = \hat{s}_1 - 2(\hat{s}_1 \cdot \hat{n}) \hat{n}$$

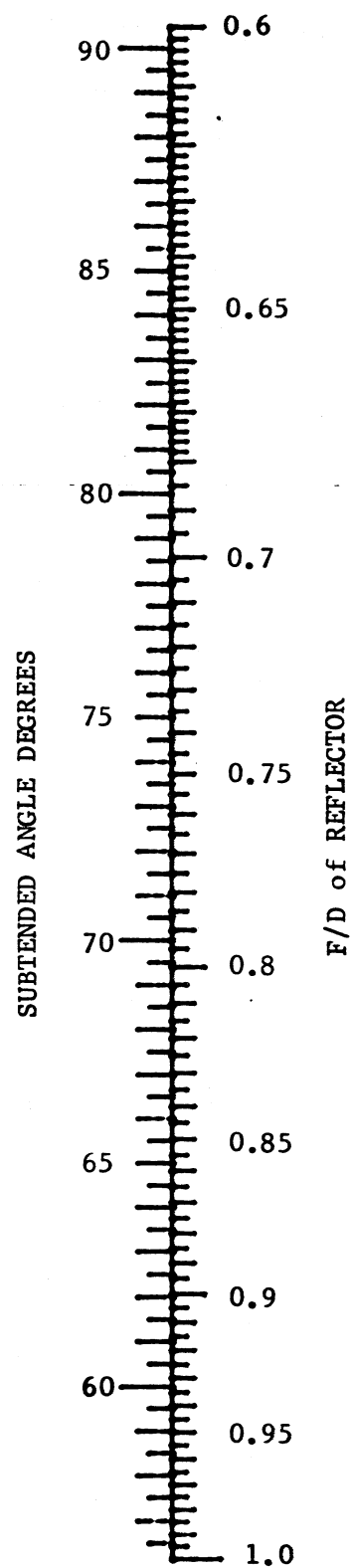
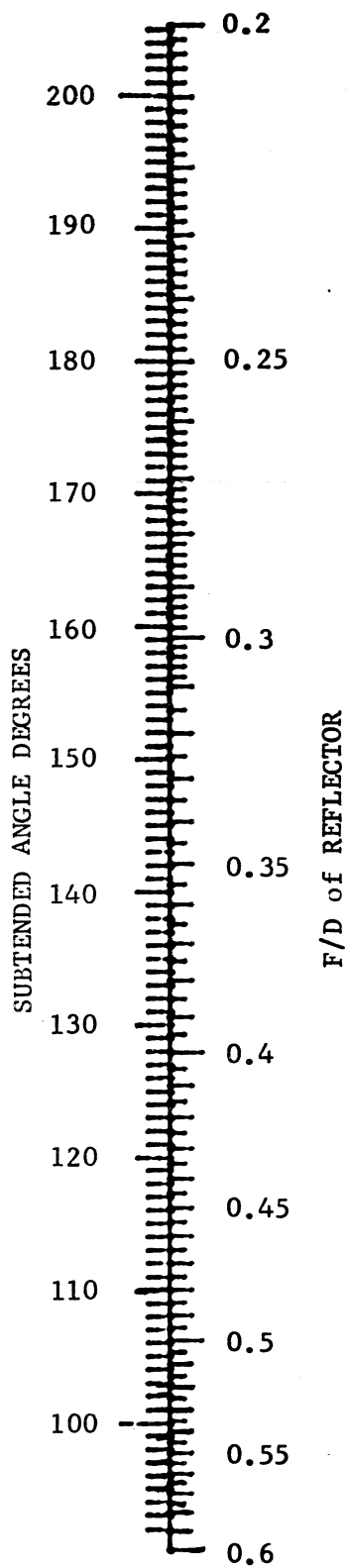
$$\hat{s}_2 = \bar{a}_\rho - 2 \cos \psi / 2 (\cos \psi / 2 \bar{a}_\rho - \sin \psi / 2 \bar{a}_\psi)$$

$$\hat{s}_2 = \bar{a}_\rho (1 - 2 \cos^2 \psi / 2) + 2 \cos \psi / 2 \sin \psi / 2 \bar{a}_\psi$$

Using the double angle formulas, this equation can be simplified.

$$\hat{s}_2 = -\bar{a}_\rho \cos \psi + \bar{a}_\psi \sin \psi = \bar{a}_z$$

All the reflected rays are parallel to the Z axis. The second thing we need



8/15/80 TAM

to find is the phase distance from the focus to a plane at the focus whose normal is the Z axis, through a reflection. The distance from the reflector to the aperture plane at the focus along the reflected ray path is given by

$$\rho \cos \psi$$

The total phase distance is $\rho + \rho \cos \psi = \rho(1 + \cos \psi)$.

$$\frac{(1 + \cos \psi)}{2} = \cos^2 \psi/2$$

$$2 \cos^2 \psi/2 = 2 F$$

The distance is the same for all reflected rays, $2 F$, and the aperture plane is an eikonal (an equal phase surface of the wave) for sources at the focus. In fact any plane in front of the reflector parallel to the plane at the focus is also an eikonal. Since the wave has no curvature, it is a plane wave. From the geometric optics solution we see that the reflected wave is a cylinder projected from the diameter of the reflector. But, of course, because the wavelength is not zero, there will be some diffraction which will broaden the beam and give sidelobes.

We have found the ray paths and an eikonal aperture, but we must also find the amplitude distribution along the rays. The rays from the source at the focus are spherical waves. At the reflector the amplitude of the ray from an isotropic spherical source is given by

$$1/\rho$$

The reflector has changed the curvature of the rays to plane waves (infinite radii of curvature). If the pattern of the source is $E(\psi, \phi)$, then the amplitude in the aperture plane is given by

$$E_a(r, \phi) = E(\psi, \phi)/\rho$$

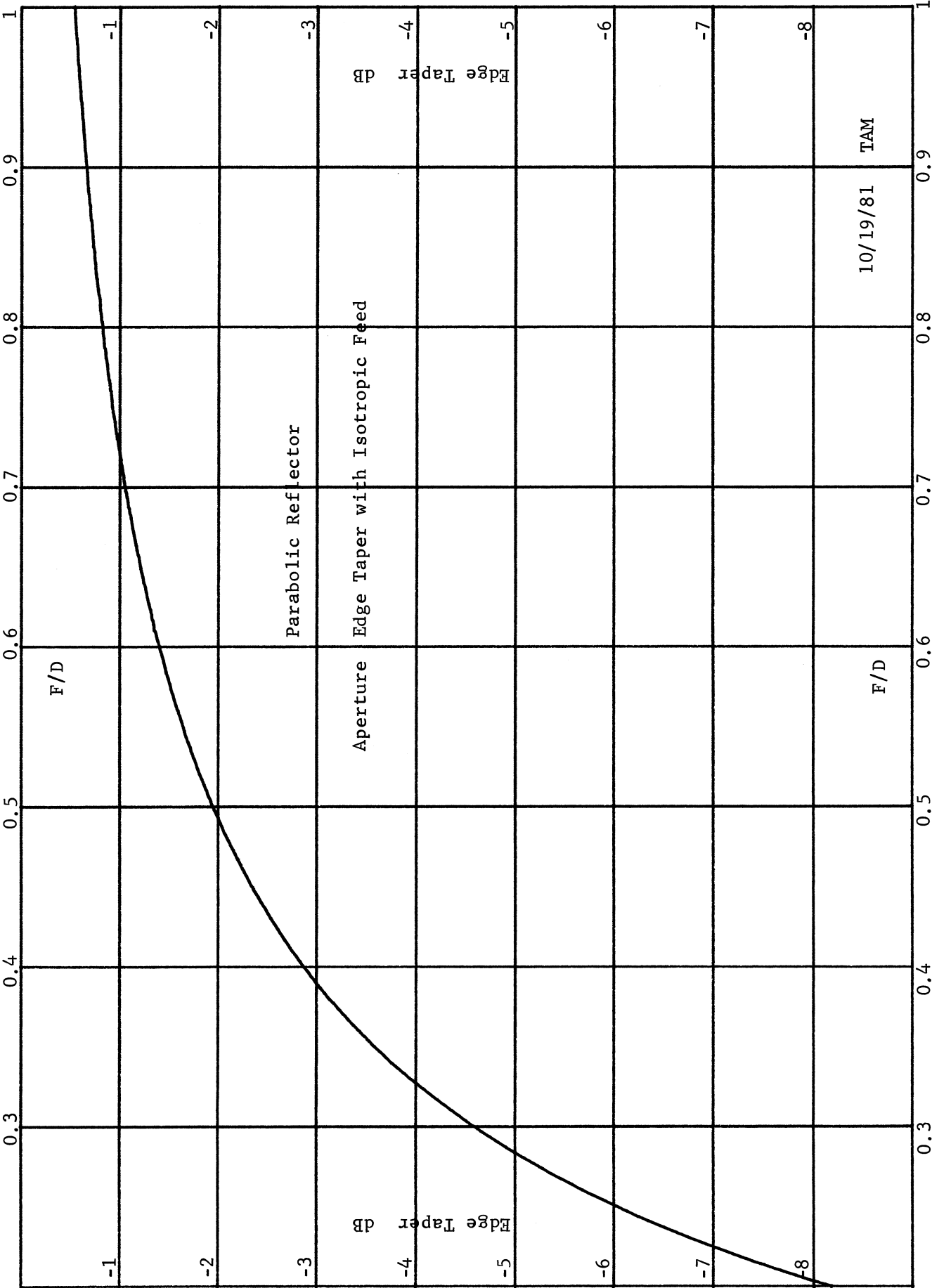
If the feed antenna is isotropic, then the distribution in the aperture plane will be tapered.

$$E_a(r) = \cos^2 \psi/2$$

$E(r)$ is referenced to the center of the parabola. On page 590 is a graph of the edge taper versus F/D for an isotropic source. We see that the edge taper is reduced for larger values of F/D and the amplitude taper loss will be less. We will find that there will be a trade-off between the amplitude taper loss and the spillover loss which is the energy from the source which does not strike the reflector. Large values of F/D will increase the spillover loss.

APERTURE DISTRIBUTION LOSSES

We can relate the aperture field to the pattern of the feed using the equation above and find the amplitude taper and phase error losses for the aperture with the feed pattern. The amplitude taper loss of a circular aperture is found



from the equation on page 576.

$$ATL = \frac{\left| \int_0^{2\pi} \int_0^a |E_a(r', \phi')| r' dr' d\phi' \right|^2}{\pi a^2 \int_0^{2\pi} \int_0^a |E(r', \phi')|^2 r' dr' d\phi'}$$

a is the radius of the aperture. The parabola parameters have the following relations:

$$\rho = F \sec^2 \psi/2$$

$$r' = \rho \sin \psi = 2 \sin \psi/2 \cos \psi/2 \frac{F}{\cos^2 \psi/2}$$

$$r' = 2 F \tan \psi/2$$

$$dr' = F \sec^2 \psi/2 d\psi = \rho d\psi$$

We will substitute these into the amplitude taper loss equation and relate the integrals to the feed pattern.

$$ATL = \frac{\left| \int_0^{2\pi} \int_0^{\psi_0} \frac{|E(\psi', \phi')|}{\rho} 2 F \tan \psi'/2 \rho d\psi' d\phi' \right|^2}{\pi a^2 \int_0^{2\pi} \int_0^{\psi_0} \frac{|E(\psi', \phi')|^2}{\rho^2} 2 F \tan \psi'/2 \rho d\psi' d\phi'}$$

ρ cancels out in the numerator integral and we can manipulate the expression in the denominator integral to eliminate it.

$$\frac{2 F \tan \psi/2}{\rho} = \frac{2 F \tan \psi/2}{F \sec^2 \psi/2} = 2 \sin \psi/2 \cos \psi/2 = \sin \psi$$

$$ATL = \frac{4 F^2 \left| \int_0^{2\pi} \int_0^{\psi_0} |E(\psi', \phi')| \tan \psi'/2 d\psi' d\phi' \right|^2}{\pi a^2 \int_0^{2\pi} \int_0^{\psi_0} |E(\psi', \phi')|^2 \sin \psi' d\psi' d\phi'}$$

We can make the substitution: $a/(2 F) = \tan \psi_0/2$ and eliminate dimensions.

$$ATL = \frac{\cot^2(\psi_0/2) \left| \int_0^{2\pi} \int_0^{\psi_0} |E(\psi', \phi')| \tan(\psi'/2) d\psi' d\phi' \right|^2}{\pi \int_0^{2\pi} \int_0^{\psi_0} |E(\psi', \phi')|^2 \sin \psi' d\psi' d\phi'}$$

This is the formula for the aperture distribution taper loss which is referenced to the feed pattern and dimensionless.

Phase Error Loss

The phase error loss of the aperture plane can be related back to the feed pattern of the source in a similar manner as the amplitude taper loss. We can find the expression for a circular aperture from the equation on page 573.

$$PEL = \frac{\left| \int_0^{2\pi} \int_0^a E_a(r', \phi') r' dr' d\phi' \right|^2}{\left(\int_0^{2\pi} \int_0^a |E_a(r', \phi')| r' dr' d\phi' \right)^2}$$

We can directly relate the aperture field to the feed pattern.

$$PEL = \frac{\left| \int_0^{2\pi} \int_0^{\psi_0} \frac{E(\psi', \phi')}{\rho} 2F \tan \frac{\psi'}{2} \rho d\psi' d\phi' \right|^2}{\left(\int_0^{2\pi} \int_0^{\psi_0} \frac{|E(\psi', \phi')|}{\rho} 2F \tan \frac{\psi'}{2} \rho d\psi' d\phi' \right)^2}$$

After cancelling terms, this becomes

$$PEL = \frac{\left| \int_0^{2\pi} \int_0^{\psi_0} E(\psi', \phi') \tan \frac{\psi'}{2} d\psi' d\phi' \right|^2}{\left(\int_0^{2\pi} \int_0^{\psi_0} |E(\psi', \phi')| \tan \frac{\psi'}{2} d\psi' d\phi' \right)^2}$$

The integral in the numerator can be divided into two integrals which is done for any calculation.

$$PEL = \frac{\left(\int_0^{2\pi} \int_0^{\psi_0} E_R(\psi', \phi') \tan \frac{\psi'}{2} d\psi' d\phi' \right)^2 + \left(\int_0^{2\pi} \int_0^{\psi_0} E_I(\psi', \phi') \tan \frac{\psi'}{2} d\psi' d\phi' \right)^2}{\left(\int_0^{2\pi} \int_0^{\psi_0} |E(\psi', \phi')| \tan \frac{\psi'}{2} d\psi' d\phi' \right)^2}$$

E_R and E_I are the real and imaginary parts of the feed pattern which is referenced to the focus of the parabola.

SPILLOVER LOSS

The spillover loss is not associated with the aperture distribution but is a measure of the amount of energy radiated from the source which is intercepted by the reflector. Since the gain of the reflector will be much larger than the feed antenna, we will ignore the direct radiation of the source to the far field. Ideally all the energy radiated by the source would be reflected by the reflector, but this is not possible. The energy which does not hit the reflector will be a loss. The energy which is radiated by the source is given by the following integral over the radiation sphere.

$$\int_0^{2\pi} \int_0^{\pi} |E(\psi, \phi)|^2 \sin \psi \, d\psi \, d\phi$$

The energy which hits the reflector is given by the integral:

$$\int_0^{2\pi} \int_0^{\psi_0} |E(\psi, \phi)|^2 \sin \psi \, d\psi \, d\phi$$

The spillover efficiency (or loss) is given by the division of the integrals.

$$\text{Spillover Loss} = \frac{\int_0^{2\pi} \int_0^{\psi_0} |E(\psi, \phi)|^2 \sin \psi \, d\psi \, d\phi}{\int_0^{2\pi} \int_0^{\pi} |E(\psi, \phi)|^2 \sin \psi \, d\psi \, d\phi}$$

CONICAL BEAM FEED LOSSES

We can use the conical beam (page 36) approximation for the pattern of the feed antenna and study the trade-off between aperture amplitude taper loss and spillover loss for various beamwidths and F/D of the reflector. The feed pattern is given by

$$E(\psi) = \cos^N(\psi/2)$$

When we substitute this feed pattern into the integrals above, we can find the spillover and amplitude taper losses.

$$\text{Let } X = \cos(\psi_0/2)$$

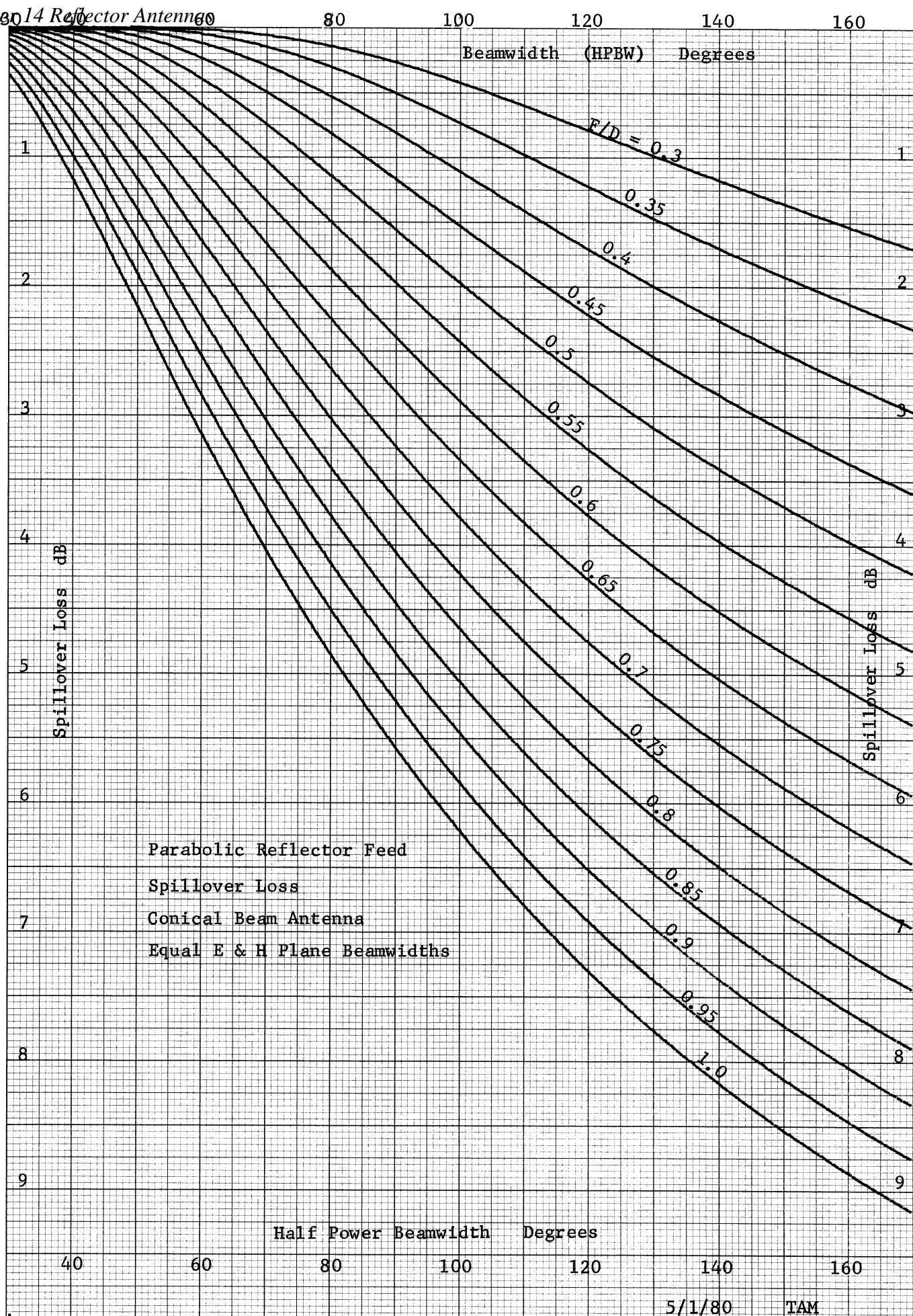
$$\text{Spillover Loss} = (1 - X^{2(N+1)})$$

$$\text{Amplitude Taper Loss} = \frac{4 \cot^2(\psi_0/2) (1 - X^N)^2 / N^2}{(1 - X^{2(N+1)}) / (N + 1)}$$

These functions have been plotted on pages 594 and 595 for various F/D and feed beamwidths. We see that as the F/D decreases the subtended angle of the reflector increases and more of the feed energy hits the reflector and the spillover loss decreases. On the other hand as the subtended angle increases (F/D decreases) the amplitude taper loss increases. There is a trade-off between these two. On page 596 is a plot of the sum of the amplitude taper loss and the spillover loss. This shows that there is an optimum feed beamwidth for each F/D. The beamwidths for minimum loss given F/D are plotted on page 597. Both the 3 and 10 dB beamwidths are given on this plot. The dashed curve is the subtended angle of the reflector which is reasonably similar to the optimum 10 dB beamwidth. A good rule of thumb would be that the 10 dB beamwidth of the feed equal the subtended angle of the reflector.

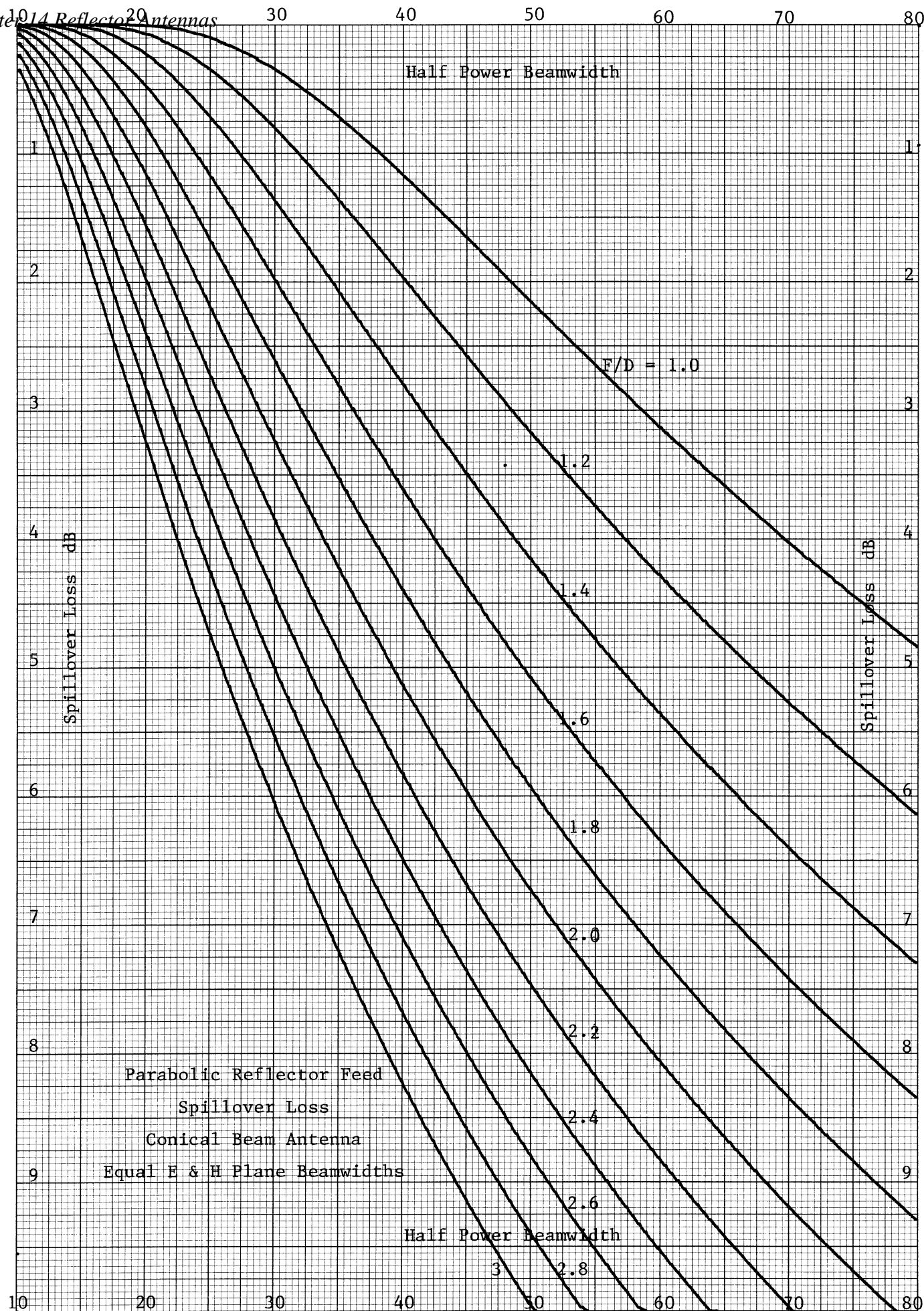
46 1320

10 X 10 TO 1/2 INCH 7 X 10 INCHES
KEUFFEL & ESSER CO. MADE IN U.S.A.



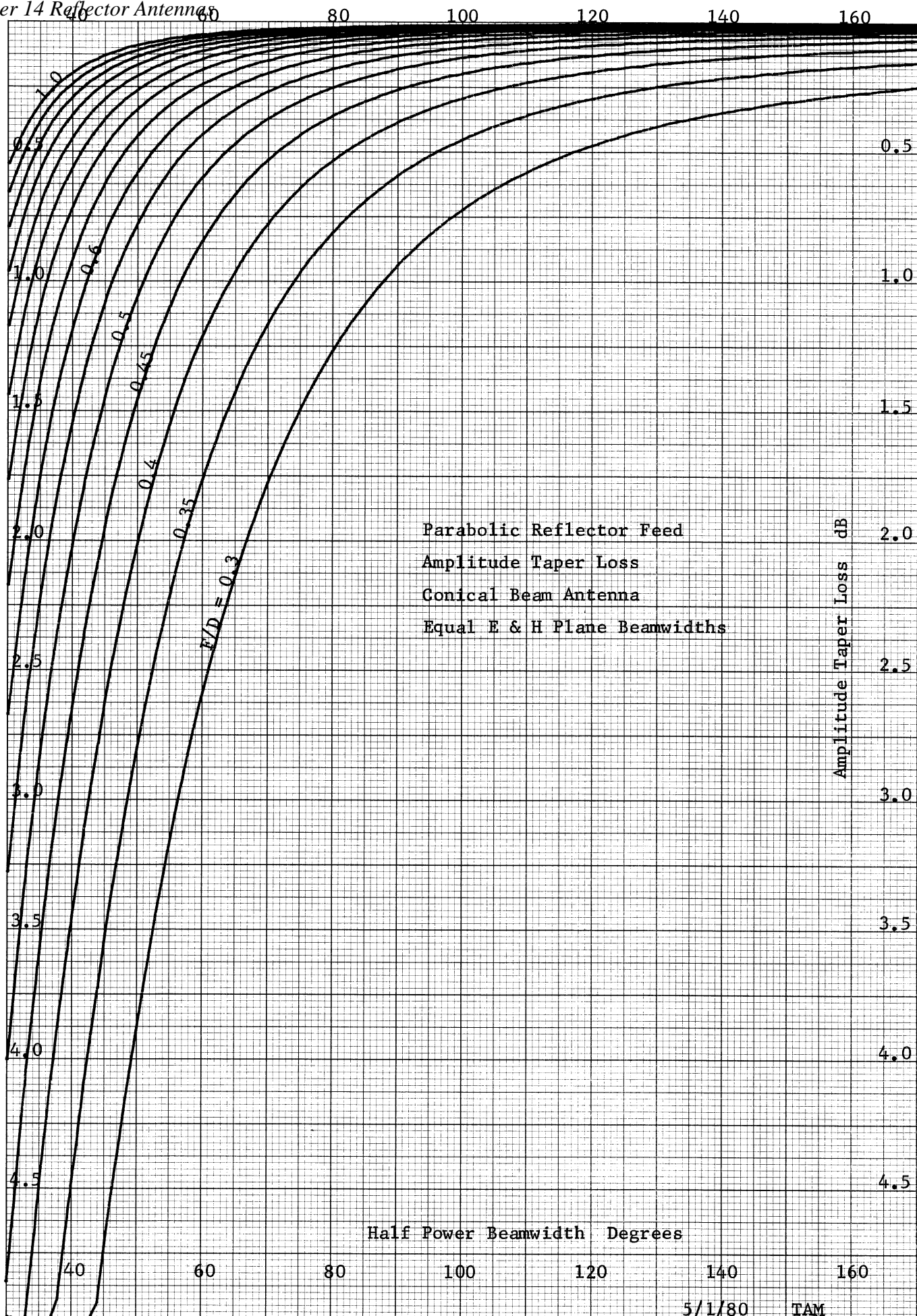
46 1320

10 X 10 TO 1/2 INCH 7 X 10 INCHES
KEUFFEL & ESSER CO. MADE IN U.S.A.

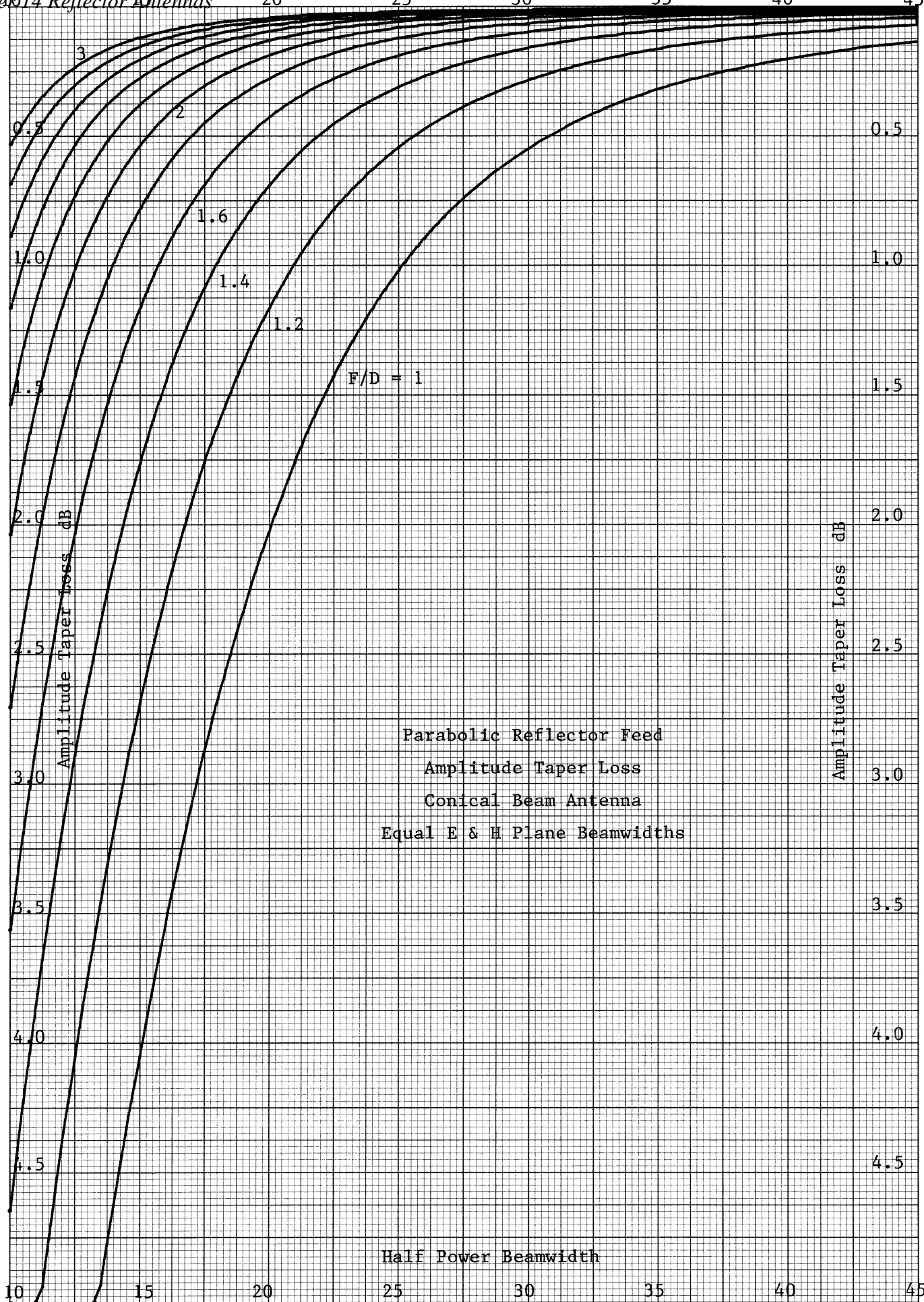


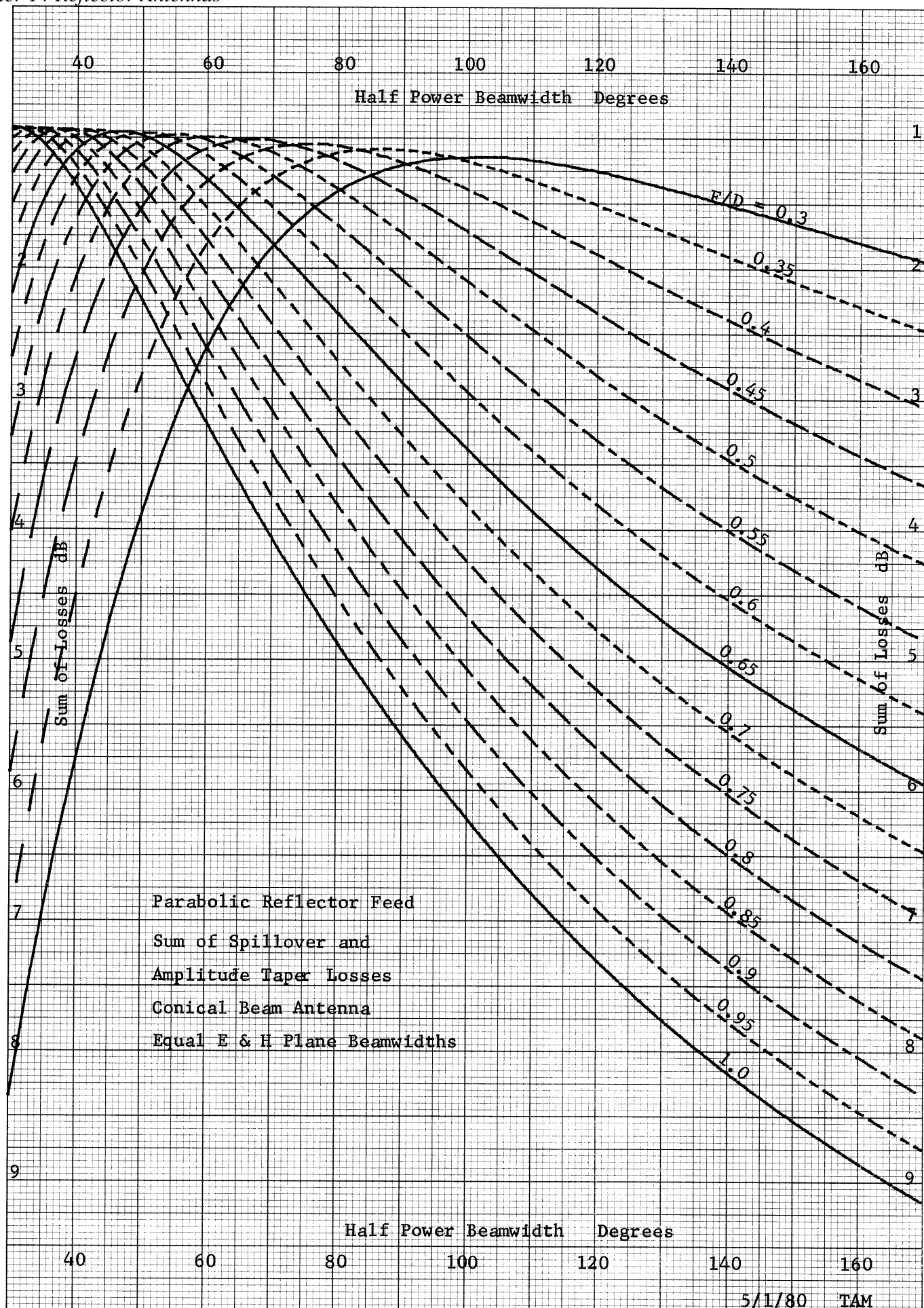
46 1320

10 X 10 TO 1/2 INCH 7 X 10 INCHES
KEUFFEL & ESSER CO. MADE IN U.S.A.



46 1320

K&E 10 X 10 TO 1/4 INCH 7 X 10 INCHES
KEUFFEL & ESSER CO. MADE IN U.S.A.

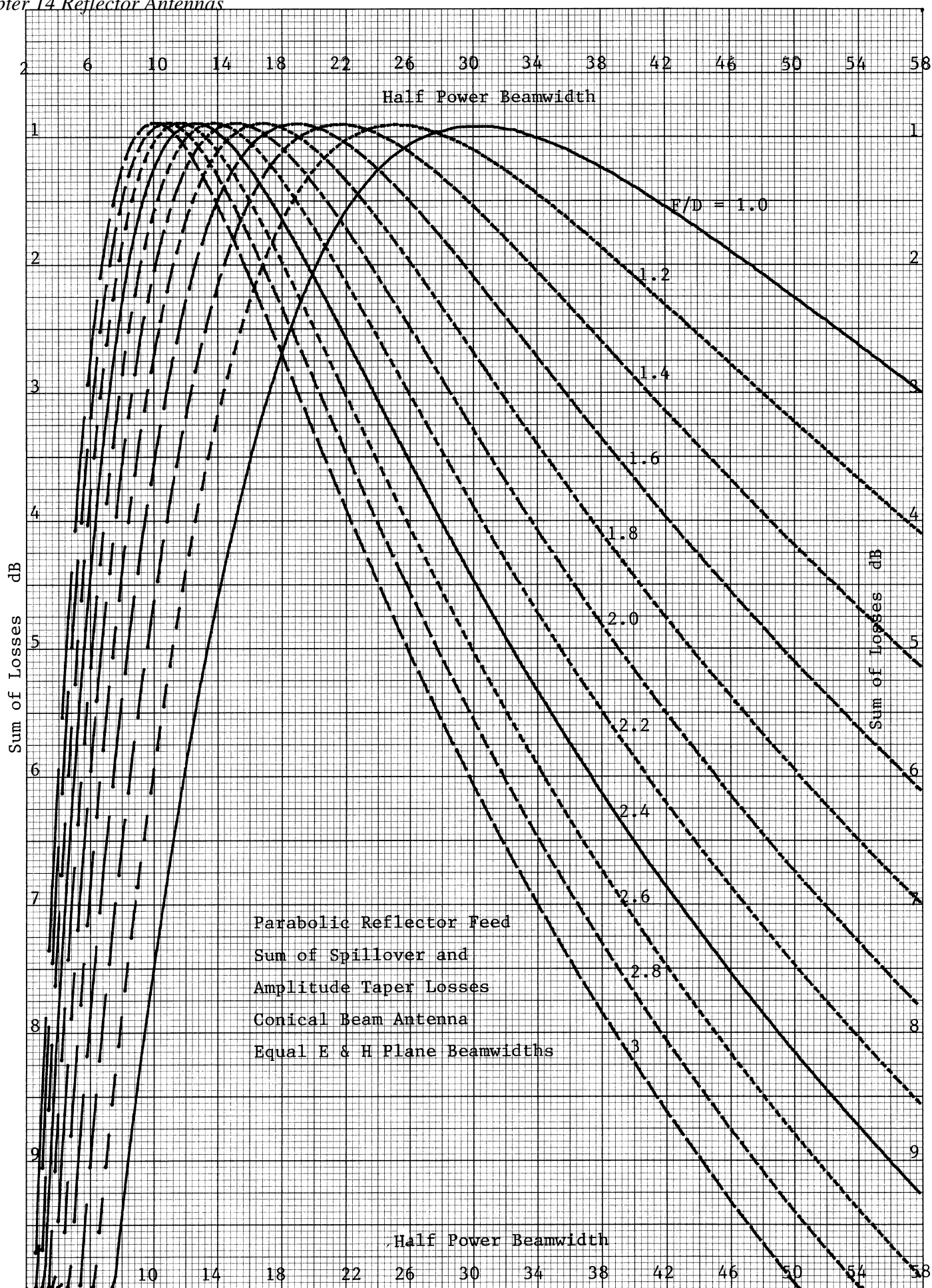


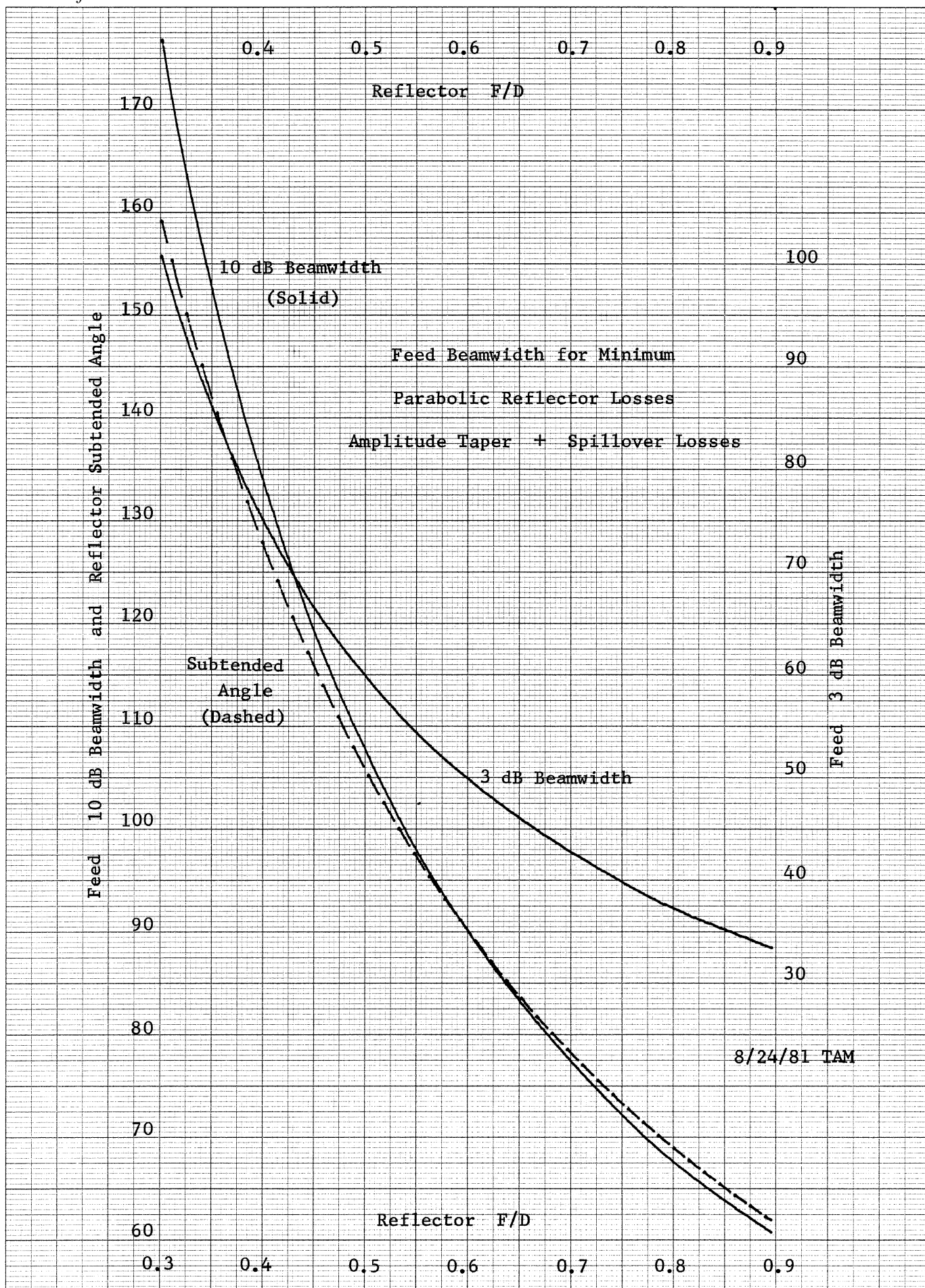
46 1320

K/E 10 X 10 TO 1/2 INCH 7 X 10 INCHES
KEUFFEL & ESSER CO. MADE IN U.S.A.

46 1320

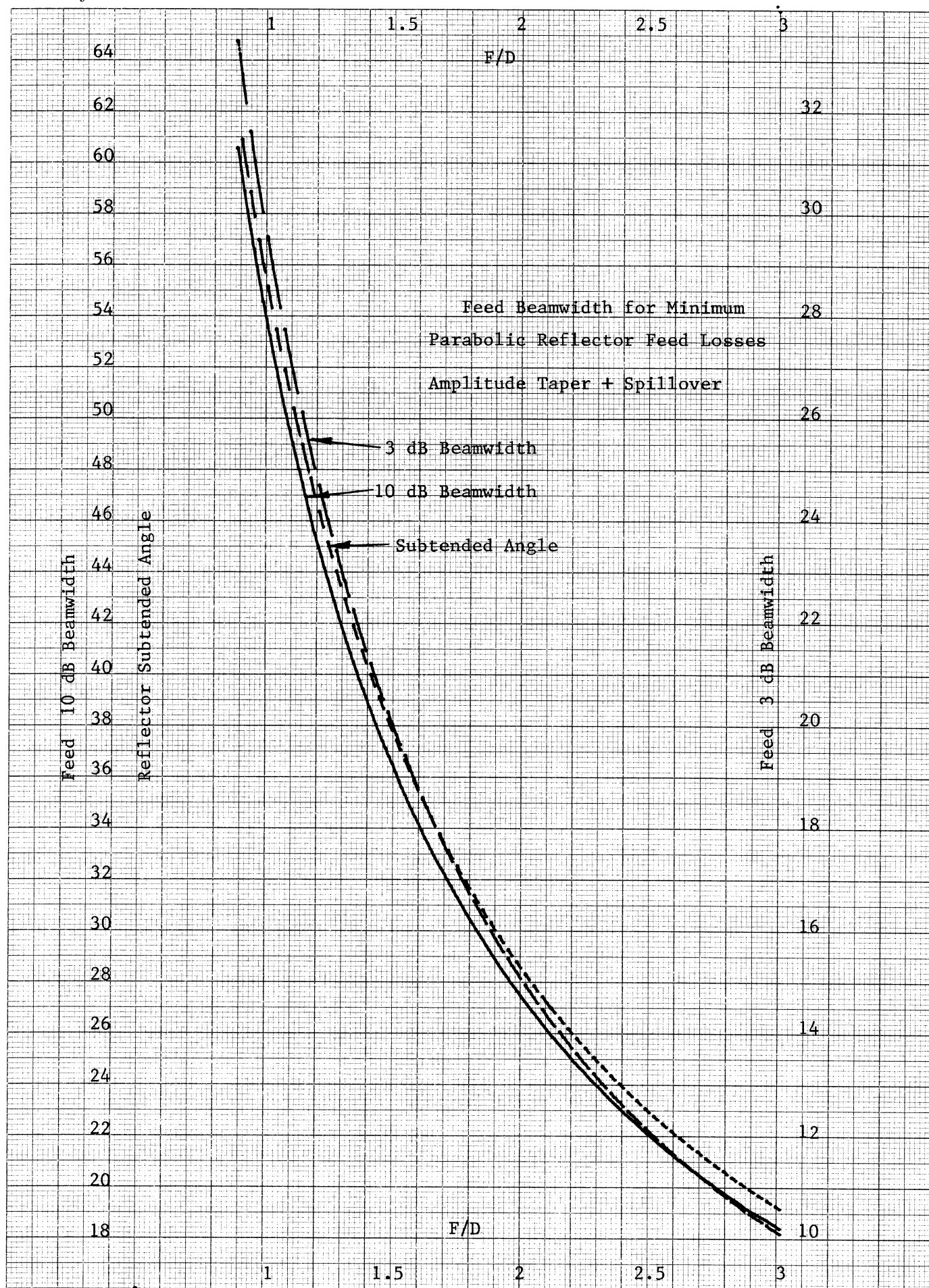
K&E 10 X 10 TO 1 1/2 INCH 7 X 10 INCHES
KEUFFEL & ESSER CO. MADE IN U.S.A.





46 1510

10 X 10 TO THE CENTIMETER 18 X 25 CM.
KEUFFEL & ESSER CO. MADE IN U.S.A.



PHASE ERROR LOSS AND DEFOCUSING

If the phase center of the antenna which is used for the feed is located at the focus of the parabola, then there will be no phase error loss in the aperture. There are some practical problems with real feeds. Some feeds like waveguide horns will not have the same phase center in both principle planes; it is an astigmatic source. The phase center may not be well defined. For different angles, ψ , the wave appears to come from different phase centers. In general the feed will have random phase errors which may be systematic but difficult to identify. These errors can be established by measuring the feed pattern phase and amplitude, and the integrals given above can be used to predict the phase error loss. There are some systematic phase error losses which can be given.

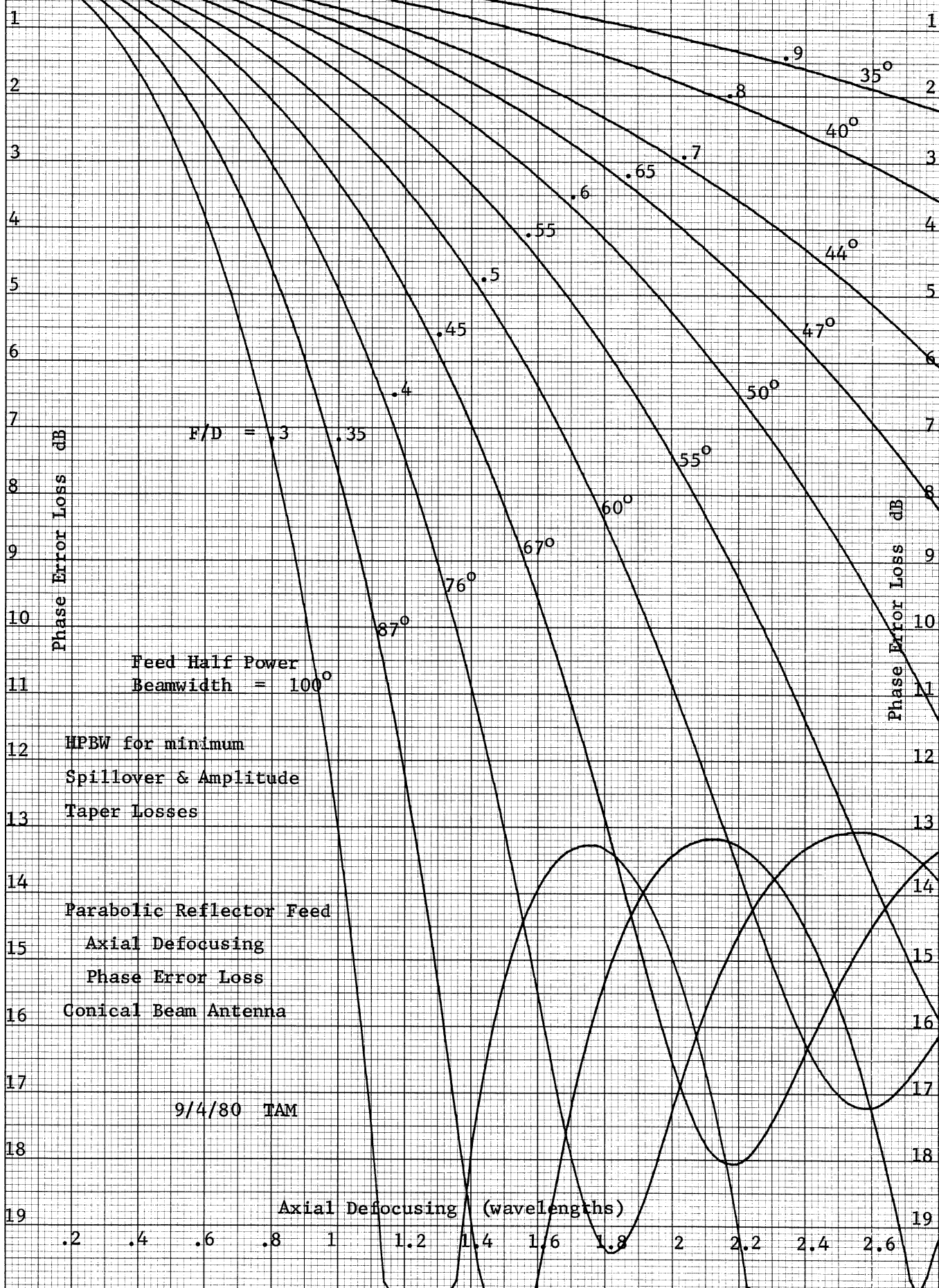
The first systematic phase error which is separated out is axial defocusing. In this case the phase center is on the axis of the reflector but not located at the focus. This can happen, for example, with a log periodic antenna feed. The phase center of the antenna will move when the frequency is changed (see page 473). If the phase center of the antenna is placed on the focus at one frequency, then for any other frequency there will be axial defocusing. One method would be to put the focus at the virtual apex of the antenna which would then give the same axial defocusing at all frequencies in the band of the feed antenna. On page 599 is a plot showing the effect of axial defocusing for various F/D . The conical beam approximation was used to find these plots with the beamwidth picked to be the optimum for the minimum sum of the spillover and amplitude taper losses. The results only change slightly for reasonable changes in the feed beamwidth. We can see from this plot that reflectors with small F/D are more susceptible to movement of the feed antenna.

The second type of defocusing is lateral offset. If the phase center of the feed antenna is moved off the axis of the reflector, then the beam will no longer be on boresight when reflected off the reflector. The phase error loss is a measure of the gain on boresight. It can only find the gain here so it does not correctly predict the gain at the peak of the beam. The effect of lateral offset on the phase error loss is plotted on page 600. We can see that like the axial defocusing, the reflectors with small F/D (large subtended angle) have higher phase error losses than reflectors with large F/D for the same lateral offset. The second thing to notice is that the parabolic reflector is more susceptible to lateral offset than to axial defocusing. We can see this by comparing the abscissa scales on the two plots.

The plots on pages 599 and 600 can be used to determine the tolerance requirements of the feed structure. Deep dishes (small F/D) will require closer tolerances than shallow dishes. Many feed supports are built with adjustments so that the feed can be accurately located at the focus. When designing a broadband feed, it will be necessary to make some compromises.

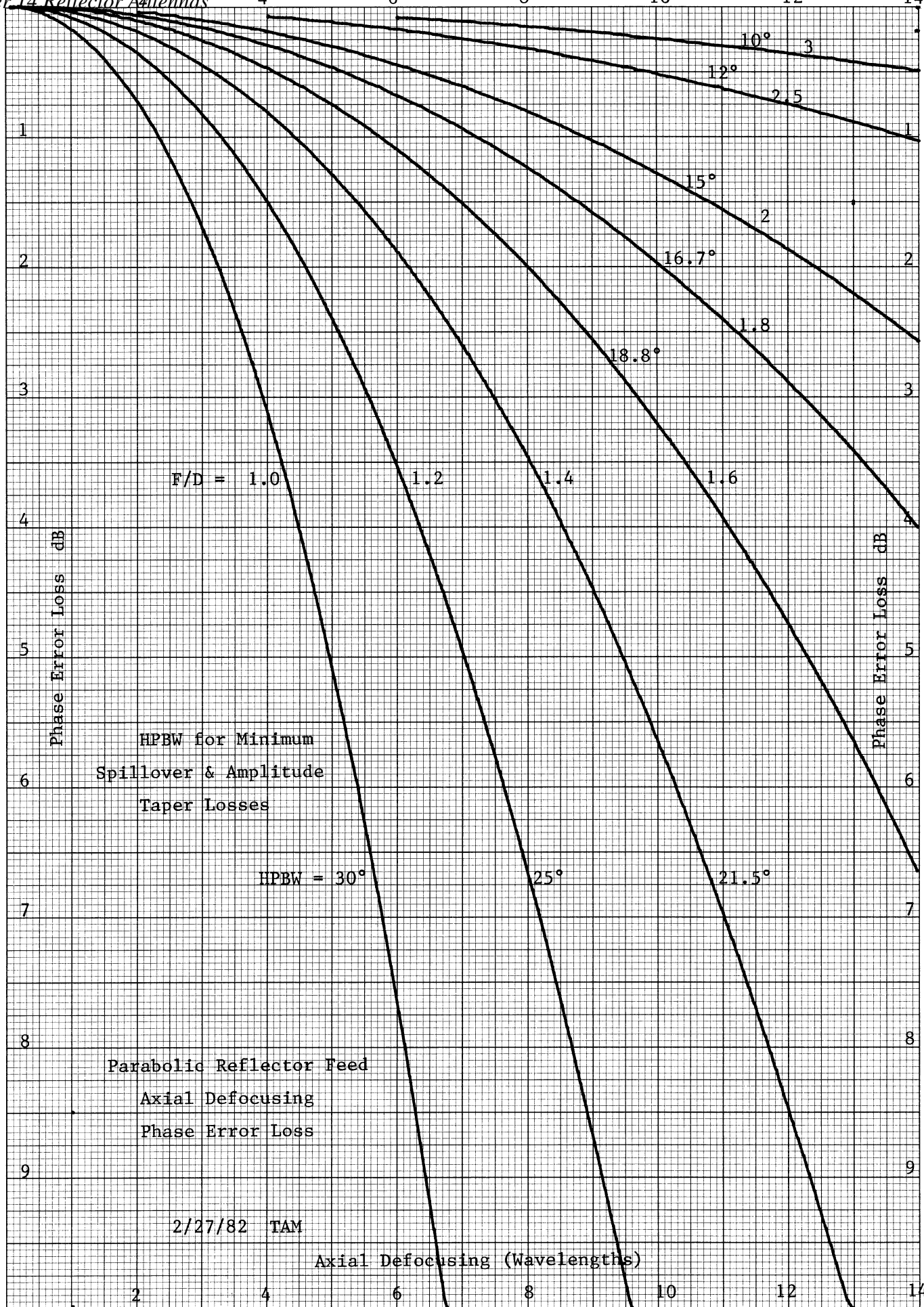
A third phase error problem with the feed is astigmatism. An investigation of this effect has been made by using the conical beam approximation for the feed and varying the Z axis offset sinusoidally with the rotation of the

Axial Defocusing (Wavelengths)



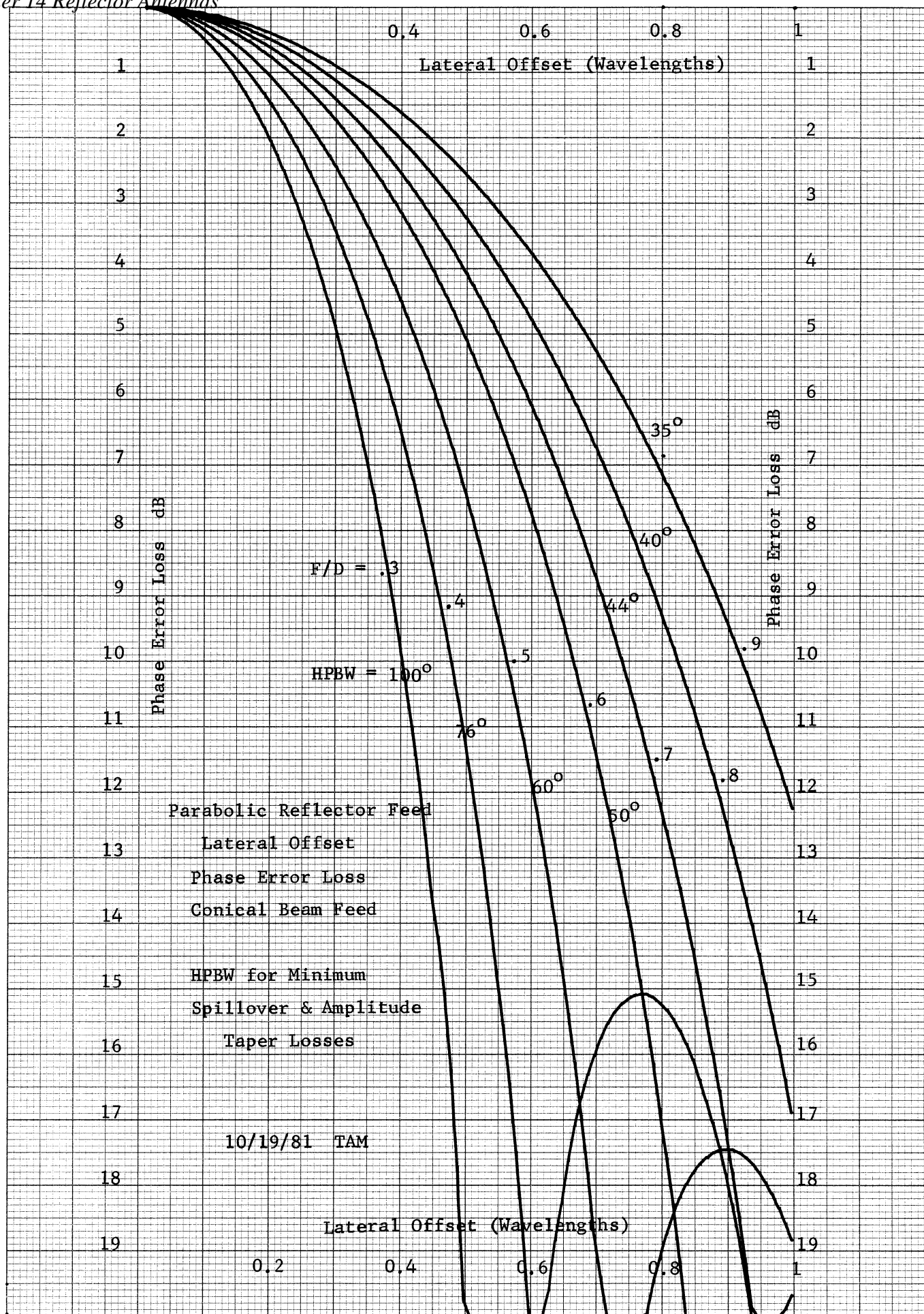
46 1320

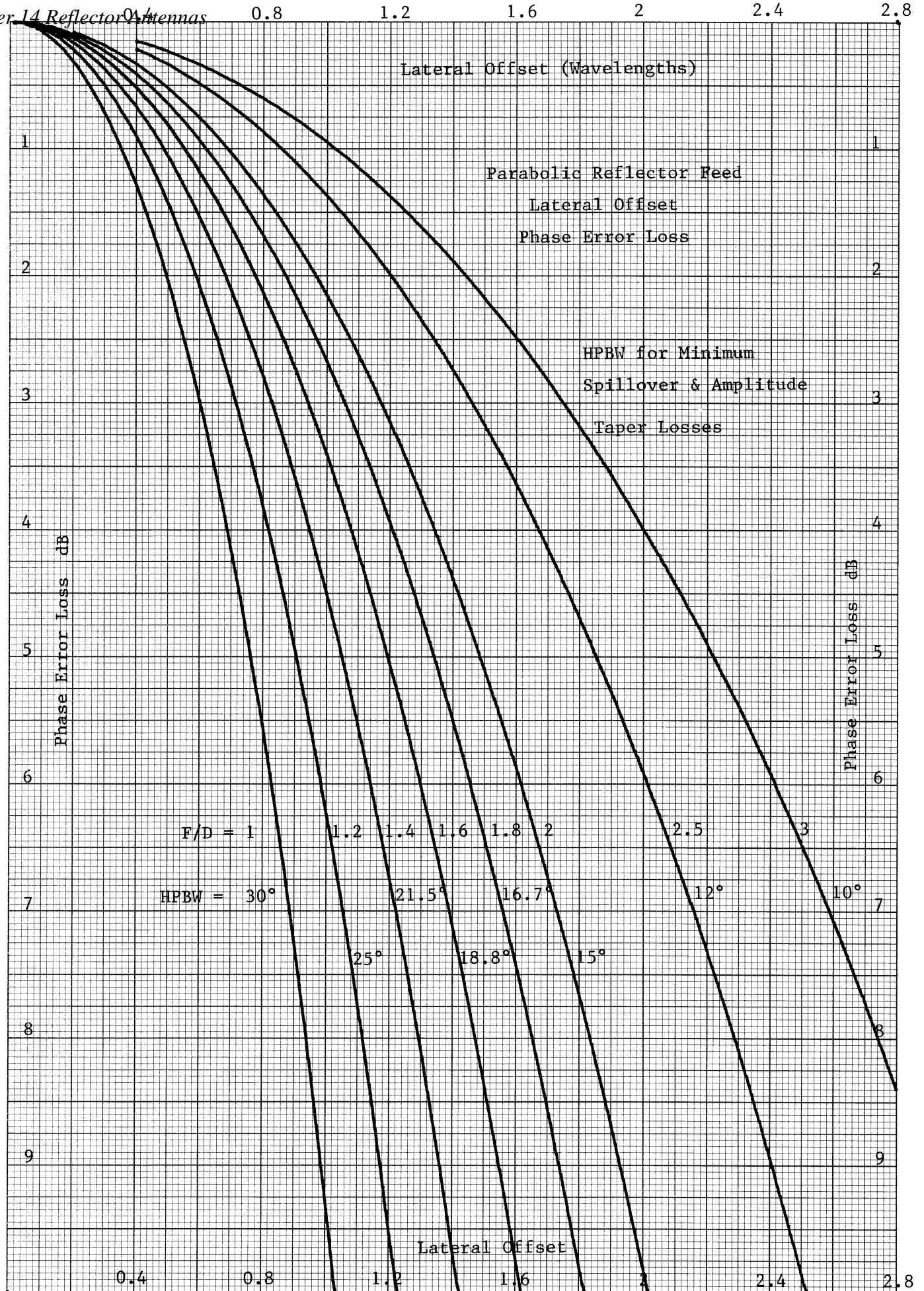
K&E 10 X 10 TO 1/2 INCH 7 X 10 INCHES
KEUFFEL & ESSER CO. MADE IN U.S.A.



46 1320

10 X 10 TO 1/2 INCH 7 X 10 INCHES
KEUFFEL & ESSER CO. MADE IN U.S.A.





phi pattern axis. The results are plotted on page 602. In these results the average phase center was placed at the focus of the parabola. We can see from the plot that the effects of astigmatism are similar to lateral offset losses, quite large. Unlike the other two types of defocusing, reflectors with small F/D are less effected by astigmatism in the feed. For example, if the phase error loss due to astigmatism is to be less than 0.5 for $F/D = 0.5$, astigmatism must be less than 0.19 wavelengths.

Another potential phase problem with the feed is random phase errors. The same reflector and feed that was studied for astigmatism was also studied with random errors. The plot of these results is given on page 603. Since only a limited pattern contours could be generated, the one sigma points are also plotted on the graph. Like all other phase error problems, deep dishes would have higher phase error losses for a given random phase errors in the feed antenna.

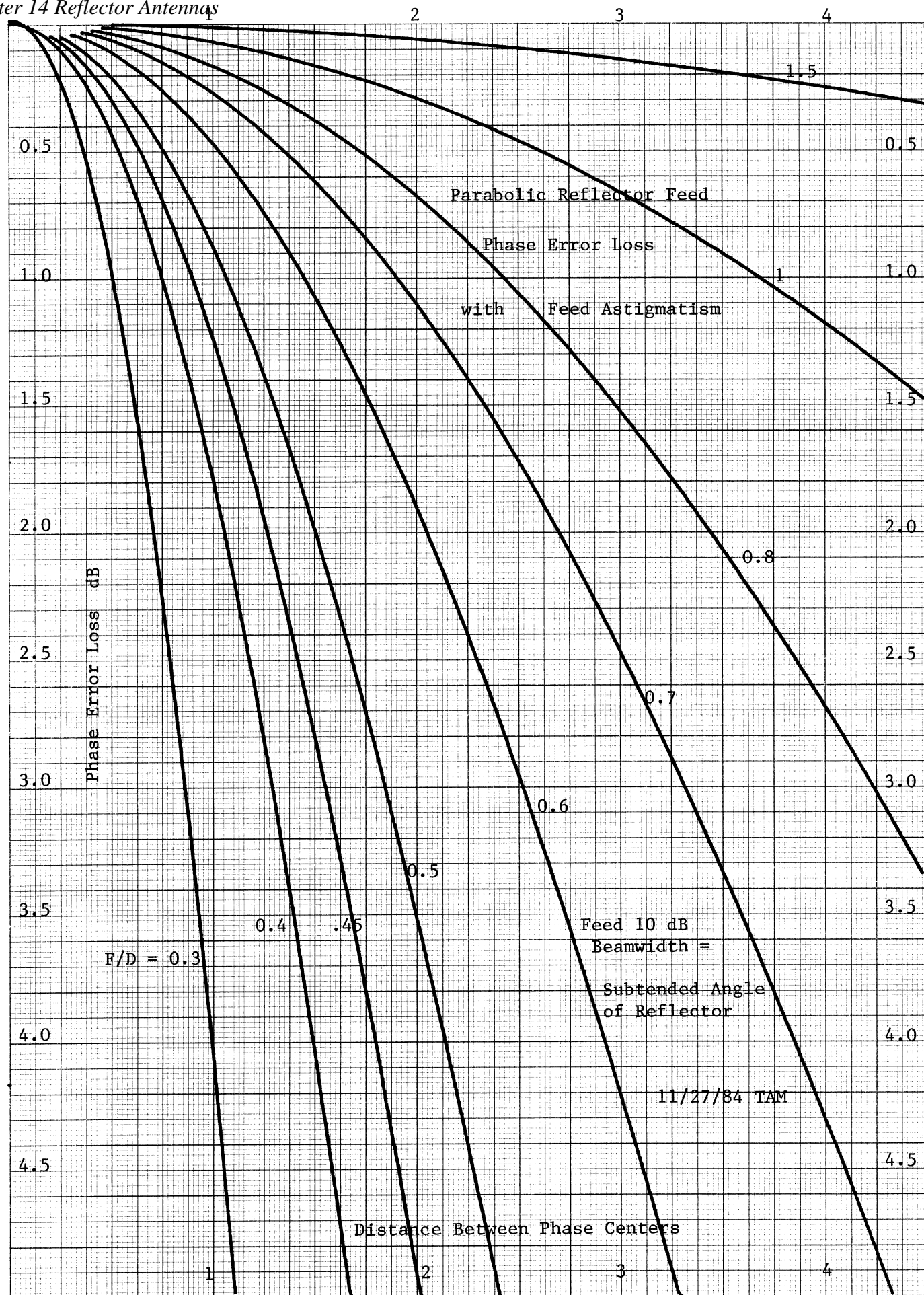
The last feed phase error problem can be the most severe. When a wide bandwidth feed is used such as a horn, we must be certain that the sidelobes of the feed are not within the subtended angle of the reflector. The sidelobes are 180 degrees out of phase with respect to the main beam. In the aperture plane these lobes will be 180 degrees out of phase as well. This portion of the aperture will subtract from the central portion in the far field radiation. It is easy to get total cancellation somewhere in the band of the antenna. This is one advantage of the log periodic feed for wide bandwidths. The beamwidth will remain constant over most of the band of the feed.

RELATIONS BETWEEN BEAMWIDTHS

Many of the graphs given here are in terms of either the 3 dB or 10 dB beamwidths. Sometimes the 6 dB beamwidth is used. We can find an approximate relationship between the different beamwidths of an antenna by using the conical beam approximation. If we refer to page 36, we can find new relations similar to the ones given there for any beamwidth level. Given one beamwidth level and one beamwidth, we can find the exponent, N . Using this exponent and another beamwidth level, we can find the new beamwidth. The expressions which result for such an operation are time consuming to calculate on a calculator. The operations can be reduced to a nomograph which has been done on pages 604 and 605.

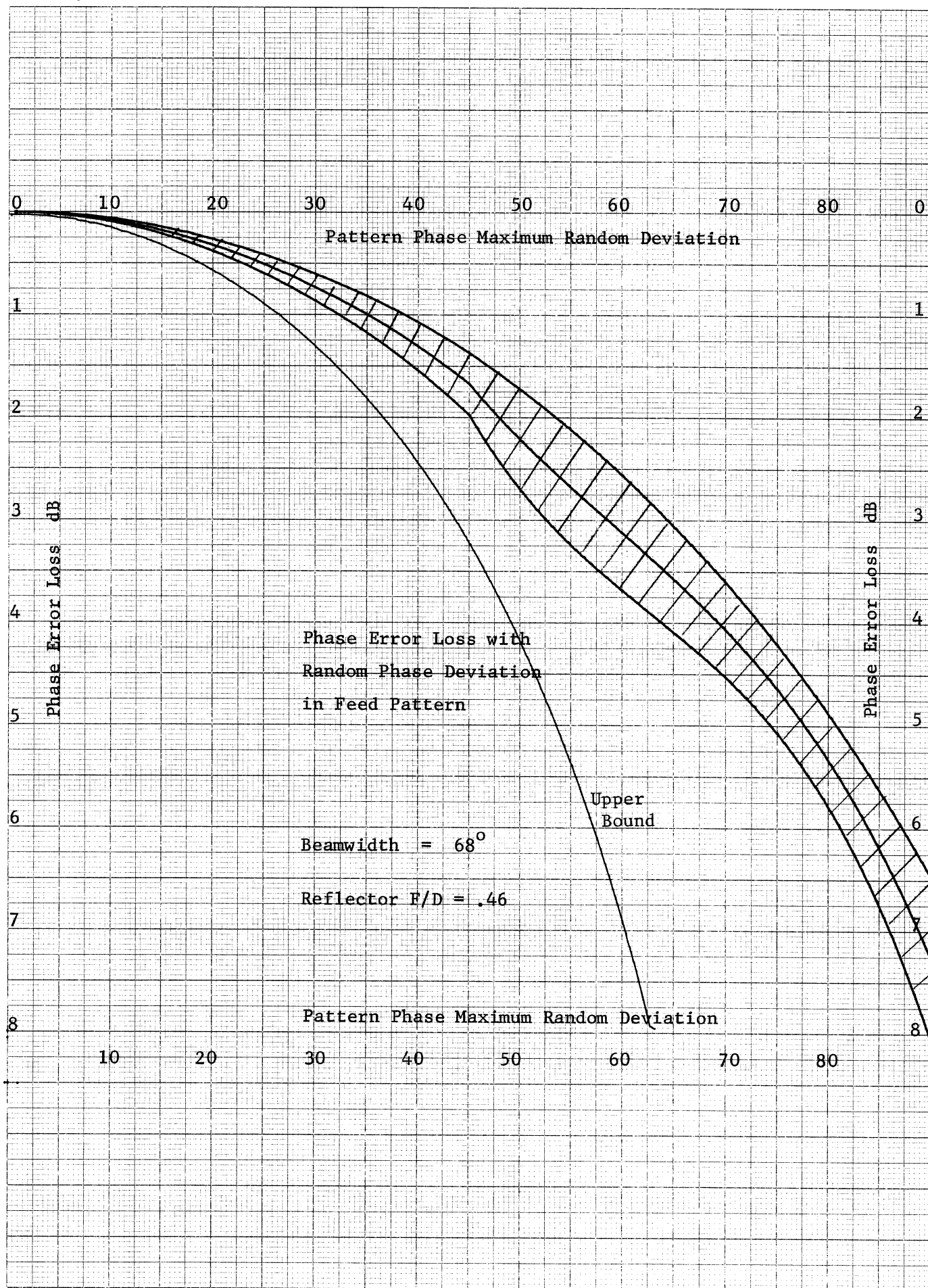
To use the nomograph, draw a line between the pattern beamwidth level and the beamwidth. Note the point where the line intersects the diagonal axis. In the example on page 604 the pattern level is 3 dB and the beamwidth is 60° . Draw a second line from the new pattern level through the intersection point of the first line and the diagonal axis to the beamwidth axis. This is the pattern beamwidth at the new level. The 6 dB beamwidth in the example on page 604 is 84.1° .

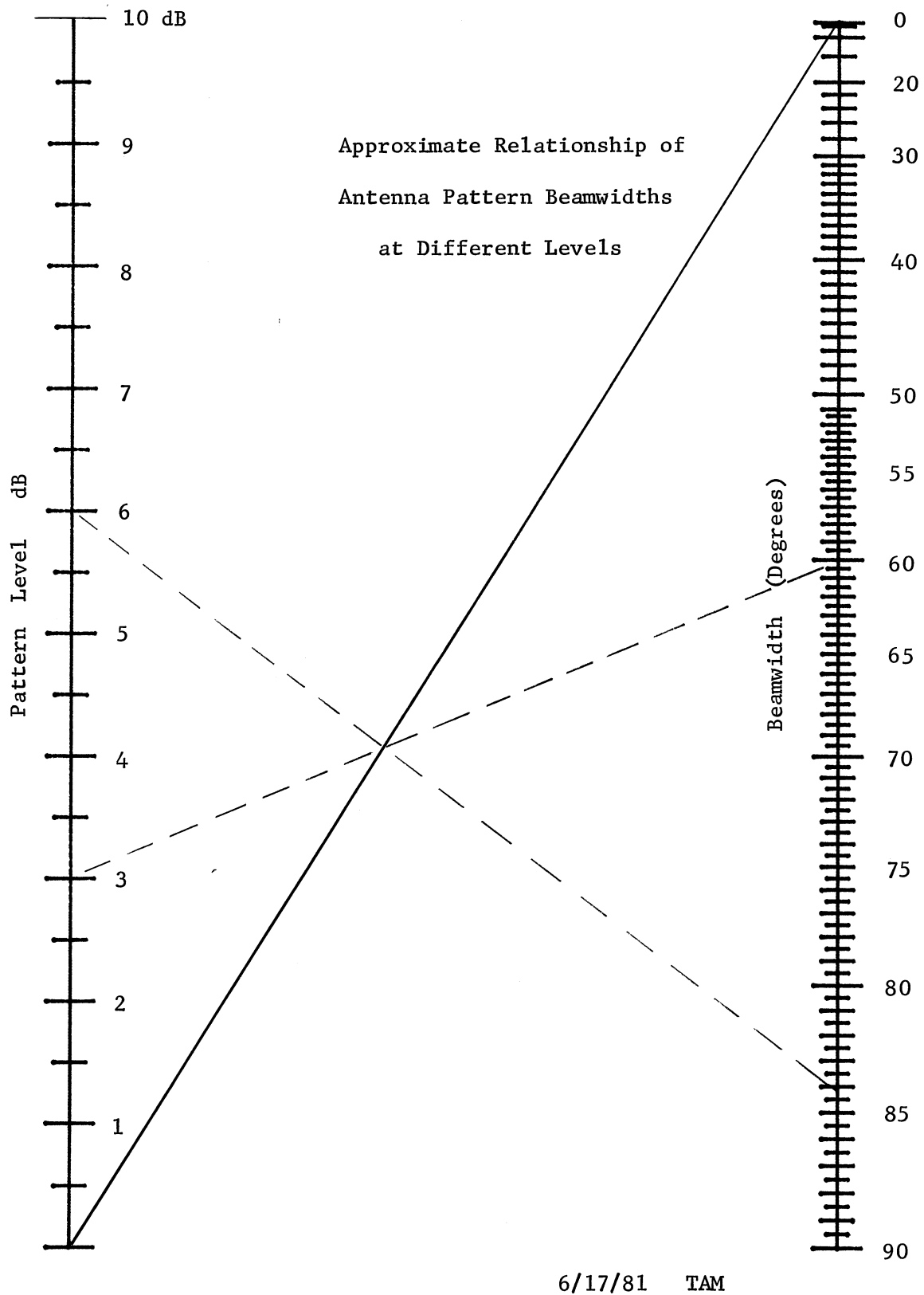
The chart can also be used to find the pattern level at different angles. For example, suppose the pattern level is 3 dB at 30° and we want to find the level at 40° . We draw a line between the 3 dB point on the pattern level and 30° on the beamwidth axis and note the intersection with the diagonal axis. Through the intersection draw another line using 40° as the second point and read the pattern level as 5.2 dB.

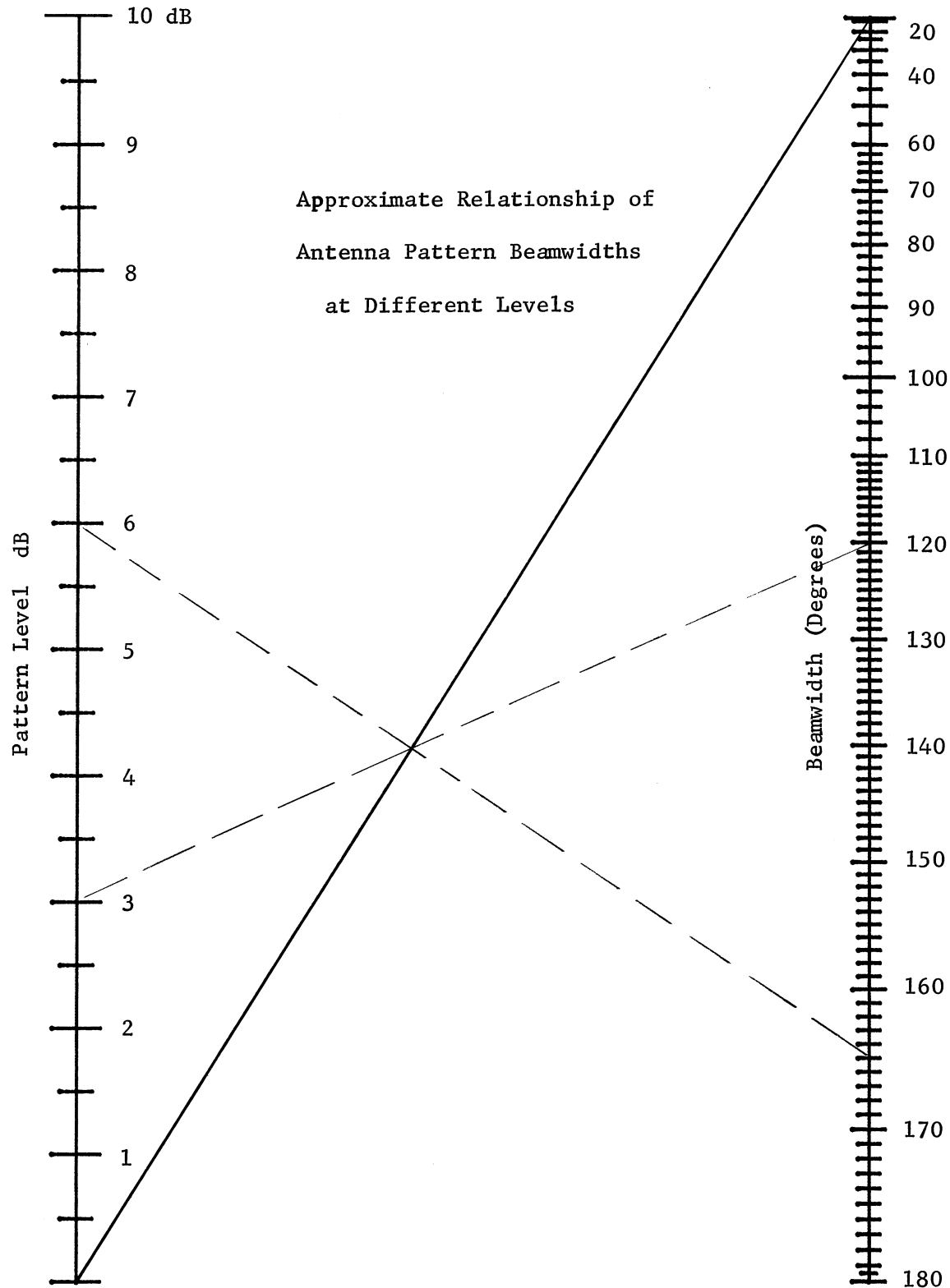


461510

10 X 10 TO THE CENTIMETER 18 X 25 CM.
KEUFFEL & ESSER CO. MADE IN U.S.A.







6/17/81 TAM

FEED CROSS POLARIZATION LOSS

If the feed has a substantial cross polarization component, then a cross polarization loss must be included. We will see later that the parabolic reflector will generate cross polarization for some feeds but the energy is located off boresight in the secondary pattern. It is necessary to divide the wave into orthogonal polarizations such as linear or circular to apply these formulas.

We must back up and consider the effect of cross polarization energy in an aperture. The formula for directivity is changed to include a cross polarization component.

$$\text{Directivity} = \frac{4\pi}{\lambda^2} \frac{\left| \iint_S E_c(x, y) dx dy \right|^2}{\iint_S |E_c(x, y)|^2 + |E_x(x, y)|^2 dx dy}$$

E_c is the co-polarization component and E_x is the cross polarization component. This is the directivity on boresight. As before we will divide the directivity formula up into pieces.

$$\text{Directivity} = \frac{4\pi A}{\lambda^2} (\text{ATL}) (\text{PEL}) (\text{XOL})$$

ATL is the aperture taper loss, PEL is the phase error loss, and XOL is the cross polarization loss. We will use the same formulas for ATL and PEL which were derived before. If we assume that there is no phase error loss, then the formula for directivity is reduced.

$$\text{Directivity} = \frac{4\pi A}{\lambda^2} (\text{ATL}) (\text{XOL}) = \frac{4\pi}{\lambda^2} \frac{\left| \iint_S |E_c| dx dy \right|^2}{\iint_S |E_c|^2 + |E_x|^2 dx dy}$$

If we substitute the expression for ATL, we can solve for XOL.

$$\text{ATL} = \frac{\left| \iint_S |E_c| dx dy \right|^2}{A \iint_S |E_c|^2 dx dy}$$

$$\text{XOL} = \frac{\iint_S |E_c|^2 ds}{\iint_S |E_c|^2 ds + \iint_S |E_x|^2 ds}$$

Above is the formula for XOL on an aperture. We need to convert this to a formula on the feed pattern. All three integrals are of the same form.

$$\iint_S |E|^2 ds = \int_0^{2\pi} \int_0^a |E(r', \phi')|^2 r' dr' d\phi'$$

The conversion of this integral to the feed pattern is given on page 591 in the denominator of the ATL formula.

$$\int_0^{2\pi} \int_0^{\psi_0} |E(\psi', \phi')|^2 \sin \psi' d\psi' d\phi'$$

Using this formula, we can find the XOL for the feed pattern.

$$XOL = \frac{\int_0^{2\pi} \int_0^{\psi_0} |E_c|^2 \sin \psi d\psi d\phi}{\int_0^{2\pi} \int_0^{\psi_0} (|E_c|^2 + |E_x|^2) \sin \psi d\psi d\phi}$$

Another consideration we must look into with a reflector feed is the spillover loss. Cross polarization patterns tend to be poorly defined beams and will spillover quite a bit of the energy contained in them. Since the spillover loss is just a measure of the energy which hits the dish, we can find the formula from the ratio of the integrals.

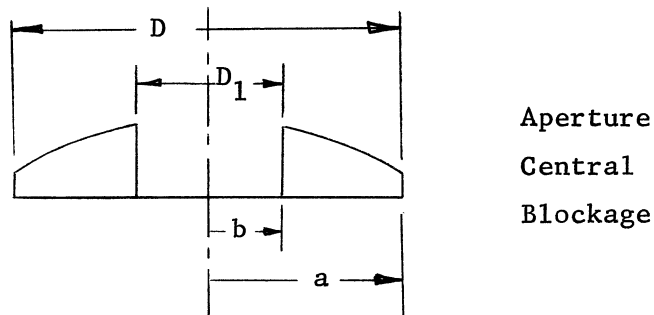
$$\text{Spillover Loss} = \frac{\int_0^{2\pi} \int_0^{\psi_0} (|E_c|^2 + |E_x|^2) \sin \psi d\psi d\phi}{\int_0^{2\pi} \int_0^{\pi} (|E_c|^2 + |E_x|^2) \sin \psi d\psi d\phi}$$

Using the above equations, we can find the boresight illumination losses when the feed antenna has a substantial cross polarization response. In many feeds the cross polarization loss is very small and can be ignored.

APERTURE BLOCKAGE

The parabolic reflector feed is placed at the focus and will block part of the aperture and eliminate radiation from that portion. This has two effects. First, it will reduce the gain because the energy from that part does not radiate. The second effect will be an increase in the sidelobes. We will only consider central blockage because we can consider it in general.

One method of handling central blockage is to modify the integrals of the illumination loss efficiencies. The central aperture blockage is as shown in the figure below.



We will want to relate the blockage to the feed pattern. To do this we can find an equivalent F/D for the blockage. The focal length, F, is the same as the full dish, but the diameter has decreased. The angle to the end of the blockage is found.

$$\psi_B = 2 \tan^{-1}(b/(2F))$$

The integrals over the feed pattern will have a changed lower limit, ψ_B . To find the amplitude taper loss efficiency, we only integrate over the aperture and reduce the area factor in the denominator.

$$ATL = \frac{\left| \int_0^{2\pi} \int_b^a E_a(r, \phi) r dr d\phi \right|^2}{\pi(a^2 - b^2) \int_0^{2\pi} \int_b^a |E_a(r, \phi)|^2 r dr d\phi}$$

Now let us relate this back to the feed pattern. We can modify the arguments and limits of the integral by inspecting the development on page 591.

$$ATL = \frac{4F^2 \left| \int_0^{2\pi} \int_{\psi_B}^{\psi_0} E(\psi, \phi) \tan \psi/2 d\psi d\phi \right|^2}{\pi(a^2 - b^2) \int_0^{2\pi} \int_{\psi_B}^{\psi_0} |E(\psi, \phi)|^2 \sin \psi d\psi d\phi}$$

The dimensions can be eliminated by making the following substitutions.

$$a/(2F) = \tan \psi_0/2 \quad b/(2F) = \tan \psi_B/2$$

With these substitutions we obtain the final form of the amplitude taper loss efficiency.

$$ATL = \frac{\left| \int_0^{2\pi} \int_{\psi_B}^{\psi_0} E(\psi, \phi) \tan \psi/2 d\psi d\phi \right|^2}{\pi(\tan^2 \psi_0/2 - \tan^2 \psi_B/2) \int_0^{2\pi} \int_{\psi_B}^{\psi_0} |E(\psi, \phi)|^2 \sin \psi d\psi d\phi}$$

The phase error loss efficiency will only require a change in the limits of the integrals.

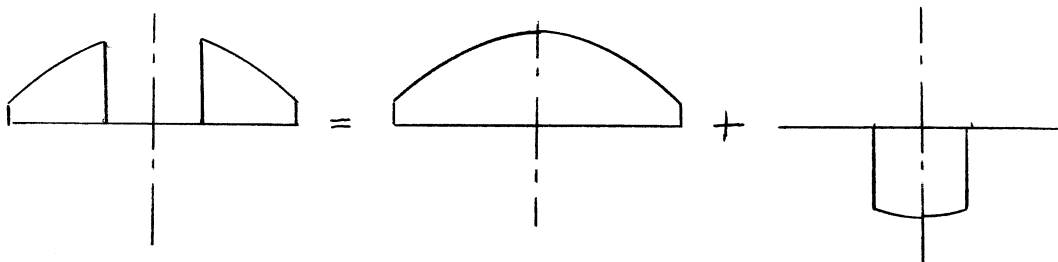
$$PEL = \frac{\left| \int_0^{2\pi} \int_{\psi_B}^{\psi_0} E(\psi, \phi) \tan \psi/2 d\psi d\phi \right|^2}{\left(\int_0^{2\pi} \int_{\psi_B}^{\psi_0} |E(\psi, \phi)| \tan \psi/2 d\psi d\phi \right)^2}$$

The limits in the spillover loss are also modified to take the ratio of the energy which hits dish and is translated to the unblocked aperture to the total radiated energy of the feed.

$$\text{Spillover Loss} = \frac{\int_0^{2\pi} \int_{\psi_B}^{\psi_0} |E(\psi, \phi)|^2 \sin \psi \, d\psi \, d\phi}{\int_0^{2\pi} \int_0^{\pi} |E(\psi, \phi)|^2 \sin \psi \, d\psi \, d\phi}$$

All the loss efficiencies except the amplitude taper, are changed to include blockage by modifying only the limits of the integrals.

The second method of handling the central aperture blockage is to divide the problem into two parts. The blocked aperture is equivalent to the sum of the two apertures given in the figure below.



To find the radiated field of the blocked aperture, find the field of the unblocked aperture and subtract from it the field radiated from the blockage aperture. This is conceptually simple but the power division in each section must be maintained before subtracting the fields. The blockage loss is more easily found from the ratio of the following integrals.

$$\text{Blockage Loss} = \frac{\left| \int_0^{2\pi} \int_{\psi_B}^{\psi_0} E \tan(\psi/2) \, d\psi \, d\phi \right|^2}{\left| \int_0^{2\pi} \int_0^{\psi_0} E \tan(\psi/2) \, d\psi \, d\phi \right|^2}$$

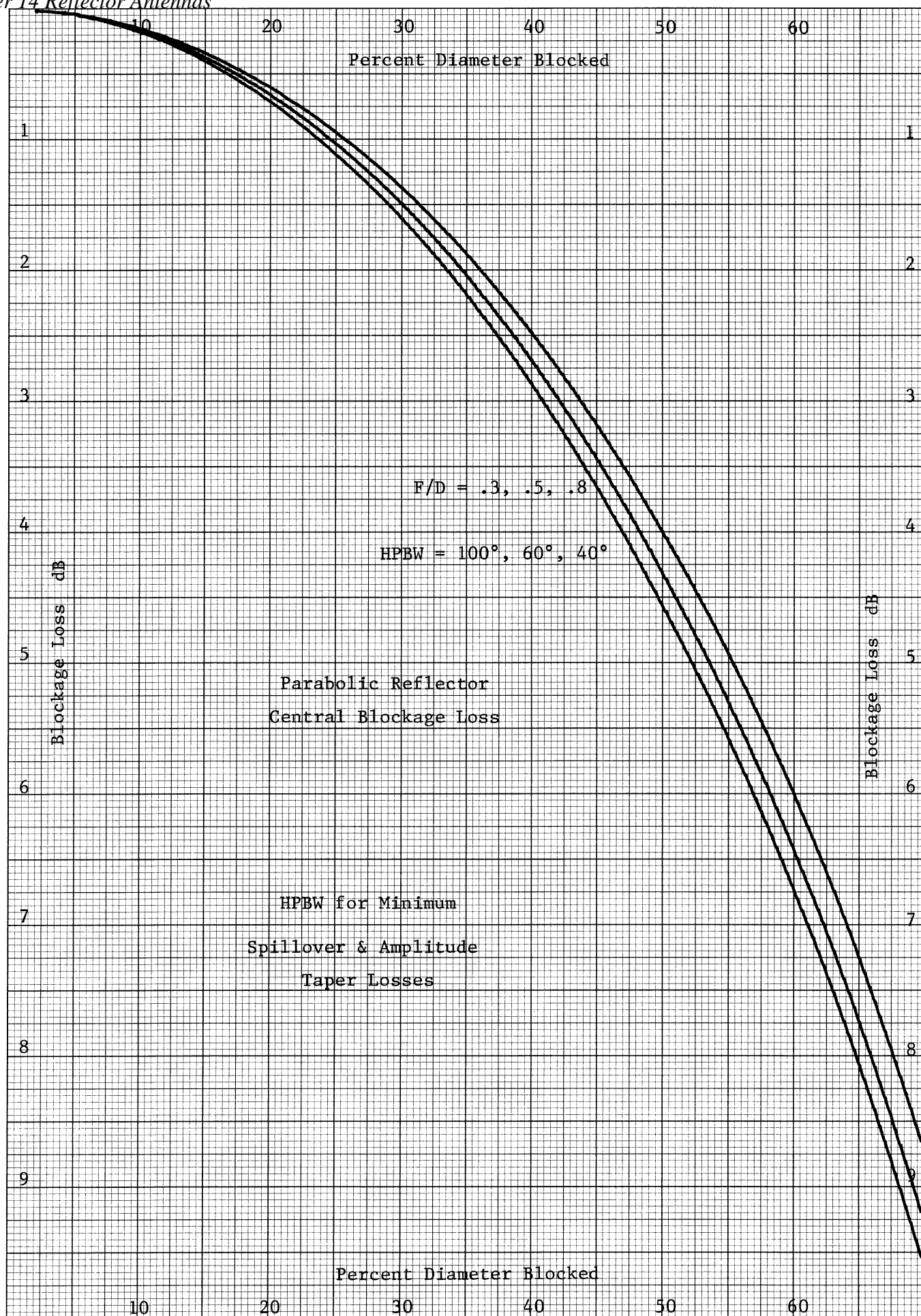
Two curves of the blockage loss of a Parabolic reflector feed are given on pages 610 and 611. On these curves a feed was picked which would give the minimum sum of spillover and amplitude taper losses. The first curve is in terms of the percent of the diameter blocked. From this we can see that the F/D of the reflector has little effect on the blockage loss for an optimum feed beamwidth. The second curve is the same blockage loss only related to the feed angle to the edge of the blocked portion of the aperture.

The second effect of aperture blockage is a change in the sidelobe level. The pattern of the full aperture will have a narrow beamwidth, but the pattern of the blockage will be broad in comparison and will cover the first few sidelobes of the full aperture pattern. The blockage pattern will subtract from the main beam of the full aperture giving lower gain, but it will add to the first sidelobe which is 180° out of phase with respect to the main beam.

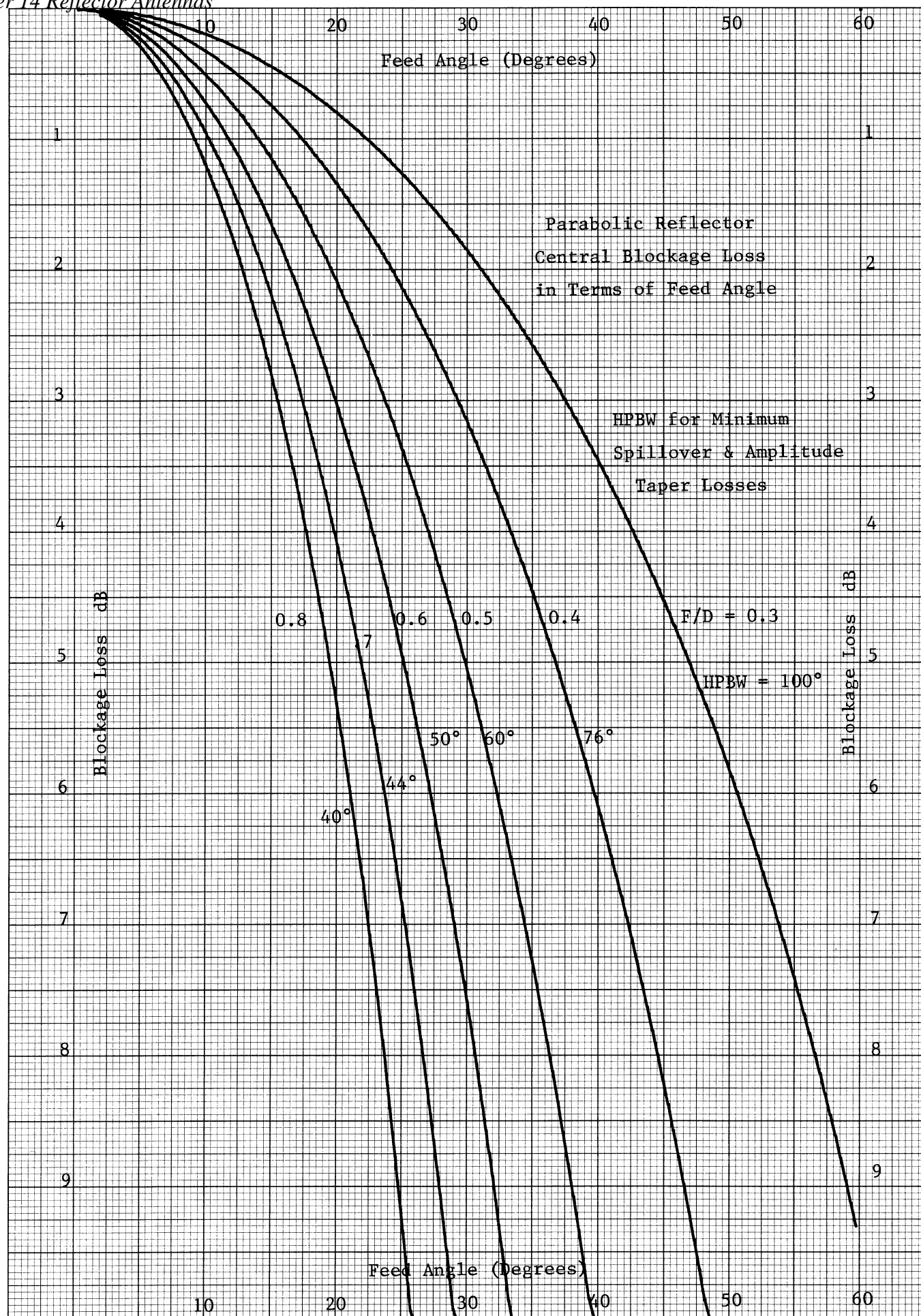
On page 612 is a pattern of a parabolic reflector with and without central blockage. The first sidelobe has been raised 4.5 dB by the blockage. The second sidelobe was lowered because it is in phase with the main beam and

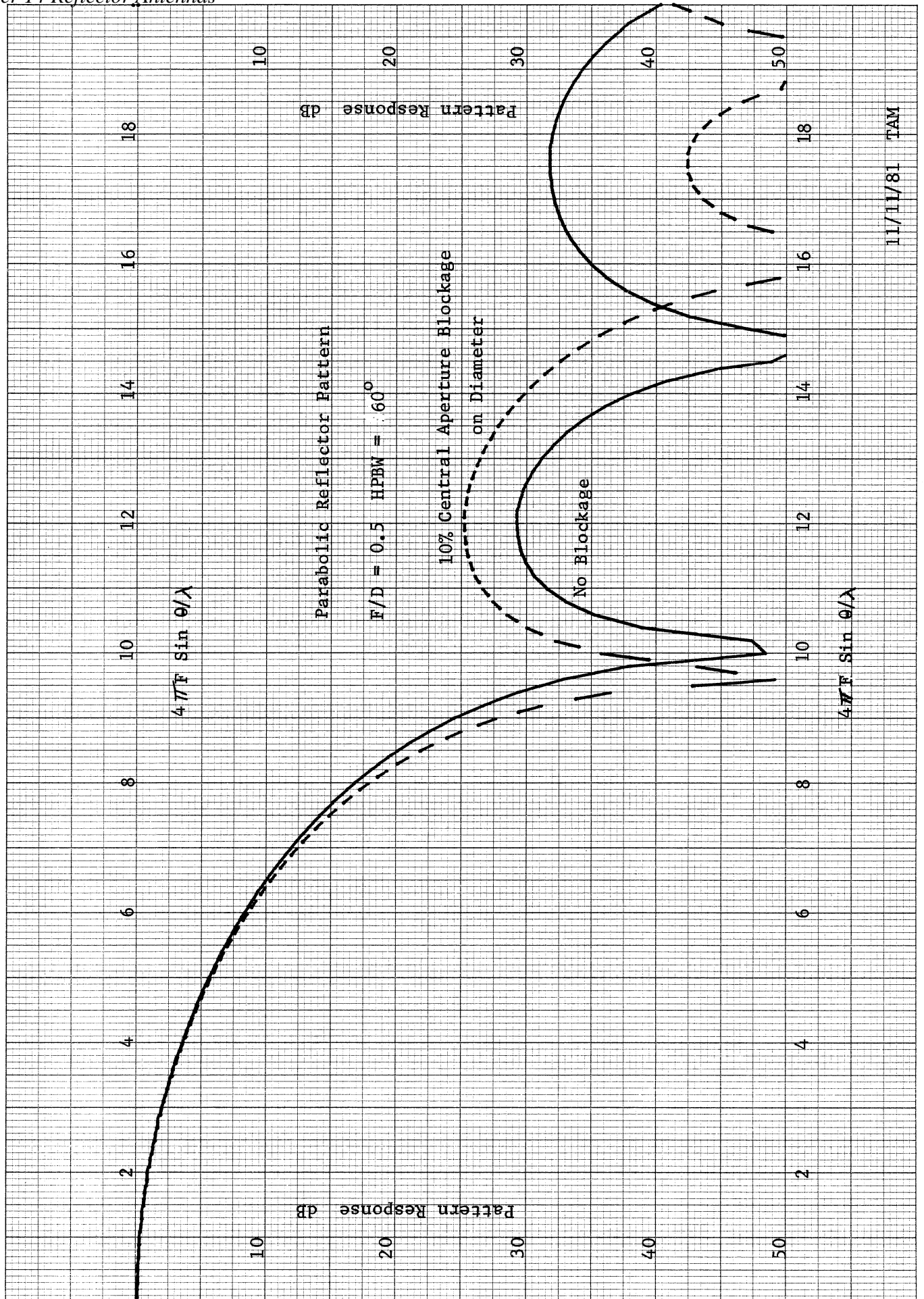
46 1320

10 X 10 TO 1/2 INCH 7 X 10 INCHES
KEUFFEL & ESSER CO. MADE IN U.S.A.



46 1320

K&E 10 X 10 TO 1/2 INCH 7 X 10 INCHES
KEUFFEL & ESSER CO. MADE IN U.S.A.



out of phase with the blockage pattern. A curve showing the effect on the sidelobes as the blockage is increased is drawn on page 614. All three cases are for a feed which will have minimum spillover and amplitude taper losses. The reflectors with smaller F/D have smaller sidelobes for the optimum feed. The feed pattern is down about 10 dB in the direction of the edge of the reflector in all three cases, but we can see from the curve on page 590 that the reflectors with smaller F/D have a greater taper across the aperture for the same edge level of the feed. The greater taper reduces the sidelobes.

The struts which hold the feed in place will also block the aperture and raise the sidelobes. These can be handled by modifying the integrals to exclude these regions from the calculation. In the case of the amplitude taper loss these areas will also have to be excluded from the area calculation in the denominator of the formula.

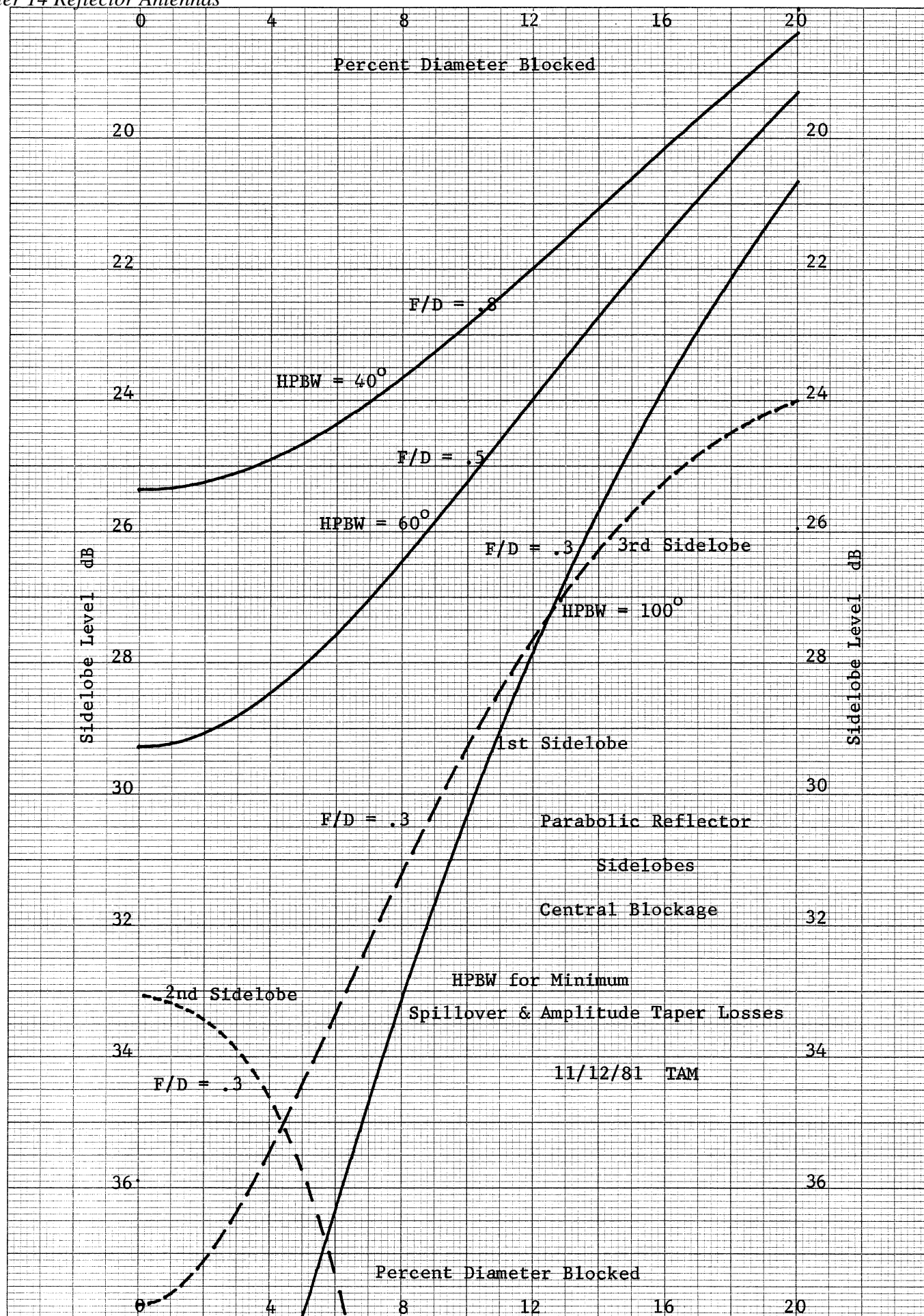
The problems with the feed blockage can be solved by using an offset feed. The reflector still has its focus at the feed, but portion of the reflector which would be projected on the feed is eliminated. These are used when low sidelobes are needed or when the feed structure is large.

The curves on pages 610 and 611 point out the importance of the feed pattern in the direction of the reflector edge. This is more clearly demonstrated by the curves on page 615. These show the ratio of the gain of the central portion of the aperture relative to the total aperture. The abscissa is in terms of the feed angles. The beamwidth for each F/D has been picked to give the minimum sum of the spillover and amplitude taper losses. There is about a 10 dB taper in the direction of the reflector edge.

Take for an example a reflector with $F/D = 0.5$. The half subtended angle is found from the alignment chart on page 583: 53° . From the plots on page 615 we can see that one half of the gain comes from the feed angles from 41° to 53° . The half power beamwidth of the feed is 60° . The level of the feed pattern at 41° can be found by using the nomograph on page 604. It is 5.7 dB down from the peak. Over the region from 41° to 53° , the average feed pattern level is 7.5 dB below the peak, but still half the gain of the reflector comes from this region. If the diameter of the reflector is doubled, then the gain increases by the square of the diameter or 6 dB. We would expect that half the gain would come from the central 70.7% of the feed pattern if it were uniform, but because there is an amplitude taper, it comes from 74%. Having a 10 dB taper across the feed pattern did not alter much the effect of the outer portion of the reflector on the total gain.

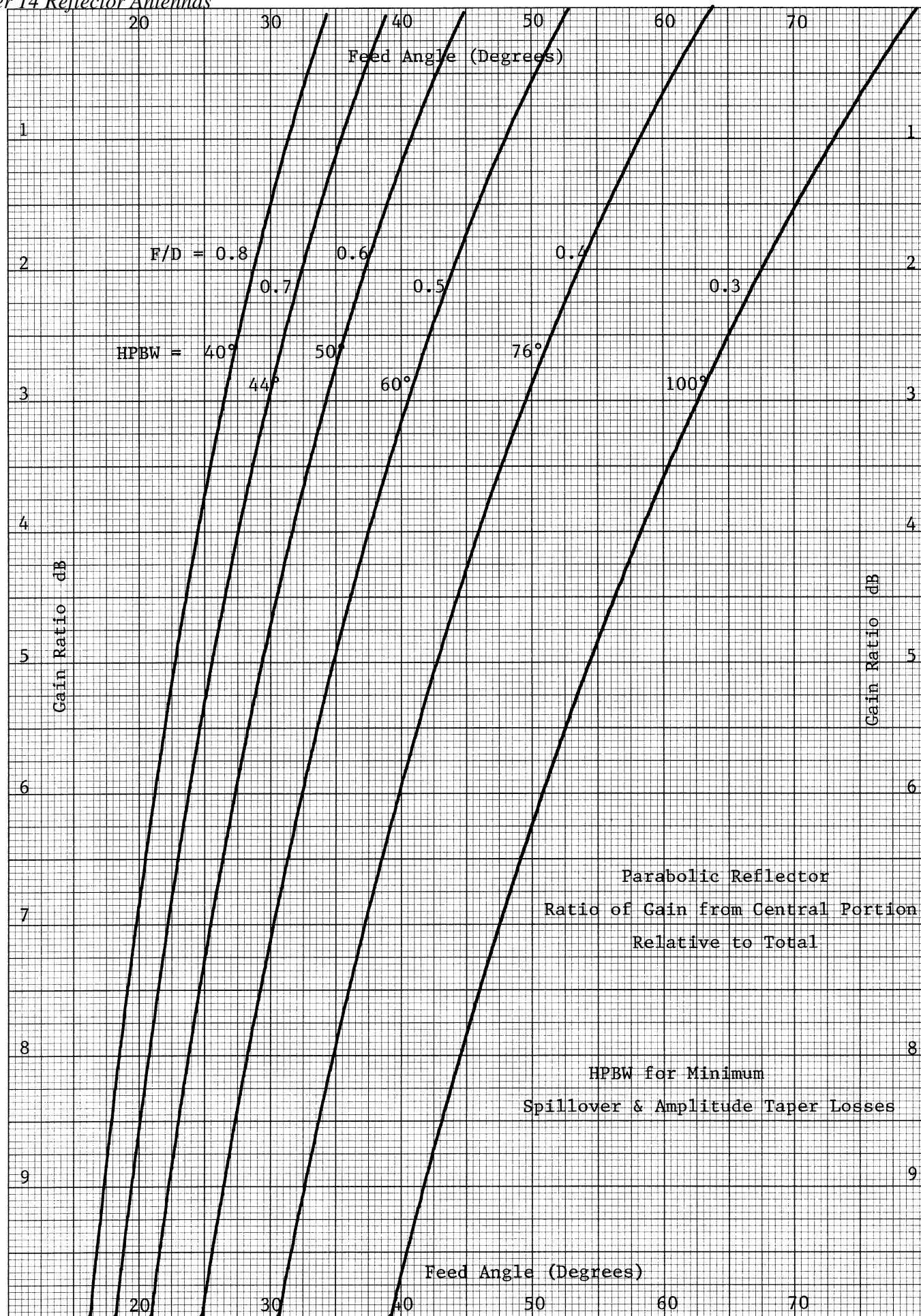
46 1320

KE 10 X 10 TO 1 1/2 INCH 7 X 10 INCHES
KEUFFEL & ESSER CO. MADE IN U.S.A.



46 1320

10 X 10 TO 1/2 INCH 7 X 10 INCHES
KEUFFEL & ESSER CO. MADE IN U.S.A.



ALTERNATE GAIN CALCULATION METHOD

The usual method of finding the gain of a parabolic reflector is to find the directivity from the feed pattern and subtract from it the spillover loss (in dB) and the feed antenna efficiency (in dB). The reflector is assumed to be 100% efficient. The directivity is the gain of a uniform aperture of the projected area of the reflector ($4\pi A/\lambda^2$) times the amplitude taper loss efficiency and the phase error loss efficiency.

$$\text{Gain} = \text{Directivity (SPL)} \eta_f$$

SPL is the spillover loss efficiency and η_f is the feed efficiency. We can combine the two formulas into one. First convert the directivity formula into one involving the feed pattern angles.

$$\text{Directivity} = \frac{4\pi}{\lambda^2} \frac{\left| \int_0^{2\pi} \int_0^a E_{ac}(r, \phi) r dr d\phi \right|^2}{\int_0^{2\pi} \int_0^a (|E_{ac}(r, \phi)|^2 + |E_{ax}(r, \phi)|^2) r dr d\phi}$$

E_{ac} is the copolarized electric field in the aperture and E_{ax} is the cross polarized field. We made similar integral conversions on page 591. Following the development given there, the directivity formula can be found in terms of the feed pattern.

$$\text{Directivity} = \frac{16\pi F^2}{\lambda^2} \frac{\left| \int_0^{2\pi} \int_0^{\psi_0} E_c(\psi, \phi) \tan(\psi/2) d\psi d\phi \right|^2}{\int_0^{2\pi} \int_0^{\psi_0} (|E_c(\psi, \phi)|^2 + |E_x(\psi, \phi)|^2) \sin \psi d\psi d\phi}$$

If we multiply this by the spillover loss efficiency given on page 607, then we can see that the denominator of the directivity formula will be cancelled by the numerator of the spillover loss.

$$\text{Gain} = \frac{16\pi F^2}{\lambda^2} \frac{\left| \int_0^{2\pi} \int_0^{\psi_0} E_c(\psi, \phi) \tan(\psi/2) d\psi d\phi \right|^2 \eta_f}{\int_0^{2\pi} \int_0^{\pi} (|E_c(\psi, \phi)|^2 + |E_x(\psi, \phi)|^2) \sin \psi d\psi d\phi}$$

The denominator is the power radiated by the feed antenna if multiplied by the impedance of free space. This is the formula for the gain at boresight, which may not be the peak gain if the feed has lateral offset from the focus. On page 569 we find a formula for the directive directivity which indicates the changes needed to modify the boresight gain to get the directive gain formula.

$$\text{Gain} = \frac{4\pi(1+\cos\theta)^2 F^2 \eta_f}{\lambda^2} \frac{\left| \int_0^{2\pi} \int_0^{\psi_0} E_c(\psi', \phi_c) \text{TAN}(\psi'/2) e^{j\beta r \sin\theta \cos(\phi - \phi_c)} d\psi' d\phi_c \right|^2}{\int_0^{2\pi} \int_0^{\pi} (|E_c(\psi', \phi_c)|^2 + |E_x(\psi', \phi_c)|^2) \sin\psi' d\psi' d\phi_c}$$

The phase factor is in terms of the radial factor of the aperture which can be converted by the formulas on page 591. Since we expect that the gain will be near boresight, we can let $\cos\theta = 1$.

$$\text{GAIN}(\theta, \phi) = \frac{16\pi F^2 \eta_f}{\lambda^2} \frac{\left| \int_0^{2\pi} \int_0^{\psi_0} E_c(\psi', \phi_c) \text{TAN}(\psi'/2) e^{j2\beta F \text{TAN}(\psi'/2) \sin\theta \cos(\phi - \phi_c)} d\psi' d\phi_c \right|^2}{\int_0^{2\pi} \int_0^{\pi} (|E_c(\psi', \phi_c)|^2 + |E_x(\psi', \phi_c)|^2) \sin\psi' d\psi' d\phi_c}$$

This is the gain near boresight from the feed pattern referenced to the focal point of the reflector. Given a measured feed pattern, we can find the far field gain pattern near boresight.

Let us separate out a feed cross polarization efficiency.

$$(\text{XOL})_f = \frac{\int_0^{2\pi} \int_0^{\pi} |E_c(\psi, \phi)|^2 \sin\psi d\psi d\phi}{\int_0^{2\pi} \int_0^{\pi} (|E_c(\psi, \phi)|^2 + |E_x(\psi, \phi)|^2) \sin\psi d\psi d\phi}$$

We can then express the gain with this efficiency.

$$\text{GAIN} = \frac{16\pi F^2 \eta_f (\text{XOL})_f}{\lambda^2} \frac{\left| \int_0^{2\pi} \int_0^{\psi_0} E_c(\psi, \phi_c) \text{TAN}(\psi'/2) e^{j2\beta F \text{TAN}(\psi'/2) \sin\theta \cos(\phi - \phi_c)} d\psi d\phi_c \right|^2}{\int_0^{2\pi} \int_0^{\pi} |E_c(\psi, \phi_c)|^2 \sin\psi d\psi d\phi_c}$$

The efficiency of the feed antenna is the gain divided by the directivity of the feed antenna.

$$\eta_f = \frac{\text{Gain}_f}{\text{Directivity}} = \frac{\text{Gain}_f \int_0^{2\pi} \int_0^{\pi} (|E_c|^2 + |E_x|^2) \sin\psi d\psi d\phi}{4\pi E_{c(\max)}}$$

The product of the feed efficiency and the feed polarization efficiency is

$$\eta_f (\text{XOL})_f = \frac{\text{Gain}_f \int_0^{2\pi} \int_0^{\pi} |E_c|^2 \sin\psi d\psi d\phi}{4\pi E_{c(\max)}}$$

We can identify this as the gain divided by the feed directivity found by

ignoring the energy in the cross polarized component. We can call this efficiency: η_{fc} . When finding the gain of the reflector from the feed pattern, it is not necessary to measure the cross polarization pattern to get accurate results. The cross polarization efficiency is included in the normal efficiency of the feed.

The gain formula can be separated into the usual illumination efficiencies and the spillover loss.

$$\text{Spillover Loss} = \frac{\int_0^{2\pi} \int_0^{\psi_0} |E_c|^2 \sin \psi \, d\psi \, d\phi}{\int_0^{2\pi} \int_0^{\pi} |E_c|^2 \sin \psi \, d\psi \, d\phi}$$

$$\text{ATL} = \frac{\cot^2(\psi_0/2) \left| \int_0^{2\pi} \int_0^{\psi_0} |E_c(\psi', \phi)| \tan(\psi'/2) \, d\psi' \, d\phi \right|^2}{\pi \int_0^{2\pi} \int_0^{\psi_0} |E_c(\psi', \phi)|^2 \sin \psi' \, d\psi' \, d\phi}$$

If we use these equations above for the for the efficiencies, then the phase error loss efficiency becomes

$$\text{PEL}(\theta, \phi) = \frac{\left| \int_0^{2\pi} \int_0^{\psi_0} E_c(\psi, \phi_c) \tan(\psi/2) e^{j2\beta F \tan \psi/2 \sin \theta \cos(\phi - \phi_c)} \, d\psi \, d\phi_c \right|^2}{\left(\int_0^{2\pi} \int_0^{\psi_0} |E_c(\psi', \phi_c)| \tan(\psi'/2) \, d\psi' \, d\phi_c \right)^2}$$

This phase error loss efficiency is no longer just at boresight, but at a general angle (θ, ϕ) . The division of the illumination losses in this manner is arbitrary but at least most of them remain the same.

$$\text{Gain}(\theta, \phi) = \frac{\pi D^2}{\lambda^2} \eta_{fc} (\text{SPL}) (\text{ATL}) (\text{PEL}(\theta, \phi))$$

If the cross polarization secondary pattern is wanted, then the cross polarization pattern of the feed needs to be measured. The efficiency of the feed antenna will be the same for both polarizations since it is a measure of the material and input reflection losses which are the same for both polarizations. It is not necessary to measure the gain of the cross polarization component.

$$\eta_{fx} = \eta_f (\text{XOL})_{fx}$$

$(\text{XOL})_{fx}$, the feed cross polarization efficiency, can be found from the ratio given on page 617 by substituting E_x for E in the numerator. η_f is the true efficiency of the antenna which can be found from the formula

$$\eta_f (\text{dB}) = \eta_{fc} (\text{dB}) - \text{Dir}_{cT} (\text{dB}) + \text{Dir}_c (\text{dB})$$

Dir_{cT} is the true directivity and Dir_c is the directivity found by ignoring the cross polarization component.

The efficiency: η_{fx} can be found from η_{fc} and various directivities.

$$\eta_{fx}(\text{dB}) = \eta_{fc}(\text{dB}) - \text{Dir}_{cT}(\text{dB}) + \text{Dir}_c(\text{dB}) + \text{Dir}_{xT}(\text{dB}) - \text{Dir}_x(\text{dB})$$

Dir_{xT} is the true directivity of the cross polarization component and Dir_x is the directivity found by ignoring the copolarization component.

We can combine these formulas for the directivities and obtain the difference between the two efficiencies as the following integral ratio.

$$\eta_{fx}(\text{dB}) - \eta_{fc}(\text{dB}) = 10 \text{ Log} \left(\frac{\int_0^{2\pi} \int_0^{\pi} |E_x(\psi, \phi)|^2 \sin \psi \, d\psi \, d\phi}{\int_0^{2\pi} \int_0^{\pi} |E_c(\psi, \phi)|^2 \sin \psi \, d\psi \, d\phi} \right)$$

FEED SCANNING

The beam of the secondary pattern can be scanned a few beamwidths by moving the feed off the axis. The problem can be handled by using the phase error loss term given on page 618. Suppose the feed has been offset from the axis by a distance, d , along the X axis. We can measure the angle from the vertex of the parabola to the feed relative to the axis.

$$d = F \tan \psi_s$$

The amplitude distribution on the reflector will be nearly the same when the feed has been moved slightly and we can ignore any change. The movement will introduce a phase factor in the feed pattern when referenced to the focus.

$$- \beta d \sin \psi \cos \phi_c$$

This assumes that the feed was moved along the negative X axis.

To find the effect of the scanning of the feed, we will restrict our attention to the pattern along $\phi = 0$. The phase error loss becomes

$$\text{PEL} = \frac{\left| \int_0^{2\pi} \int_0^{\psi_0} E(\psi, \phi_c) \tan(\psi/2) e^{j\beta F \cos \phi_c (2 \tan(\psi/2) \sin \theta - \tan \psi_s \sin \psi)} d\psi d\phi_c \right|^2}{\left(\int_0^{2\pi} \int_0^{\psi_0} |E(\psi, \phi_c)| \tan(\psi/2) d\psi d\phi_c \right)^2}$$

The beam peak occurs when this factor is a maximum. The equation can be simplified if there is no dependence on ϕ_c in the feed pattern.

$$\int_0^{2\pi} e^{j u \cos \phi_c} d\phi_c = 2\pi J_0(u)$$

The phase error loss becomes

$$PEL = \frac{\left| \int_0^{\psi_0} E(\psi) \tan(\psi/2) J_0(\beta F (2 \tan(\psi/2) \sin \theta - \tan \psi_s \sin \psi)) d\psi \right|^2}{\left(\int_0^{\psi_0} |E(\psi)| \tan(\psi/2) d\psi \right)^2}$$

The conical beam approximation will be used to obtain approximate results, but, of course, the integral will have to be evaluated numerically. On page 621 is a plot of the secondary pattern of a reflector which has been scanned about two beamwidths by moving the feed. The unscanned pattern has been drawn for comparison. The beamwidth of the feed antenna has been picked to give a minimum sum of the spillover and amplitude taper losses. The unscanned pattern is very similar to the parabolic distribution pattern given on page 559. The gain of the scanned pattern has decreased slightly (0.13 dB) but the beamwidth has not been effected much. The most significant change has occurred in the sidelobes. The level of the sidelobe toward the axis of the reflector has increased by 8.3 dB while the first sidelobe away from the axis has become a vestigial lobe. These are called coma lobes. They are not new sidelobes but merely have become unequal. Coma is one of the standard optical aberrations and is due to a cubic phase error term in the aperture.

As the beam is scanned even further, the pattern becomes more distorted. On page 622 is a plot of the secondary pattern which has been scanned about 4.76 beamwidths. The first sidelobe away from the axis has merged into the main beam and the sidelobe level has increased to 13.5 dB. Notice the amplitude at zero. The loss is 38 dB which is the value that is given by the standard phase error loss formula on page 592. Even the curve on page 621 has 24 dB phase error loss for the scanned beam. These patterns explain the curve on 600. The phase error loss increases rapidly as the first null is approached when the beam is scanned by the feed position and there will be a cycling through the sidelobes as shown on page 600, 621, and 622. The true loss of the feed scanned antenna is 0.81 dB.

BEAM DEVIATION FACTOR

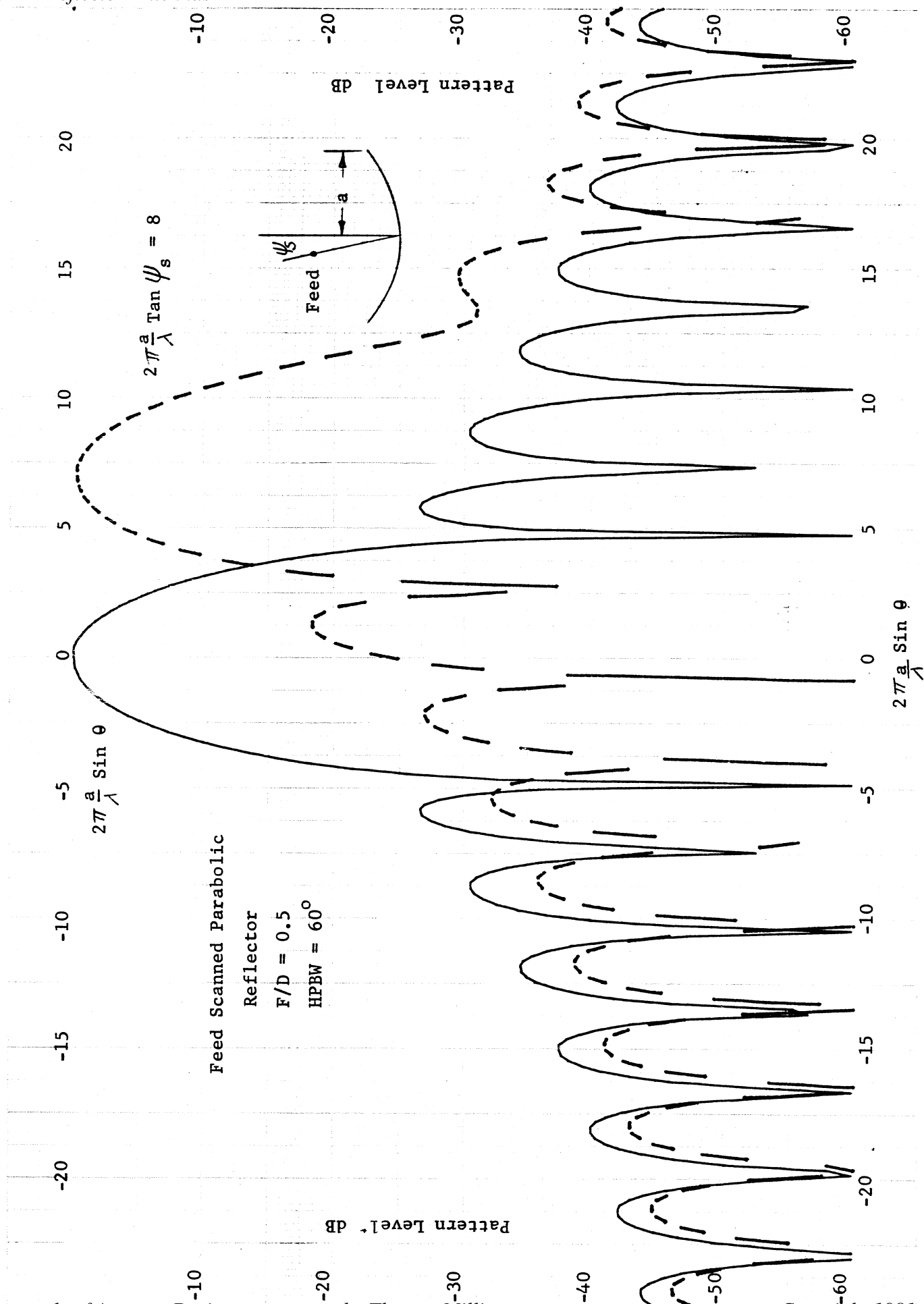
Since we are dealing with a large aperture antenna, the beamwidth will be small and we can make the following approximations.

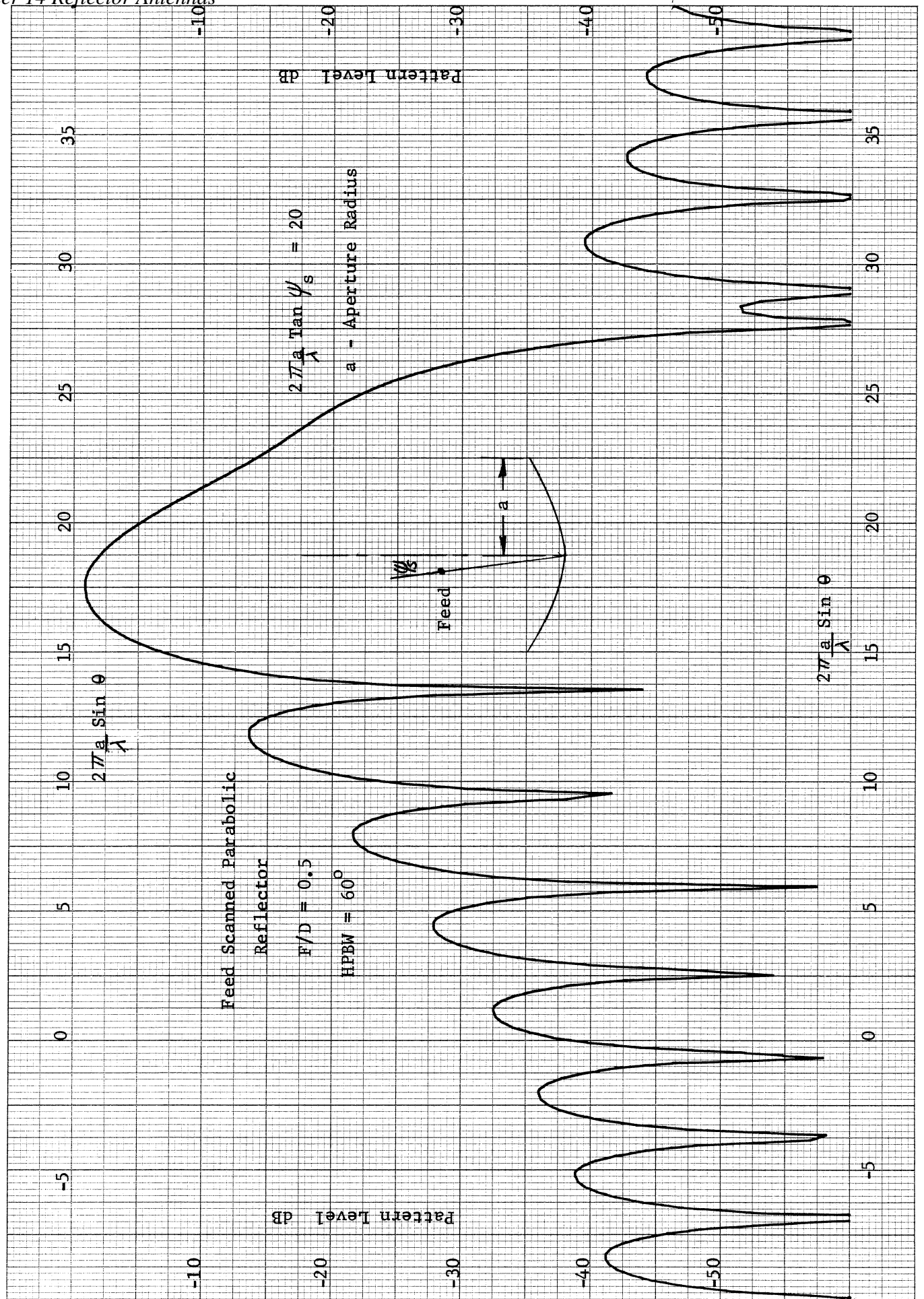
$$\psi_s \cong \tan \psi_s \quad \text{and} \quad \theta \cong \sin \theta$$

The pattern scale becomes: $2\pi \frac{a}{\lambda} \theta$

and the offset phase factor becomes: $2\pi \frac{a}{\lambda} \psi_s$

On the plot on page 621 the offset phase factor, $2\pi \frac{a}{\lambda} \tan \psi_s$, is 8 and the beam peak, $2\pi \frac{a}{\lambda} \sin \theta_m$, is at 7. If we use the approximations, then the ratio of





the offset angle to the maximum beam angle becomes

$$\theta_m / \psi_s = 7/8$$

This ratio is called the beam deviation factor and is a measure of the incremental change of the beam direction with respect to the feed angle relative to the vertex.

$$\theta_m = \text{BDF } \psi_s$$

If we had a flat reflector, then the beam deviation factor would be one: angle of reflection equals angle of incidence. For a concave reflector $\text{BDF} < 1$ and for a convex reflector $\text{BDF} > 1$. On page 624 is a plot of the beam deviation factor versus the F/D of a parabola. The curve has a slight dependence on the beamwidth of the feed. This curve is for about a 10 dB feed taper. If the feed taper is increased, it is equivalent to increasing F/D since the outer portion of the dish will have a less effect. The beam deviation factor will be greater for more feed taper.

The peak of the beam will decrease as it is scanned. On page 625 is a plot of the scanning loss in terms of the beamwidths of scan for various F/D . From this we can see that reflectors with larger F/D can be scanned further for the same loss.

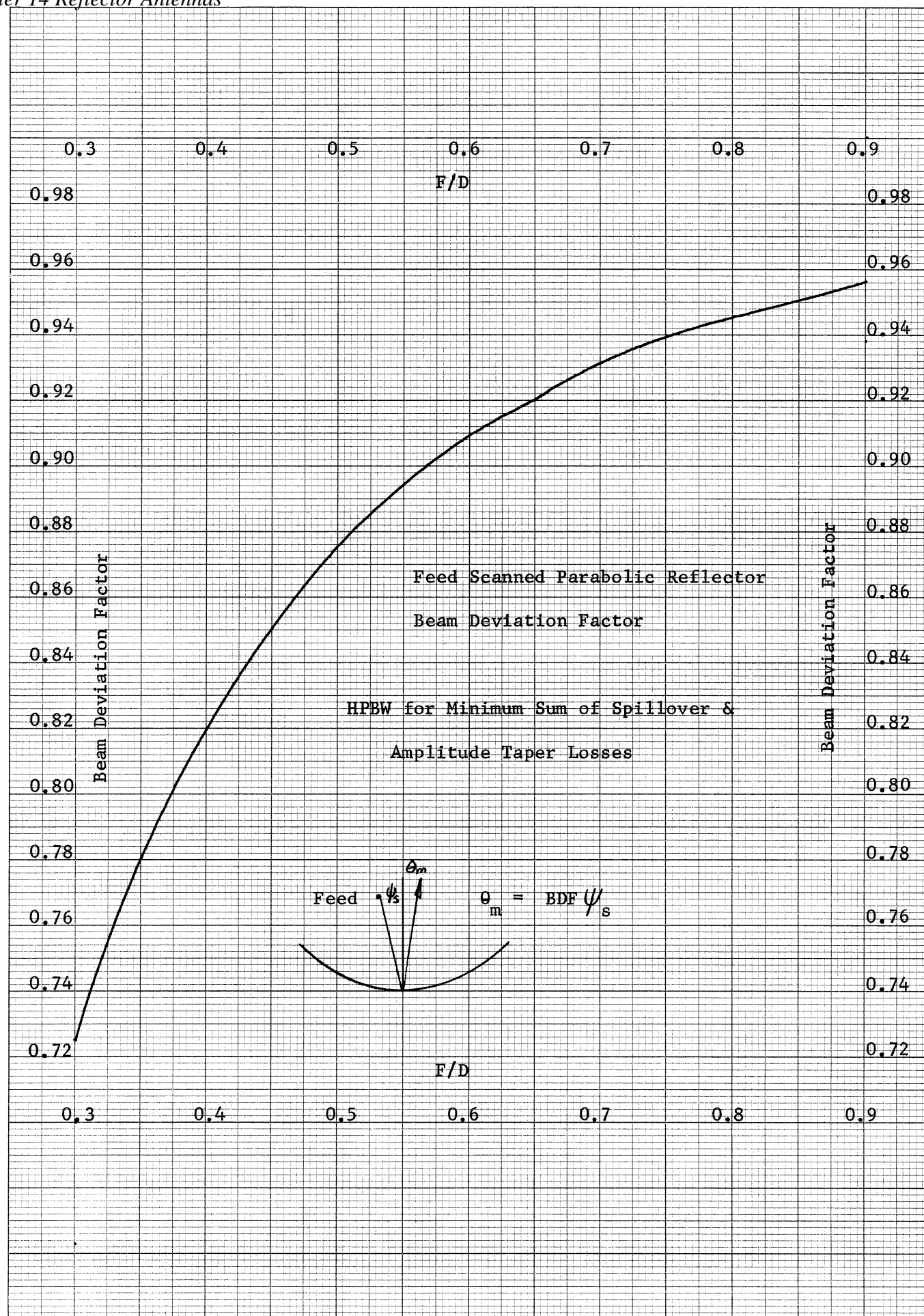
For an example let us look at the pattern for a scanned reflector with $F/D = 0.5$ that has 3 dB of scanning loss. On page 626 is this plot. If we compare this pattern with the one on page 622 for 4.76 beamwidths of scan, we can see that the main beam pattern has broadened some more, but it has the same general shape. The pattern on page 626 is scanned 9.5 beamwidths. The sidelobe level continues to rise and is now only 8.5 dB. The pattern shape is quite degraded.

On page 627 is a plot of the sidelobe level of a feed scanned parabolic reflector versus the beamwidths of scan. The sidelobes rise with increased scanning. Like the scanning loss, the sidelobe level changes the least for high values of F/D . The initial sidelobe level is dependent on the aperture distribution, but it will increase as the antenna is feed scanned.

AXIAL DEFOCUSING

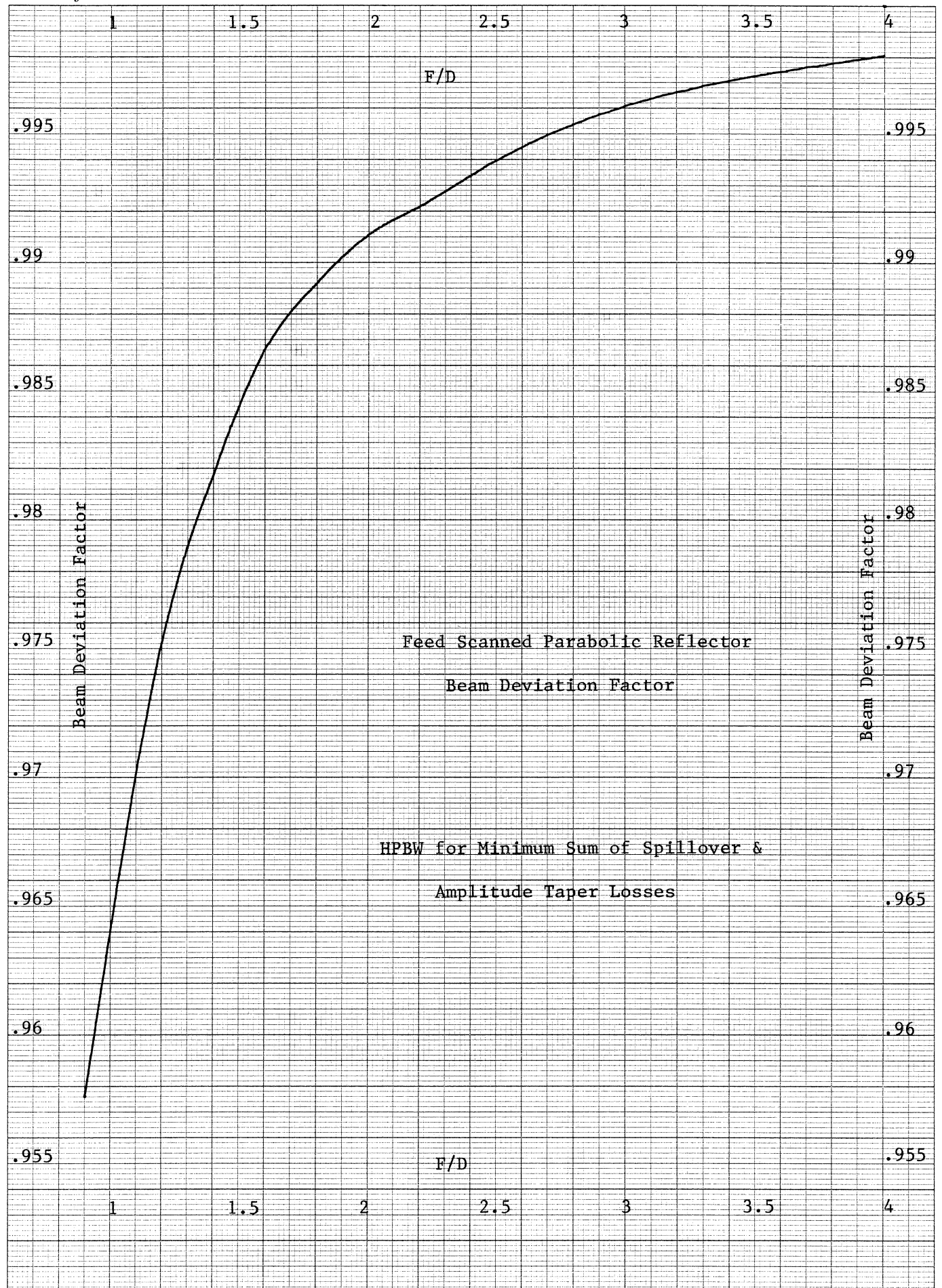
By using the alternate gain calculation method and the generalized phase error loss derived for any scan angle, we found that the losses given on page 600 for lateral offset were not representative of the real loss because the beam had been scanned and the plot is for boresight phase error loss. Is the plot on page 599 for the axial defocusing representative or has the peak of the beam moved off boresight? On page 628 is a plot of the secondary pattern of the reflector when there is axial defocusing of the feed. The patterns are symmetrical about boresight which would be expected, but it appears that the losses are real. For large offsets the beam starts to bifurcate but the loss is still on the order of 10 dB. Axial defocusing shows in the lack of deep nulls between sidelobes.

46 1320

K&E 10 X 10 TO 1/2 INCH 7 X 10 INCHES
KEUFFEL & ESSER CO. MADE IN U.S.A.

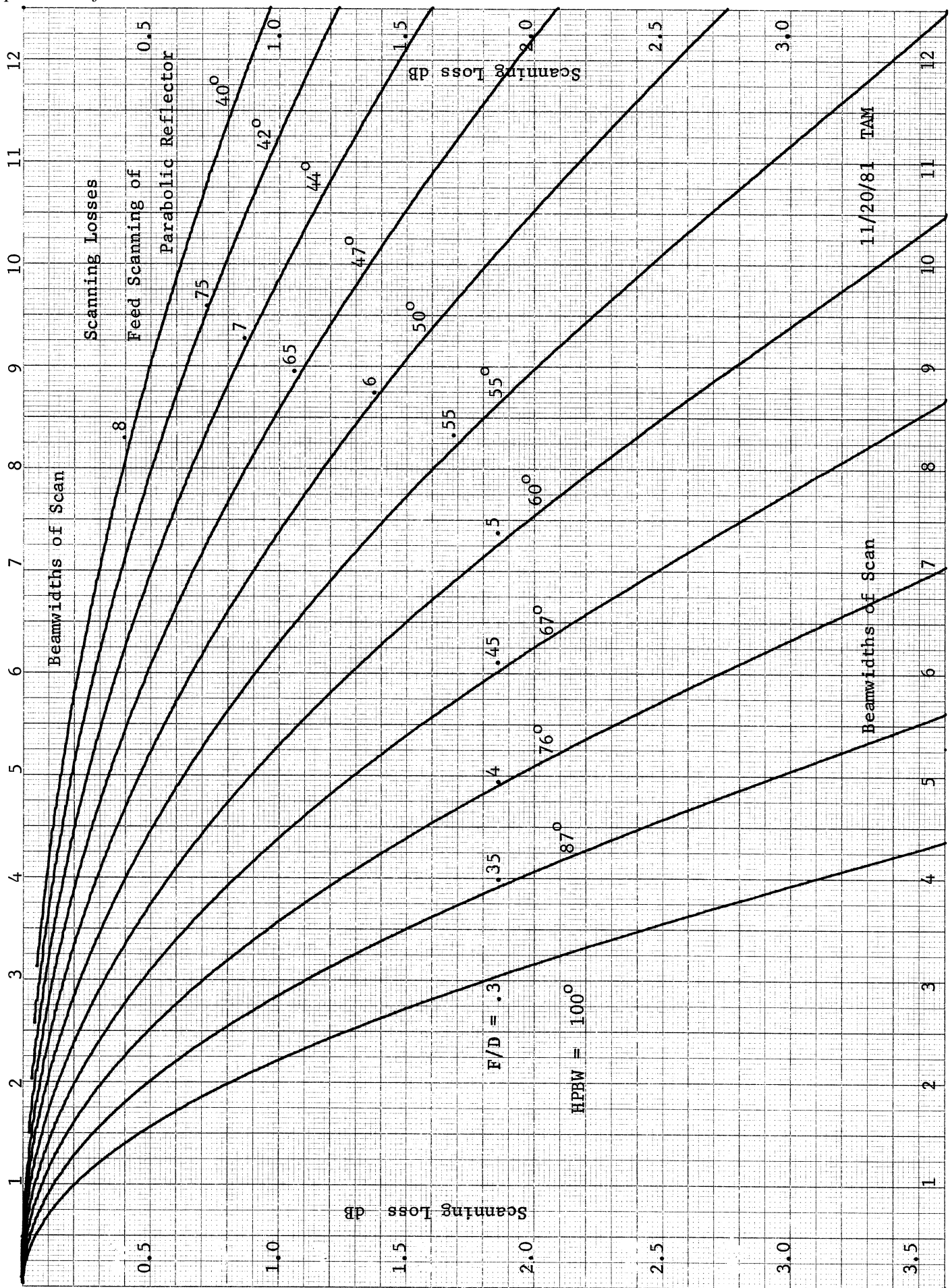
46 1510

10 X 10 TO THE CENTIMETER 18 X 25 CM.
KEUFFEL & ESSER CO. MADE IN U.S.A.



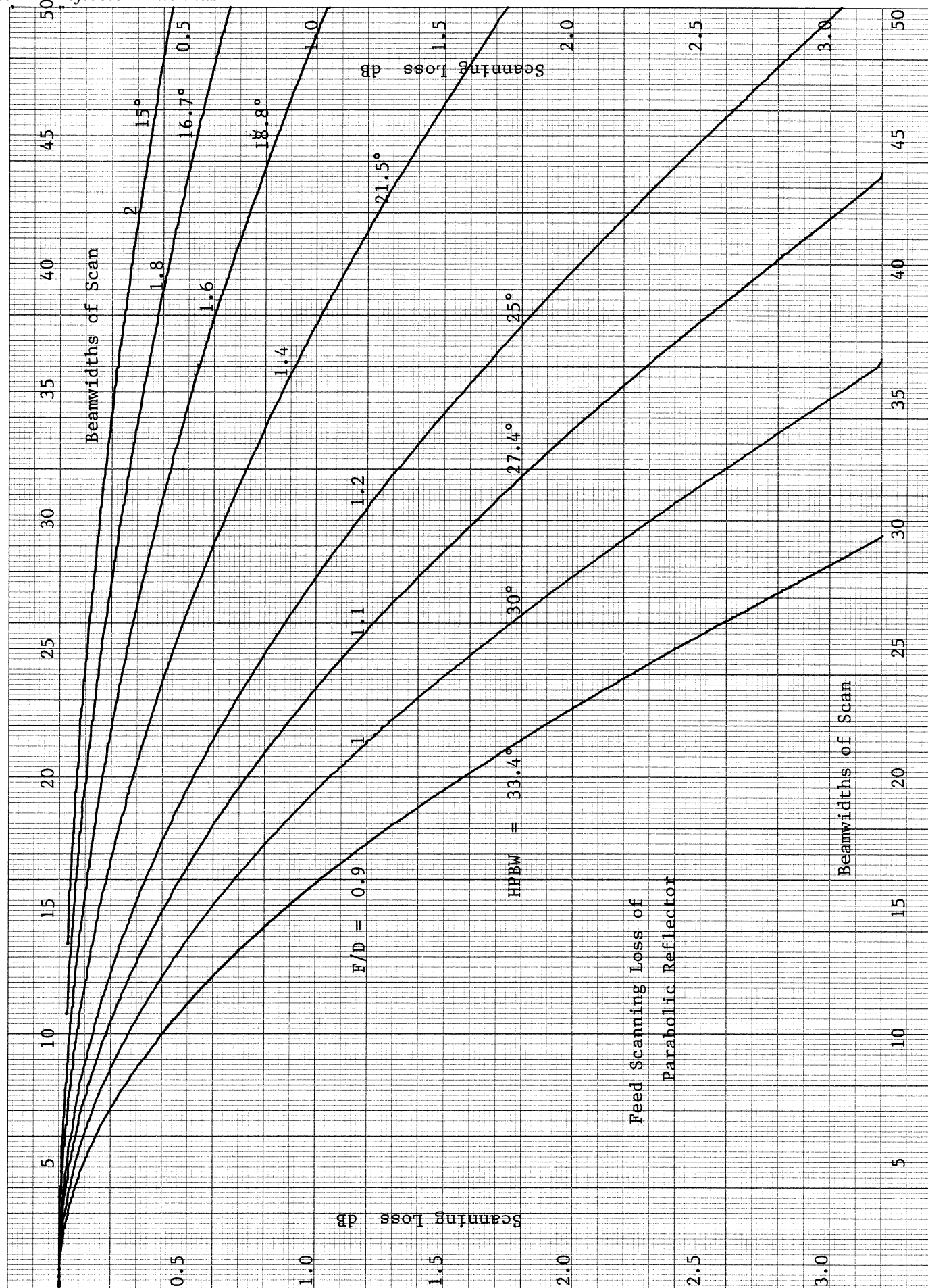
461510

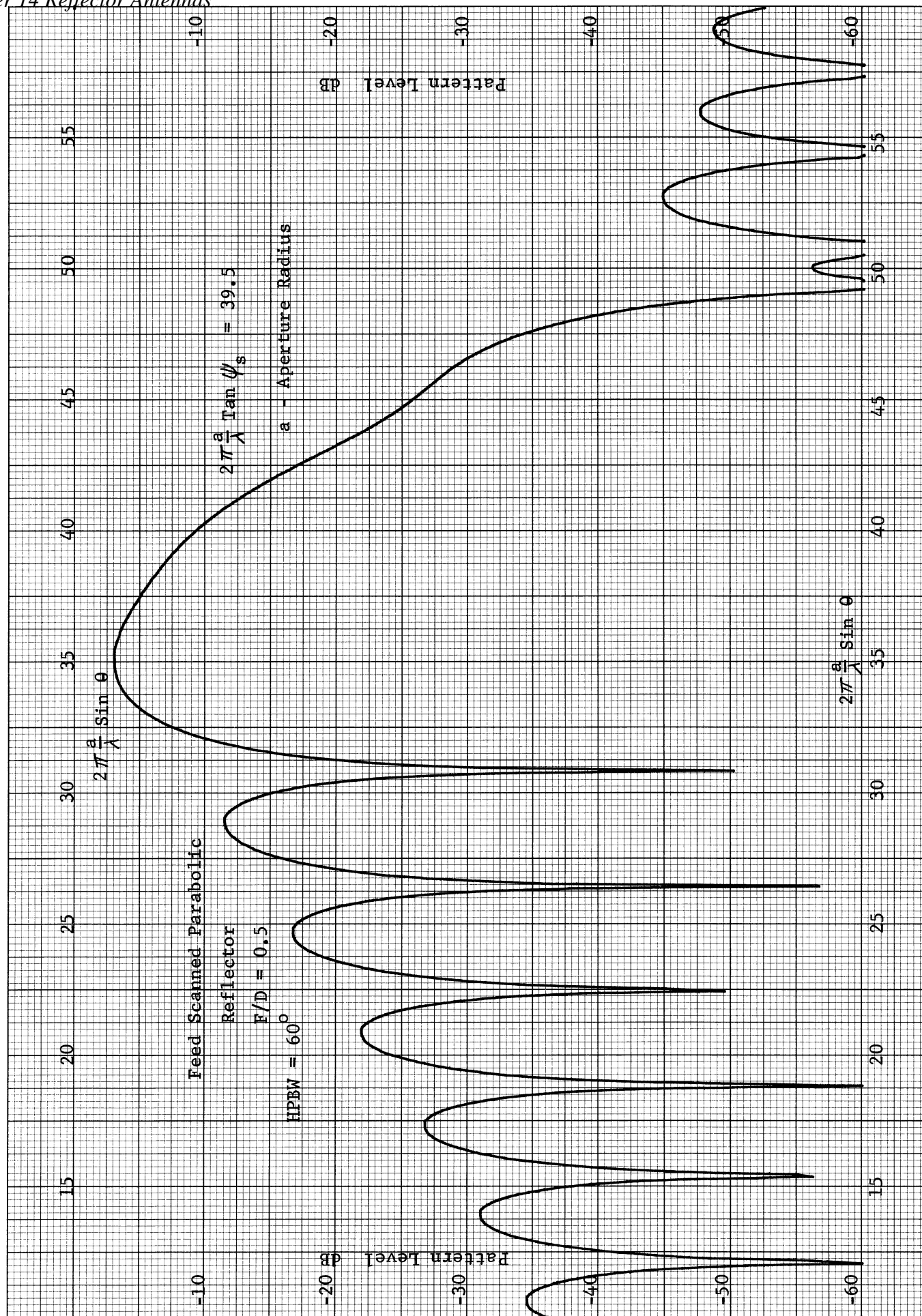
K&E 10 X 10 TO THE CENTIMETER 18 X 25 CM.
KEUFFEL & ESSER CO. MADE IN U.S.A.



46 1510

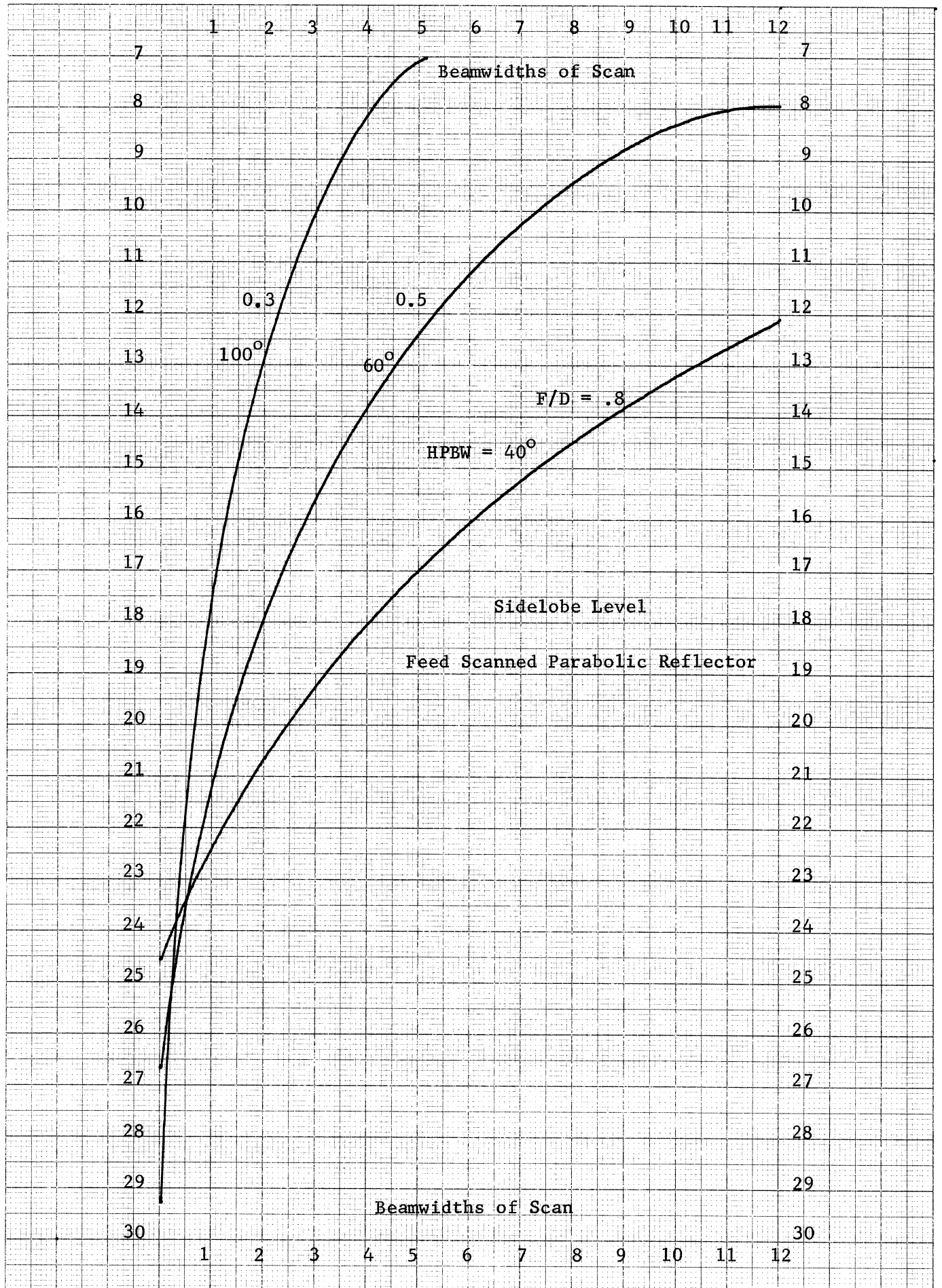
K&E 10 X 10 TO THE CENTIMETER 18 X 25 CM.
KEUFFEL & ESSER CO. MADE IN U.S.A.

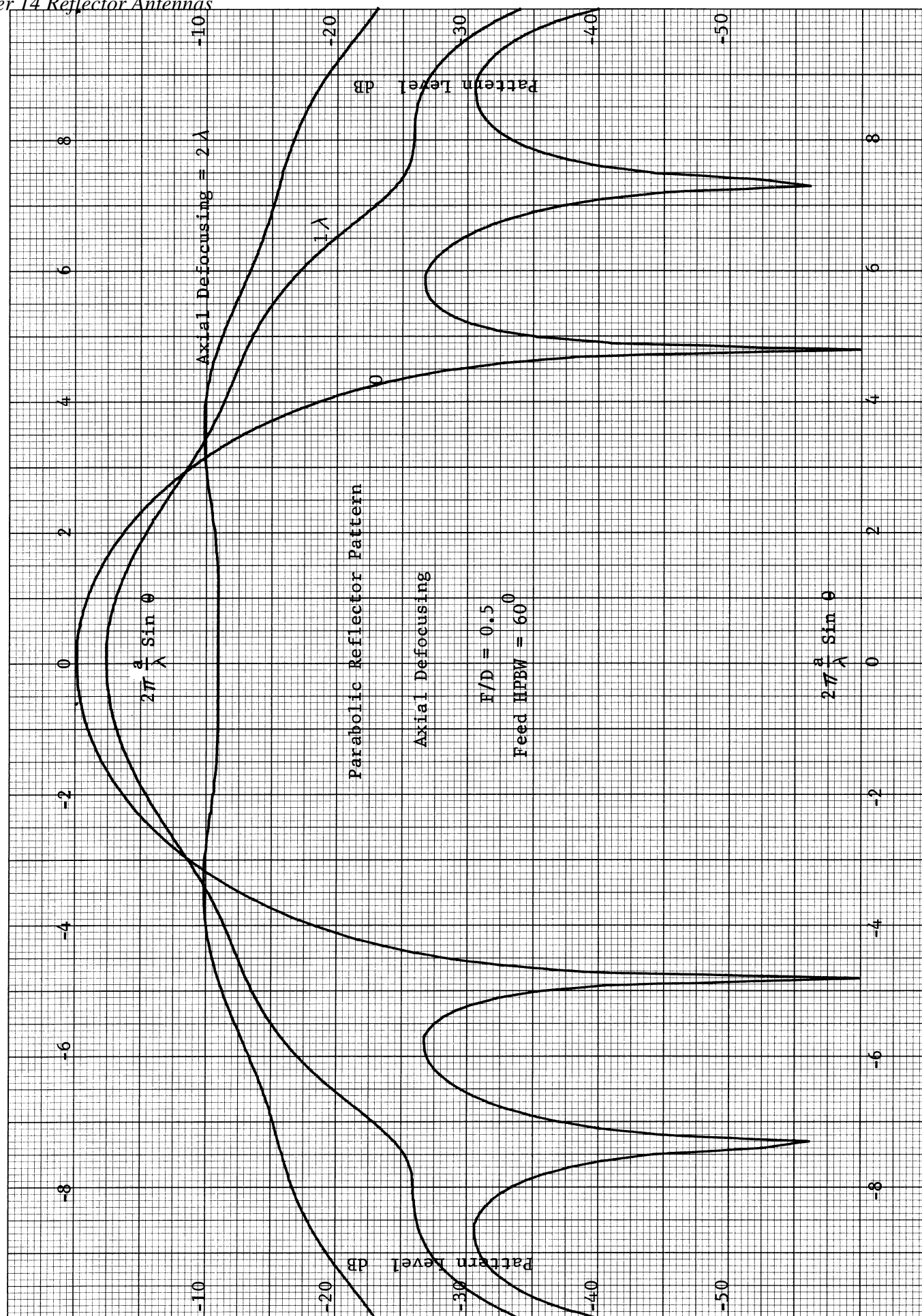




46 1510

10 X 10 TO THE CENTIMETER
KEUFFEL & ESSER CO. MADE IN U.S.A.





PHYSICAL OPTICS

Another method of finding the far field is to obtain the currents induced on the reflector by the feed antenna radiation and using the magnetic vector potential to find the fields. If we could find the exact currents on the reflector, then the exact solution could be found. We could find various approximations by expanding in a Fourier series using plane wave or spherical wave eigenvalue solutions to the boundary value problem. This would involve infinite series which would be truncated to a few terms for evaluations. We will take an even simpler approach. Geometric optics (ray tracing) will be used to find the fields at the surface of the reflector. The fields will induce currents on the surface. Using these currents, the far field will be found through the magnetic vector potential.

Consider a plane wave incident on a flat conductor. From the boundary conditions given on page 153, we know that the fields inside the conductor are zero and that the tangential electric field is continuous across the boundary. The tangential electric field at the boundary must be zero. The electric field can be zero only if there is a reflected wave 180° out of phase with respect to the incident wave at the boundary. Suppose the incident wave is polarized in the X direction; H is the Y direction, for a wave traveling in the Z direction. The reflected wave will be in the negative Z direction with the electric field in the negative X direction at the surface. For a wave traveling in the negative Z direction with the electric field in the negative X direction, the magnetic field, H, will be in the positive Y direction. The field at the surface of the conductor is the sum of the two waves with the electric field zero but the magnetic field double the amplitude of the incident wave. From the boundary conditions given on page 154, we find the surface current induced on the conductor.

$$\bar{K}_s = \bar{n} \times 2\bar{H}_i$$

\bar{H}_i is the incident wave magnetic field and \bar{n} is the unit normal of the reflector.

The parabolic reflector is not a flat reflector, but if the radius of curvature is much larger than a wavelength, then the surface currents will be approximately the same as for a flat reflector. This is the first term of an asymptotic expansion. We do not have to assume that the reflector is parabolic; it can be any shape which has large radii of curvature relative to a wavelength. The physical optics approximation can be used for any reflector shape. We have assumed that locally a wave is reflected from a surface as it were a flat plate conductor.

The reflector is in the far field of the feed antenna. Since we assume that it is the far field of the feed, the magnetic field can be found in terms of the electric field.

$$\bar{H}_i = \frac{1}{\eta} \bar{S}_1 \times \bar{E}_i$$

\bar{S}_1 is the incident ray direction and η is the impedance of free space. The surface current can be found in terms of the incident electric field by using this assumption that the reflector is in the far field of the feed and the above equation for the surface current in terms of the magnetic field.

$$\bar{K}_s = \frac{2}{\eta} (\bar{n} \times (\bar{S}_1 \times \bar{E}_i))$$

Similarly, the surface current can be found in terms of the reflected wave electric field, \bar{E}_r , and the reflector wave ray direction, S_2 .

$$\bar{K}_s = \frac{2}{\eta} (\bar{n} \times (\bar{S}_2 \times \bar{E}_r))$$

There will also be a surface charge induced on the reflector surface for waves at oblique incidence.

$$\sigma_s = 2 \epsilon (\bar{n} \cdot \bar{E}_i) = 2 \epsilon (\bar{n} \cdot \bar{E}_r)$$

Since this charge does not radiate in the far field, we will not be concerned with it.

Given the surface current, we can find the magnetic vector potential. (pp. 122)

$$\bar{A} = \iint_S \frac{\bar{K}_s e^{-jk|\bar{r} - \bar{r}'|}}{4\pi|\bar{r} - \bar{r}'|} dS$$

The far field is found from the vector potential (pp. 124).

$$\bar{E} = -j\omega\mu\bar{A}$$

The aperture field method is restricted to analyzing reflectors which focus the wave from the feed, whereas, the physical optics approximation can be used with shaped reflectors.

The gain pattern of the feed antenna is found from a formula similar to directivity.

$$G_f(\psi, \phi) = \frac{4\pi P(\psi, \phi)}{P_T}$$

P_T is the total input power and $P(\psi, \phi)$ is the power pattern per unit solid angle (radiation intensity). The power pattern is related to the electric field on a unit sphere.

$$P(\psi, \phi) = \frac{|\bar{E}(\psi, \phi)|^2}{\eta}$$

Using the two formulas above, we can find the electric field on a unit sphere from the feed antenna.

$$|\bar{E}_f(\psi, \phi)| = \left[\frac{P_T \eta}{4\pi} G_f(\psi, \phi) \right]^{1/2}$$

If we include polarization, then the electric field becomes

$$\bar{E}_f(\psi, \phi) = \left[\frac{P_T \eta}{4\pi} \right]^{1/2} \left[\sqrt{G_\psi(\psi, \phi)} \bar{\Phi}_\psi \bar{a}_\psi + \sqrt{G_\phi(\psi, \phi)} \bar{\Phi}_\phi \bar{a}_\phi \right]$$

$\bar{\Phi}_\psi$ and $\bar{\Phi}_\phi$ are the normalized phased factors of the two polarizations, and G_ψ and G_ϕ are the gains to the two far field polarization components.

Suppose we have a parabolic reflector, then the electric field at the surface of the reflector is given by

$$E_f(\psi, \phi) = \frac{e^{-jk\rho}}{\rho} \left[\frac{P_T \eta}{4\pi} \right]^{\frac{1}{2}} \left[\sqrt{G_\psi(\psi, \phi)} \Phi_\psi \bar{a}_\psi + \sqrt{G_\phi(\psi, \phi)} \Phi_\phi \bar{a}_\phi \right]$$

The incident wave vector for a feed at the focus is \bar{a}_ρ and the unit normal to the reflector is found on page 587. Using these we can find the surface currents.

$$\bar{K}_s = \frac{2}{\eta} (\bar{a}_\rho \sin \psi/2 E_\psi + \bar{a}_\psi \cos \psi/2 E_\psi + \bar{a}_\phi \cos \psi/2 E_\phi)$$

E_ψ and E_ϕ are given by the following expressions.

$$E_\psi = \frac{e^{-jk\rho}}{\rho} \left[\frac{P_T \eta}{4\pi} G_\psi(\psi, \phi) \right]^{\frac{1}{2}} \Phi_\psi(\psi, \phi) \quad E_\phi = \frac{e^{-jk\rho}}{\rho} \left[\frac{P_T \eta}{4\pi} G_\phi(\psi, \phi) \right]^{\frac{1}{2}} \Phi_\phi(\psi, \phi)$$

The phase of the feed radiation will be a function of the feed angles and polarization as shown. The surface currents are given in terms of the feed pattern unit vectors (ρ, ψ, ϕ) and cannot be integrated because they change direction with location on the reflector surface. These must be changed to an invariant coordinate vector system such as rectangular. The X axis will occur when $\phi = 0$. The following scalar products relate the two coordinate systems. Note that the Z axis of the feed coordinate system is the negative Z axis of the secondary pattern of the reflector.

$$\begin{array}{lll} \bar{a}_\rho \cdot \bar{a}_x = \sin \psi \cos \phi & \bar{a}_\psi \cdot \bar{a}_x = \cos \psi \cos \phi & \bar{a}_\phi \cdot \bar{a}_x = -\sin \phi \\ \bar{a}_\rho \cdot \bar{a}_y = -\sin \psi \sin \phi & \bar{a}_\psi \cdot \bar{a}_y = -\cos \psi \sin \phi & \bar{a}_\phi \cdot \bar{a}_y = -\cos \phi \\ \bar{a}_\rho \cdot \bar{a}_z = -\cos \psi & \bar{a}_\psi \cdot \bar{a}_z = \sin \psi & \bar{a}_\phi \cdot \bar{a}_z = 0 \end{array}$$

The (X, Y, Z) coordinate system is with respect to the secondary pattern coordinates. If we substitute these relationships into the above equation for the surface current, after some manipulation, we get the currents in terms of the feed pattern in rectangular coordinates.

$$\bar{K}_s = \frac{2}{\eta} (\cos \psi/2 (\bar{a}_x (\cos \phi E_\psi - \sin \phi E_\phi) - \bar{a}_y (\sin \phi E_\psi + \cos \phi E_\phi)) + \bar{a}_z E_\psi \sin \psi/2)$$

If we restrict our attention to small patterns angles, then we can project this current on to the aperture plane. The phase of the current on the aperture plane will then only be a function of the feed pattern. When θ is small, then E_θ due to the Z component of the current will be small and can be ignored. This is the same as the null portion of the dipole pattern.

We will now look at particular feed antennas and their corresponding surface currents and fields in the aperture plane. By proceeding with this analysis we will obtain the cross polarization lobes of the parabolic reflector which have become called Condon lobes after their discoverer.

SHORT DIPOLE FEED

If the feed is a short dipole at the focus in the X direction, then the field at the reflector can be found from the magnetic vector potential.

$$\bar{A} = \frac{Il}{4\pi r} e^{-jkr} \bar{a}_X$$

$$\bar{E} = -j\omega\mu\bar{A} = \frac{-j\omega\mu Il}{4\pi r} e^{-jkr} \bar{a}_X$$

$$E_\psi = \frac{-j\omega\mu Il}{4\pi r} e^{-jkr} \cos\psi \cos\phi$$

$$E_\phi = \frac{j\omega\mu Il}{4\pi r} e^{-jkr} \sin\phi$$

We can use the formula on page 631 to find the surface currents on the reflector.

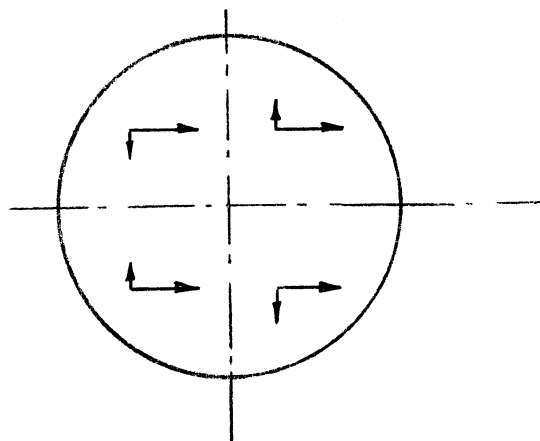
$$\begin{aligned} \bar{K}_s = \frac{-j\omega\mu Il}{4\pi r} \frac{2}{\eta} e^{-jkr} \cos\psi/2 & (\bar{a}_X (\cos\psi \cos^2\phi + \sin^2\phi) \\ & + \bar{a}_Y \sin\phi \cos\phi (1 - \cos\psi)) \end{aligned}$$

We can project this current into an aperture electric field which will remove the phase factor,

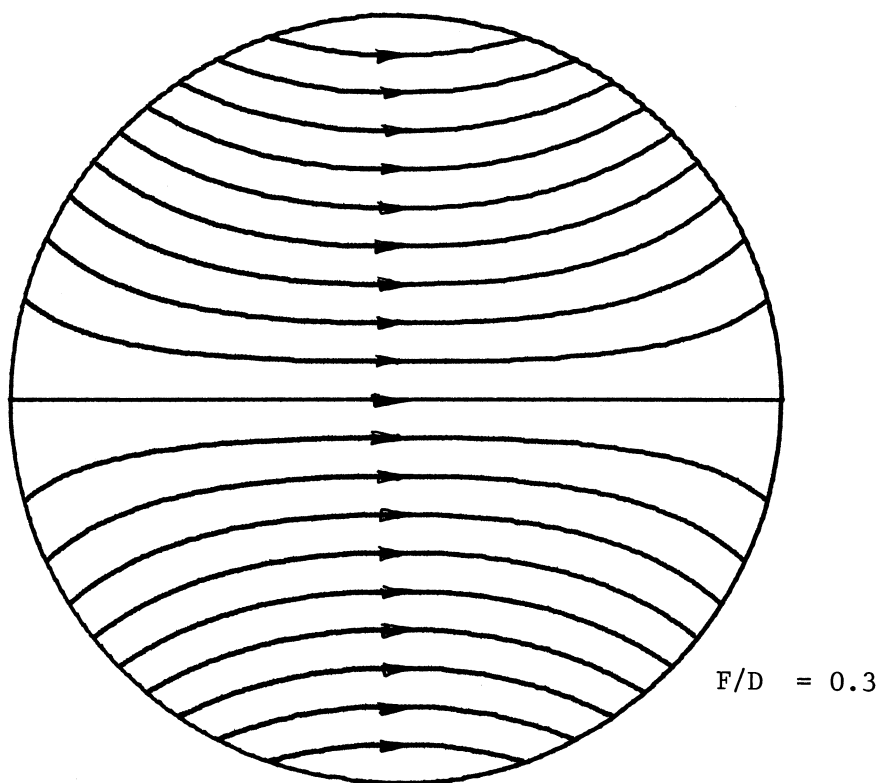
$$\bar{E}_a = - \frac{\bar{K}_s \eta}{2 \cos\psi/2}$$

$$\bar{E}_a = \frac{j\omega\mu Il}{4\pi r} (\bar{a}_X (\cos\psi \cos^2\phi + \sin^2\phi) + \bar{a}_Y \sin\phi \cos\phi (1 - \cos\psi))$$

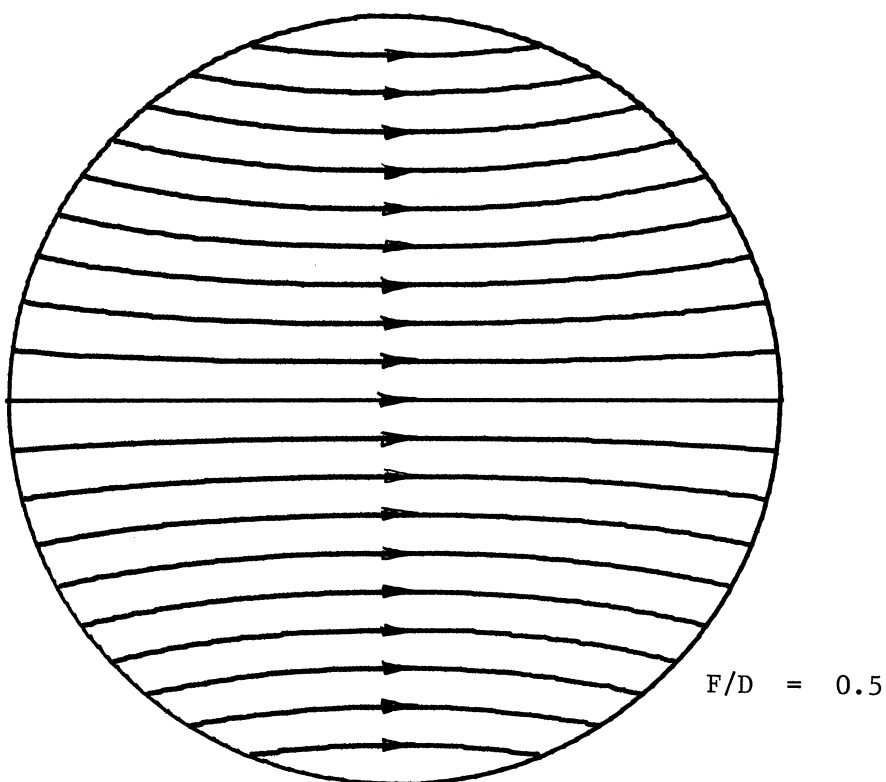
The aperture field for a short dipole has been drawn on page 633 for F/D of 0.3 and 0.50. Notice that fields have a Y component when the point is removed from the E and H plane axes of the aperture. These Y directed components will give cross polarized lobes in the secondary pattern. Second, notice that the reflector with an F/D of 0.3 has greater Y components. Deeper dishes (smaller F/D) will give higher cross polarization lobes (Condon lobes). The fields in the aperture plane are given schematically below.



Aperture Fields with Short Dipole Feed



Parabolic Reflector



If we consider the pattern along the E plane or the H plane, we can see that the Y component is exactly cancelled at the same location on the aperture about the line of symmetry in these two planes. There is no cross polarization component in these two planes from the short electric dipole. In the plane which is 45° with respect to the E plane or H plane, the cross polarization components are in the odd mode and will give a difference pattern in the far field. We will find the maximum cross polarization lobes in this plane which is defined by $\phi = 45^\circ$.

SHORT MAGNETIC DIPOLE FEED

We will align the magnetic dipole with the Y axis so that it will also give a field in the aperture which is aligned with the X axis. The field can be found from the electric vector potential.

$$\bar{F} = \frac{Ml}{4\pi r} e^{-jkr} \bar{a}_y$$

$$\bar{H} = -j\omega\epsilon\bar{F} = -j\omega\epsilon\frac{Ml}{4\pi r} e^{-jkr} \bar{a}_y$$

$$H_\psi = -j\omega\epsilon\frac{Ml}{4\pi r} e^{-jkr} \cos\psi \sin\phi \quad H_\phi = -j\omega\epsilon\frac{Ml}{4\pi r} e^{-jkr} \cos\phi$$

The far field electric field is found from the magnetic field by assuming spherical waves.

$$E_\psi = \eta H_\phi \quad E_\phi = -\eta H_\psi$$

$$E_\psi = -j\omega\epsilon\eta\frac{Ml}{4\pi r} e^{-jkr} \cos\phi \quad E_\phi = j\omega\epsilon\frac{Ml}{4\pi r} e^{-jkr} \cos\psi \sin\phi$$

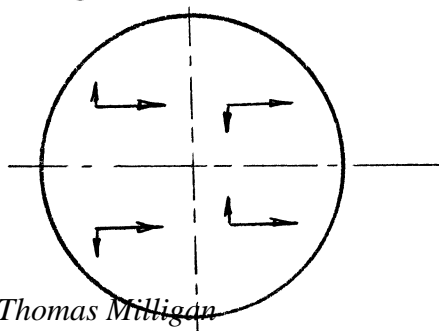
We can find the surface currents from the equation on page 631.

$$\bar{K}_s = -j\omega\epsilon\frac{2Ml}{4\pi p} e^{-jkr} \cos\psi/2 (\bar{a}_x (\cos^2\phi + \cos\psi \sin^2\phi) - \bar{a}_y \sin\phi \cos\phi (1 - \cos\psi))$$

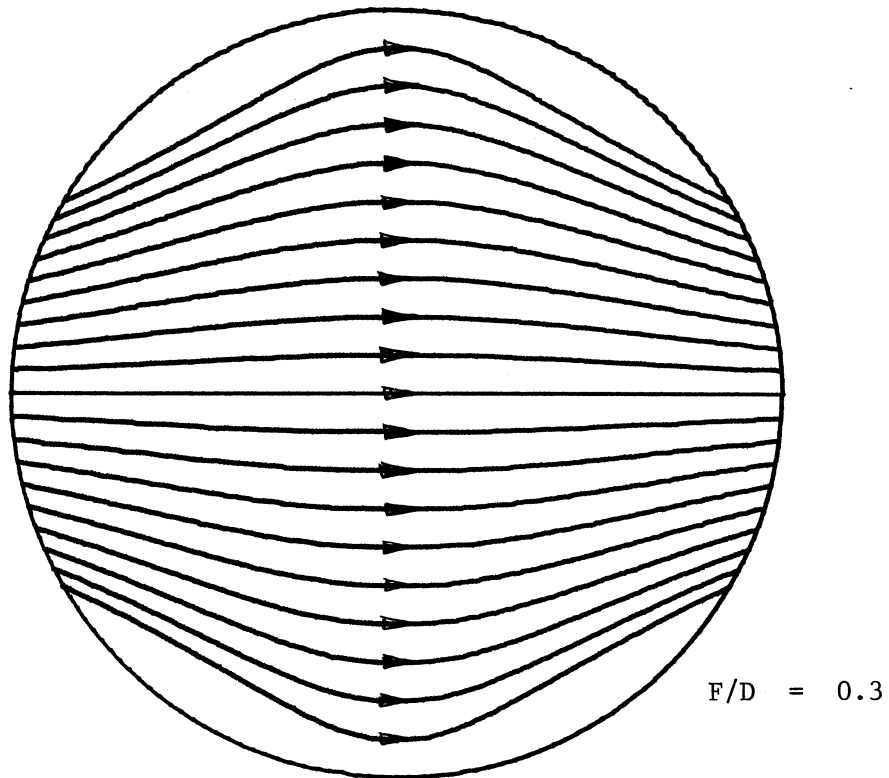
This surface current can be projected on to the aperture plane as before.

$$\bar{E}_a = \frac{j\omega\epsilon\eta Ml}{4\pi p} (\bar{a}_x (\cos^2\phi + \cos\psi \sin^2\phi) - \bar{a}_y \sin\phi \cos\phi (1 - \cos\psi))$$

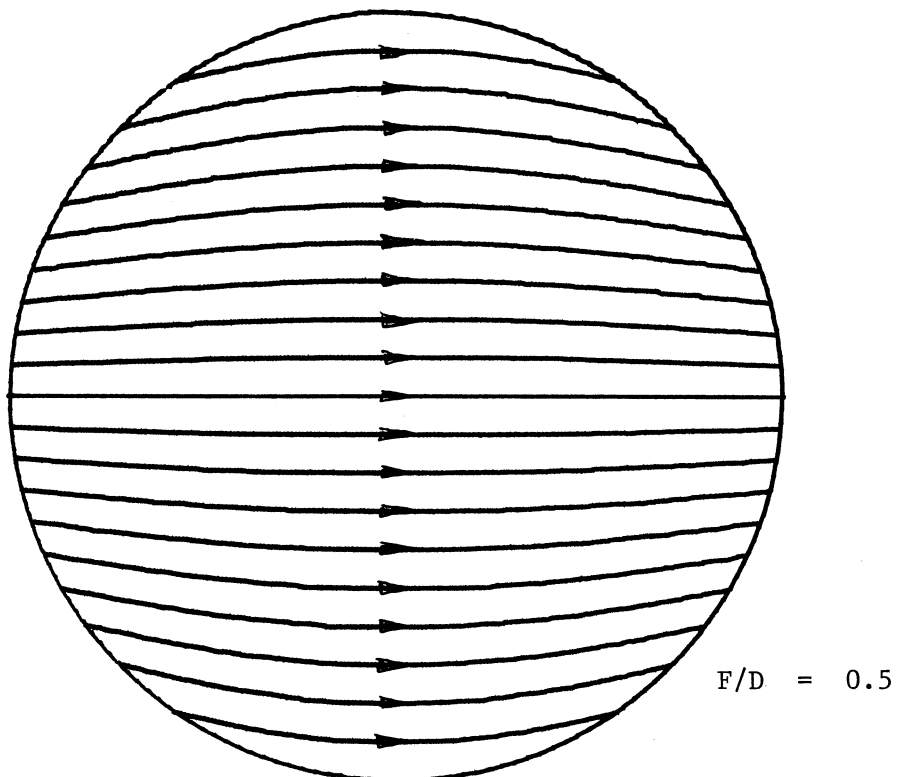
The distribution of the electric field in the aperture is drawn on page 635. Like the short electric dipole distribution, the electric field in the aperture due to a short magnetic dipole has curvature and a Y component when off the E or H plane axes of the aperture. Second, the deeper dishes have greater curvature than shallow dishes and will have higher cross polarization lobes for this feed. A simplified diagram of the fields is given below.



Aperture Fields with Short Magnetic Dipole Feed



Parabolic Reflector



Like the aperture pattern of the short electric dipole, the patterns along the E plane or H plane have cancelling Y components of the field at the same location across the lines of symmetry. There is no cross polarization component in either the E or H planes of the secondary pattern. In the 45° plane there will be a difference pattern which is also called the Condon lobes.

HUYGENS SOURCE FEED

The Huygens source is the combination of an electric and magnetic sources which are in the same ratio as a plane wave.

$$M = \eta I$$

We can combine the formulas for the two types of sources given above and we get the following aperture field.

$$\bar{E}_a = \frac{j\omega\mu I l}{4\pi\rho} \bar{a}_x (1 + \cos\psi)$$

In this aperture field there is no Y component and the far field will not have cross polarization lobes. A Huygens source such as a horn will give a secondary pattern without Condon lobes. Of course, a horn will not be a perfect Huygens source and there will still be some cross polarization in the secondary pattern.

FEED POLARIZATION

A feed which is a linearly polarized Huygens aperture feed will give a secondary pattern without Condon lobes (cross polarization). An aperture which is polarized in the X direction has a far field which is given by the following components.

$$E_\theta = E_c \cos \phi \quad E_\phi = -E_c \sin \phi$$

We can define the cross polarization component to be due to an aperture field in the Y direction.

$$E_\theta = E_x \sin \phi \quad E_\phi = E_x \cos \phi$$

E_c is the co-polarized component and E_x is the cross polarized component.

We are ignoring the factor $\cos \theta$ which is due to an obliquity factor of the flat aperture. The components which are measured on the feed antenna are E_θ and E_ϕ . We can solve the above equations for the co-polarization and cross polarization components from the measurements.

$$\begin{bmatrix} E_\theta \\ E_\phi \end{bmatrix} = \begin{bmatrix} \cos \phi & -\sin \phi \\ -\sin \phi & \cos \phi \end{bmatrix} \begin{bmatrix} E_c \\ E_x \end{bmatrix}$$

$$\begin{bmatrix} E_c \\ E_x \end{bmatrix} = \begin{bmatrix} \cos \phi & -\sin \phi \\ +\sin \phi & \cos \phi \end{bmatrix} \begin{bmatrix} E_\theta \\ E_\phi \end{bmatrix}$$

This definition of co- and cross polarization for the feed will give secondary patterns which are linearly polarized in each direction. This corresponds to

Ludwig's 3rd definition of polarization. ("The Definition of Cross Polarization", A. C. Ludwig, IEEE Trans. on Antennas and Propagation, January 1973) If we use this definition of polarization for the feed, then we do have to use surface currents to find the secondary cross polarization pattern but can use aperture theory on the parabolic reflector. For a shaped reflector we must still use the surface current method or a ray tracing technique such as GTD.

REFLECTIONS FROM CONIC SECTIONS

We can make reflectors from any of the conic sections. We have already discussed parabolic reflectors, but we can also make reflectors using ellipses or hyperbolae. These can be used with spherical waves when the two dimensional figure has been used to define the reflector by rotating about its axis or with cylindrical waves by moving the two dimensional figure in the Z axis direction to define the surface. The ellipse and hyperbola are useful as subreflectors in a two reflector antennas because they can change the focal point of the spherical waves. Because they do not have a well defined far field, they are not used as primary reflectors.

We need to review the geometry of the conic sections. All these conic sections can be described by the same polar equation.

$$r = \frac{e P}{1 - e \cos \theta}$$

(r, θ) are the polar variable. P is the distance between the origin, which is also the focus, and a line called the directrix; e is the eccentricity.

$e = 0$	Circle
$e < 1$	Ellipse
$e = 1$	Parabola
$e > 1$	Hyperbola

The polar equation becomes undefined when $e = 0$, but we will not consider this case ($r = \text{constant}$). The general curve is defined in the figure on page 638. As drawn this is part of an ellipse. The ratio of the distance, r_1 , from the origin to a point on the curve to the distance from the same point on the curve to the directrix is the eccentricity.

$$r_1 = e r_2$$

The ellipse is a closed figure with two focii. The curve is defined as the sum of the distances from the two focii is equal to a constant which is greater than the distance between the focii. The minimum and maximum distances from the origin are given by

$$R_{\max} = \frac{e P}{1 - e} \quad R_{\min} = \frac{e P}{1 + e}$$

The distance between the focii is the difference, which is named: $2c$.

$$R_{\max} - R_{\min} = 2c = e P \frac{2e}{1 - e^2}$$

The total width of the ellipse is the sum.

$$R_{\max} + R_{\min} = 2a = \frac{2 e P}{1 - e^2}$$

The maximum Y dimension can be found by differentiation of an expression for Y as a function of θ .

$$Y(\theta) = R \sin \theta = \frac{e P \sin \theta}{1 - e \cos \theta}$$

$$\frac{dY}{d\theta} = \frac{e P}{(1 - e \cos \theta)^2} (\cos \theta - e) = 0 \quad \cos \theta_{\max} = e$$

$$Y_{\max} = \frac{e P \sin(\cos^{-1} e)}{1 - e^2}$$

The width the ellipse is given the symbol: $2b = \frac{2 e P \sin(\cos^{-1} e)}{1 - e^2}$

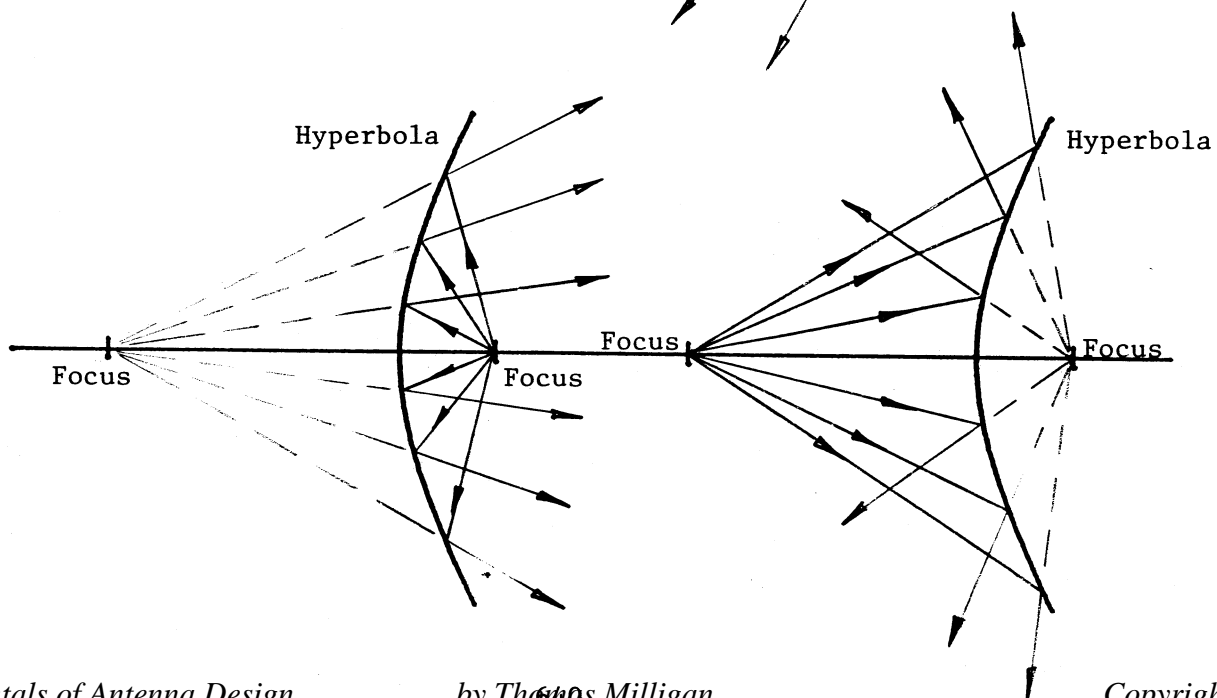
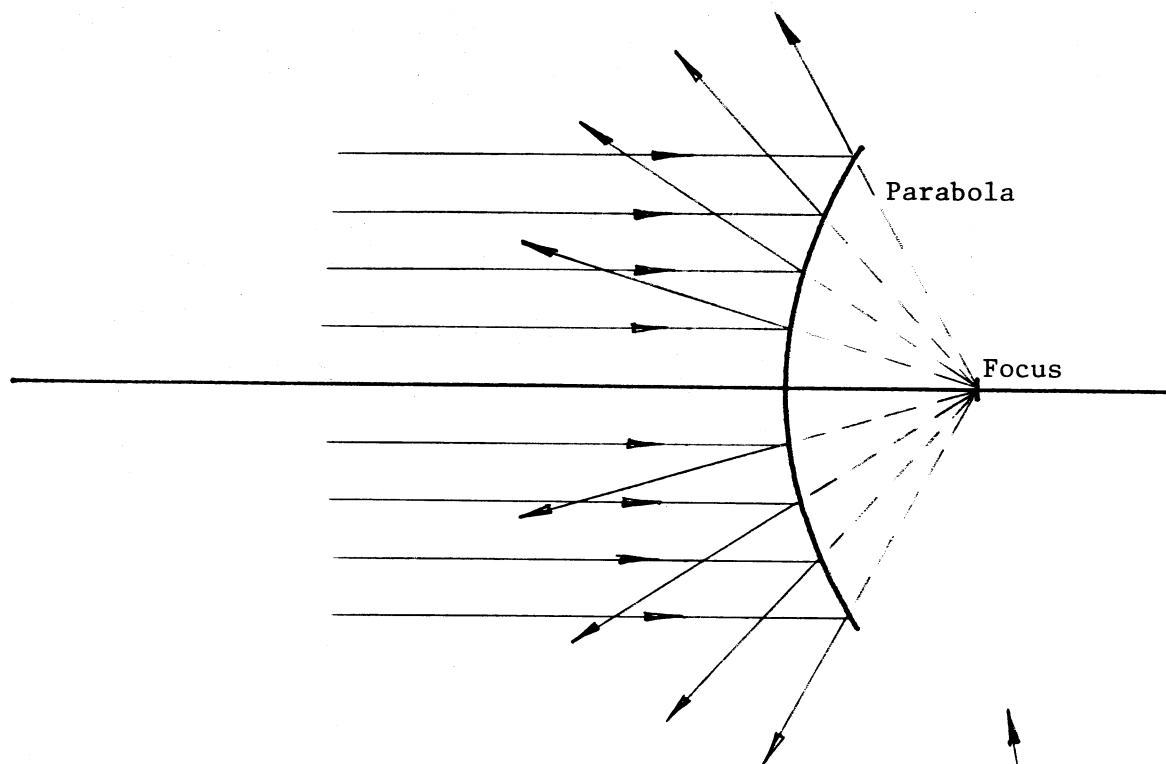
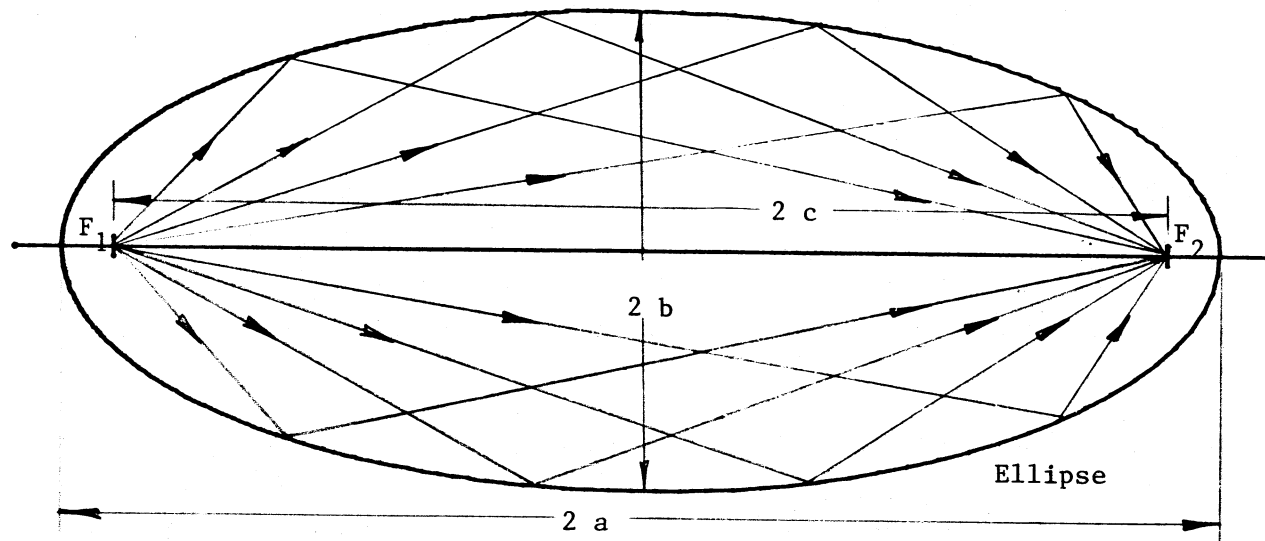
If the ellipse is centered between the two focii, then the equation for the ellipse in rectangular coordinates becomes:

$$\frac{x^2}{a^2} + \frac{y^2}{b^2} = 1 \quad a^2 = b^2 + c^2$$

We will find the polar representation more convenient.

On the top of page 640 is a plot of an ellipse. If we place a source at one of the focii of the ellipse, then the surface will reflect the waves into the other focus as shown. If the source is a spherical wave, then we assume that the figure is an ellipsoid. For cylindrical waves we assume that the figure as been moved along a Z axis out of the paper to define the surface. If we generalize the ellipse into the other conic sections, we will see the same effect. Consider the equation for the distance between the focii. If we take the limit as the eccentricity, e , approaches one, then the distance, $2c$, approaches infinity. The curve becomes a parabola and we can say that a source placed at one focus reflects off the surface to the other focus. Suppose we have a source at infinity on the other side of the parabola as shown in the middle figure of page 640. Since the surface is convex, the reflected wave will diverge. Infinity on the positive X axis is the same point as infinity on the negative X axis. The wave will be reflected into the focus. But since the wave cannot reach the focus, it will become the virtual focus of the wave. The plane wave is converted into a spherical wave with the center at the focus.

The eccentricity, e , of the hyperbola is greater than one. The distance between the focii becomes negative. We could consider the distance between the focii as having grown to infinity as e approached one and then rotates to negative as e becomes greater than one. On the bottom of page 640 are two drawings of one side of the hyperbola. Because the surface separates the two focii, if a source is placed at one focus, the reflection will be a spherical wave with the virtual focus at the other focus. The hyperbola converts a spherical wave from one of its focii to a spherical wave from the other.



DUAL REFLECTOR ANTENNAS

Dual reflector antennas have been derived from their optical telescope counterparts. The most often used dual reflector antennas are the Cassegrain and Gregorian reflector systems. Both of these have the effect of increasing the effective focal length of the reflector without physically increasing it. The Cassegrain antenna uses a hyperbolic subreflector while the Gregorian antenna has an elliptical subreflector. Since both conic sections can be described by the same polar equation, we can deal with both at the same time. The main reflector is still parabolic.

The hyperbola and the ellipse have a finite distance between the two foci. If a source is placed at one focus, then the reflector will focus the wave into the other. We will place one focus of the subreflector at the focus of the main reflector. The effective feed is then at the other focus of the subreflector. A diagram of the Cassegrain antenna is on page 642. A spherical wave from the feed point when reflected from the hyperbola has its curvature changed to a wave with its radius of curvature at the second focus of the hyperbola which is located at the focus of the main reflector. In the case of the Gregorian reflector system which is drawn on page 643, the spherical wave from the focus is refocussed into the second focus by the subreflector and becomes the focal point source for the main reflector.

In both diagrams on pages 642 and 643, the effective F/D has been increased from 0.3 to 1.0. In terms of the feed pattern the reflector is analyzed by using the effective parabola as shown in the diagrams. The half subtended angle of the main reflector is given as ψ_0 , but the effective subtended angle at the feed point is θ_0 . The eccentricity of the secondary reflector is found from the following formulas.

Cassegrain	Gregorian
$e = \frac{\sin(\frac{1}{2}(\psi_0 + \theta_0))}{\sin(\frac{1}{2}(\psi_0 - \theta_0))}$	$e = \frac{\sin(\frac{1}{2}(\psi_0 - \theta_0))}{\sin(\frac{1}{2}(\psi_0 + \theta_0))}$
Hyperbola	Ellipse

We can also find the eccentricity from a magnification factor. The ratio of the effective focal length of the system to the actual focal length of the reflector is the magnification.

$$m = F_e/F$$

Cassegrain	Gregorian
$e = \frac{m + 1}{m - 1}$	$e = \frac{m - 1}{m + 1}$

The magnification factor is used to establish the eccentricity of the subreflector and one focus of the subreflector is located at the focus of the main reflector but we must still locate the second focus and feed point of the subreflector. The distance, $2c$, is given on page 637.

Cassegrain

$$2c = \frac{2 e^2 P}{e^2 - 1}$$

Gregorian

$$2c = \frac{2 e^2 P}{1 - e^2}$$

We now have an arbitrary factor, P , which can be selected. In some applications we may want to select the distance, $2c$, to be equal to the focal length of the main reflector so that the feed structure can be located behind the main reflector. Two reflector antennas are usually limited to large apertures where it is convenient to place the receiver or transmitter behind the main dish and avoid a long run of cable to a prime focus feed. This will not usually be the optimum gain location for the feed. We can easily solve for the length P in terms of the distance: $2c$.

Cassegrain

$$P = \frac{2c(e^2 - 1)}{2 e^2}$$

Gregorian

$$P = \frac{2c(1 - e^2)}{2 e^2}$$

APERTURE BLOCKAGE

The secondary reflector will be a substantial central aperture blockage. We can use the results on page 607 along with the effective focal length to find the effects of aperture blockage. The plot on page 610 shows that the F/D of the effective reflector is only a minor factor in the loss. It would appear that the smallest possible secondary reflector would give the best solution. The subreflector must be at least a few wavelengths in diameter before the geometric optics approximation applied here can be used. There is however another factor. Because the overall reflector system seen from the feed has a large F/D , the feed must have a narrow beamwidth or the spillover losses will be large. To obtain small beamwidths, the aperture of the feed must be large in wavelengths and is not a point source. The feed antenna can become a source of aperture blockage. The blockage of the source is shown on the diagram on page 645 along with the subreflector blockage. An optimum solution would have the two blockages equal. For the case shown, the feed should be moved closer to the subreflector which would reduce the factor: P and the size of the subreflector. The required size of the feed is dependent on the frequency and the F/D of the reflector, so it is not possible to find the optimum independent of frequency. Each case must be solved independently.

Example: Design a 10 m. main reflector Cassegrain antenna given a main reflector $F/D = 0.3$ and the required $F/D = 1.5$ to operate at 3.9 GHz. Minimize the aperture blockage.

Using the ratio of the F/D , we find the magnification factor and the eccentricity of the subreflector.

$$m = 1.5/0.3 = 5 \quad e = \frac{m+1}{m-1} = \frac{5+1}{5-1} = 1.5$$

The effective subtended angle at the feed is found from the formula on page 587.

$$\theta_o = 2 \tan^{-1}(1/(4 F/D)) = 18.9^\circ$$

The feed antenna will be a circular corrugated horn with a 10 dB beamwidth equal to the subtended angle of the subreflector. The maximum aperture phase deviation in wavelengths will be picked to be 0.5 which is close to the optimum design. The obliquity factor must be found before the universal pattern curves can be used.

$$\frac{1 + \cos(18.9^\circ)}{2} = .973$$

The required pattern level to design from is $\sqrt{.1} / .973 = 0.325$. From the curve on page 292, we can find the radius of the horn aperture.

$$\frac{2\pi A}{\lambda} \sin \theta = 4.7 \lambda \quad A = 2.3 \lambda$$

$$\lambda = 0.0769 \text{ m} \quad A = .1774 \text{ m} \quad (7 \text{ inches})$$

In this case we should not ignore the thickness due to the corrugations. The radius will be increased by $3/8\lambda$.

$$(\text{feed radius}) \quad A = 2.7\lambda = .2077 \text{ m} \quad (8.2 \text{ inches})$$

It only remains to pick the distance, $2c$, between the focii of the subreflector. The half subtended angle of the main reflector and also the subreflector seen from the virtual focus is 79.6° . The radius of the blockage due to the subreflector is given by the following.

$$Y(\psi) = \frac{e P \sin(180^\circ - \psi_o)}{1 - e \cos(180^\circ - \psi_o)} = 1.161 P$$

To find the aperture blockage of the feed, we must find the projection of the feed on the main reflector.

$$\alpha = \tan^{-1}(0.2077/(3.6 P)) \quad 2c = 3.6 P$$

The value P_o of the main reflector is twice the focal length.

$$P_o = 2(F/D) \quad D = .6 \text{ m.}$$

$$Y(\alpha) = \frac{P_o \sin(180^\circ - \alpha)}{1 - \cos(180^\circ - \alpha)} = \frac{.6 \sin(\tan^{-1}(.2077/(3.6 P)))}{1 + \cos(\tan^{-1}(.2077/(3.6 P)))}$$

The minimum aperture blockage is obtained when these blockages are equal. This gives us a transcendental equation in P . The solution can be found numerically.

$$P = 0.3850 \text{ m} \quad 2c = 1.386 \text{ m}$$

$$\text{Diameter of the Subreflector} = 0.8940 \text{ m}$$

Suppose we also design a Gregorian reflector antenna and compare the results. The feed antenna will be the same as for the Cassegrain because it only depends on the effective F/D of the system.

$$e = \frac{5 - 1}{5 + 1} = 2/3$$

The half subtended angle from the focus of the ellipse and main parabola is 79.6° . The blockage radius of the subreflector can be found.

$$Y(\psi_o) = \frac{e P \sin(180^\circ - \psi_o)}{1 - \cos(180^\circ - \psi_o)} = 0.5854 P$$

The blockage radius of the feed antenna is given by a similar equation as for the Cassegrain. By equating the two expressions we get another transcendental equation in P .

$$2c = 1.6 P \quad 0.5854 P = \frac{6 \sin(\tan^{-1}(.2077/(1.6 P)))}{1 + \cos(\tan^{-1}(.2077/(1.6 P)))}$$

When this is solved numerically, we get the following results:

$$P = 0.8131 \text{ m} \quad 2c = 1.301 \text{ m}$$

$$\text{Diameter of the Subreflector} = 0.952 \text{ m}$$

The Gregorian subreflector must be about 6 cm. larger than the Cassegrain reflector for the minimum aperture blockage. The difference is about 0.04 dB from the curve on page 610. A drawing with both designs is given on page 648.

If the Cassegrain subreflector is required to change the effective F/D to one instead of 1.5, we can obtain another optimum design using the same type of corrugated horn feed by the same type of solution to a transcendental equation. The results are given below.

$$\text{Eccentricity} \quad e = 1.857$$

$$\text{Feed Diameter} \quad = 0.1485 \text{ m}$$

$$P = 0.3389 \text{ m}$$

$$\text{Spacing between Foci} = 0.9547 \text{ m}$$

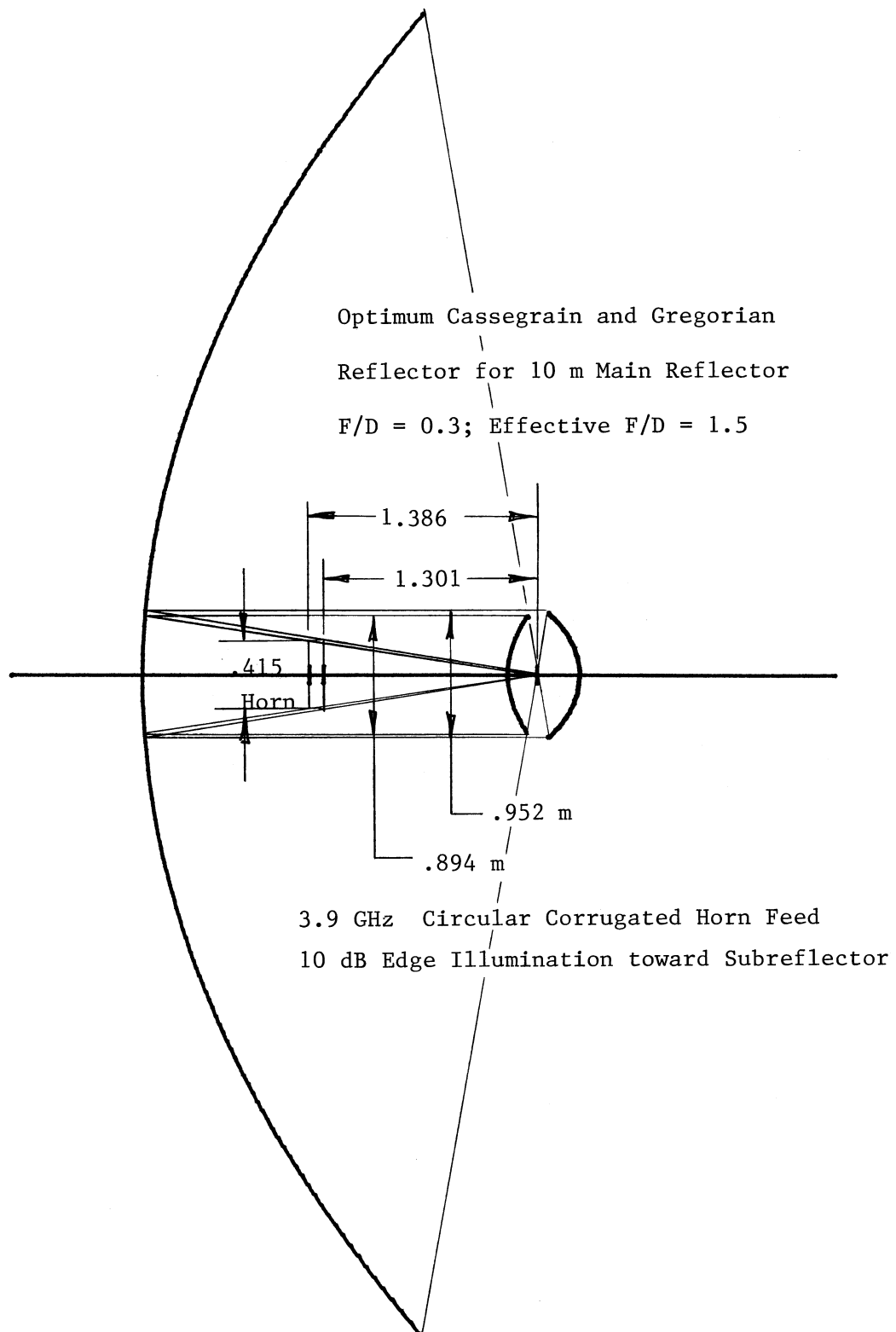
$$\text{Subreflector Diameter} = 0.9277 \text{ m}$$

The longer effective focal length design gives less aperture blockage, but only slightly.

RAY TRACING IN CASSEGRAIN ANTENNA

It will be helpful when considering general ray tracing through reflectors to first use it on the Cassegrain antenna where we know the answer from the equivalent parabola. Included in the figure on page 645 is a general ray tracing through the antenna from the feed to the main reflector. After the main reflector, the amplitude along the ray remains constant since it is converted into a plane wave. We will trace the amplitude ratio of the wave through the antenna by assuming we have spherical waves radiating from the feed. That is, the subreflector is in the far field of the feed. From page 582 we find that the amplitude varies as $1/R$ along the spherical wave. The ratio of the amplitude at the feed to the amplitude at the subreflector is ρ_1 .

$$\rho_1 = \frac{e P}{e \cos \theta - 1}$$



At the surface of the subreflector the curvature of the wave is changed. We know from the geometric optics of the hyperbola that the reflected wave is also spherical with its center of curvature at the second focus. The ratio of the amplitude along the reflected wave to the amplitude at the surface is given by ρ_3/ρ_2 .

$$\rho_2 = \frac{e P}{1 + e \cos \psi} \quad \rho_3 = \frac{2 F}{1 + \cos \psi}$$

The equation for ρ_3 is just that of the parabolic main reflector. The ratio of the amplitude at the feed to the amplitude at the main reflector becomes:

$$\frac{\rho_1 \rho_3}{\rho_2} = \frac{(1 + e \cos \psi) 2 F}{(e \cos \theta - 1)(1 + \cos \psi)}$$

The first thing we notice is that there is no dependence on the length, P , which says that the amplitude distribution in the aperture plane is independent of P . P is an arbitrary factor.

We can reduce this expression by the radial distances when expressed in terms of the two angles: θ and ψ .

$$Y(\psi) = Y(\theta) \quad \frac{\sin \psi}{1 + e \cos \psi} = \frac{\sin \theta}{e \cos \theta - 1}$$

When we substitute this in the expression above, we get a simpler expression for the effective radius.

$$\frac{\rho_1 \rho_3}{\rho_2} = \frac{2 F \sin \psi}{\sin \theta (1 + \cos \psi)} = \rho_e$$

ρ_e is the effective radius of the spherical wave. We can make a number of half angle substitutions.

$$\rho_e = \frac{2 F \sin \psi/2 \cos \psi/2}{2 \sin \theta/2 \cos \theta/2 \cos^2 \psi/2} = \frac{F \tan \psi/2}{\sin \theta/2 \cos \theta/2}$$

We can recognize $F \tan \psi/2 = D$, the diameter. We can define an equivalent focal length, F_e , then the diameter is related to F_e .

$$F_e \tan \theta/2 = D$$

$$\rho_e = \frac{F_e \tan \theta/2}{\sin \theta/2 \cos \theta/2} = \frac{F_e}{\cos^2 \theta/2}$$

This is just the equation for the equivalent parabola.

The important thing to remember when ray tracing is that the radii of curvature of a wave will change when there is a reflection. In this case the wave remained a spherical wave. In general it will become an astigmatic wave. We established the amplitude at the surface of the reflector and used that as the starting amplitude of the reflected wave with the changed radius of curvature.

EQUIVALENT PARABOLA

The feed efficiencies of the dual reflector systems can be found by using the equivalent parabola. All the results given before for the prime focus parabola can be carried over to the Cassegrain and Gregorian dual reflector antennas once the equivalent parabola is found.

The dual reflector antenna can be scanned by moving the feed laterally off the axis similar to the prime focus parabola. For a limited range the equivalent parabola can be used to find the scanned beam location using a beam deviation factor as shown on the graph on page 624. We can see from the graph on page 625 that the scanning losses of an antenna with large F/D are smaller. If the feed has to be moved a distance, X, off axis at the primary focus to scan the beam to a given angle, then the feed must be moved a distance, mX, in the dual reflector system to scan to the same angle. The offset must be increased by the magnification. Because the focal length is large, the amount of movement off axis required to scan the beam is large and the equivalent parabola approximation will not hold up very far. The coma lobes will rise fast with scanning. When analyzing the off axis feed, the physical optics approximation will give more accurate results than the aperture approximation. The work is much more involved because the currents on both reflectors must be found, but it is the only way to get good results.

EQUIVALENT NOISE TEMPERATURE OF ANTENNA

When performing system studies of communication, radar, or radiometer systems, it is necessary to assign a noise temperature to the antenna. The antenna will have conductor losses which can be given an equivalent noise temperature.

$$T_e = (L - 1)T_o$$

T_o is the temperature of the antenna, L is the loss, and T_e is the noise temperature of the antenna due to conductor losses. From a systems point of view we would also include the losses in the cable leading to the first amplifier or mixer of the receiver. This expression is for the noise temperature of an attenuator. There is however another source of noise. Because the antenna is receiving signals from all directions, it will receive blackbody noise from the environment. The noise temperature of the antenna will be a function not only of the antenna pattern but also the direction of the main beam. The noise temperature due to blackbody radiation into the antenna is the average of the product of the gain and environment temperature over the radiation sphere.

$$T_a = \frac{1}{4\pi} \int_0^{2\pi} \int_0^\pi G(\theta, \phi) T_s(\theta, \phi) \sin \theta \, d\theta \, d\phi$$

$T_s(\theta, \phi)$ is the temperature (K) of space in the direction (θ, ϕ) and G is the corresponding gain. T_a is the antenna noise temperature due to blackbody radiation. The noise temperature of the sky is quite low (3 to 10 K) while the temperature of the ground is quite high (290 K). Because there is such a difference, even small sidelobes are important to the noise temperature if they hit the ground. In most systems it is necessary to maximize the ratio G/T_a for the best performance.

If we have a prime focus parabolic dish pointed toward the sky, radiation will be received directly from the ground because of the spillover radiation pattern of the feed antenna. We will find a trade-off because when we reduce the spillover loss by decreasing the beamwidth, we will also reduce the gain of the reflector. In all cases we will maximize the ratio of the gain to noise temperature for the optimum system. One method of eliminating this trade-off is to use a dual reflector system. Now the spillover radiation of the feed is also pointed toward the cool sky. For this reason most radio astronomy telescopes and large satellite ground stations use a dual reflector system for the antenna. In the case of space borne antennas pointed toward the earth it may be an advantage to again use the prime focus reflector so that the spillover radiation will point into space. But in these cases the main beam of the antenna will be pointed at the warm earth and mechanical considerations may out-weigh any small system advantages.

FOCAL PLANE

Because large reflectors are so expensive to build, a large amount of effort has been done to improve the efficiency of the antenna by matching the fields in the focal plane to the feed horn. This careful matching of the horn feed to the focal plane fields has narrowed the frequency bandwidth but improved the overall efficiency. Here we will consider the prime focus reflectors, the efficiency may also be improved by shaping the subreflector of a dual reflector antenna. We will discuss this method later.

The fields in the focal plane were found for optical instruments to be the Fraunhofer diffraction pattern of a circular aperture.

$$E = \frac{J_1(k r \psi_o)}{k r \psi_o}$$

ψ_o is the half subtended angle of the reflector (radians), r is the radial coordinate, and k is the propagation constant. This is called the Airy function which is plotted on page 557, but with a different abscissa. The Airy function is only valid for reflectors with large F/D . Traditionally the feed horn was extended out to the first null of the Airy function with the substitution of $\sin \psi_o$ for ψ_o . The general pattern of the focal plane is sometimes referred to as Airy rings because of the pattern's concentric rings.

More exact fields can be found by using the induced currents on the reflector ($2 \hat{n} \times \vec{H}$) to calculate the fields in the focal plane. The fields are described by axial hybrid modes, HE_{1n} . These modes are a combination of TE_{1n} and TM_{1n} modes in a circular coordinate system. Both these modes have the same phase velocity. Hybrid modes can only propagate in waveguides with anisotropic walls such as corrugated walls with slots $\lambda/4$ to $\lambda/2$ deep. The highest efficiency is obtained when the feed fields conjugate match the focal plane fields. Because the feed horn can only a limited size only a few modes can be used to match the focal plane fields.

If we have a linearly polarized wave incident on the reflector, then the focal plane fields can be described by the following equations.

$$E_r = E_1(U) \cos \phi \quad U = k r \sin \psi$$

$$E_\phi = -E_2(U) \sin \phi$$

E_r is the radial component and E_ϕ is the ϕ component in the focal plane.

$$E_1(U) = E_o(F_1 + F_2)$$

$$E_2(U) = E_o(F_1 - F_2)$$

$$F_1 = \int_0^{\psi_0} \sin(\psi) J_0(U) d\psi$$

$$F_2 = \int_0^{\psi_0} \sin(\psi) \tan^2(\psi/2) J_2(U) d\psi$$

J_0 is the zeroth order Bessel function of the first kind and J_2 is the second order Bessel function.

The total number of hybrid modes which can propagate is a function of ka , where a is the radius of the corrugated horn feed. The eigenvalue, $u_n = ka \sin \theta_n$, is found from the following transcendental equation for each mode.

$$1 - \frac{u_n J_0(u_n)}{J_1(u_n)} = \cos \theta_n$$

The fields in the waveguide hybrid modes are found from the following.

$$E_r = E_3(kr) \cos \phi$$

$$E_\phi = -E_4(kr) \sin \phi$$

$$E_3 = C(G_1 + G_2)$$

$$E_4 = C(G_1 - G_2)$$

with

$$G_1 = \sin(\theta_n) J_0(kr \sin \theta_n)$$

$$G_2 = \sin(\theta_n) \tan^2(\theta_n/2) J_2(kr \sin \theta_n)$$

The fields of all these modes vanish as the walls of the waveguide. If we are matching the fields over a finite waveguide, then we must pick the waveguide radius to be at one of the nulls of the focal plane fields. The size which is picked for the feed will determine the number of modes possible in the waveguide. A method for determining the coefficients of the mode amplitudes is given by Vu The Bao (Optimisation of Efficiency of Reflector Antennas: Approximate Method, Proc. IEE, Vol. 117, pp. 30-34, Jan. 1970). The amplitudes are equated at n points where n corresponds to the number of modes. The amplitude at $r = 0$ is one of the points and the other $n - 1$ points are the zeros of the focal plane field. Using this method, the problem reduces to the solution of a set of linear equations in the mode amplitudes.

The actual amplitudes of the modes are obtained by putting steps in the waveguide and performing a Fourier Bessel series expansion using the mode functions

to find the level of the modes at the step. It is then necessary to adjust the length from the steps to the aperture plane until the different modes arrive in the proper phase. Each mode will travel with different phase velocities in the guide so it is possible to get any phase difference between them. The phase velocity is found from the mode TE_{1n} mode. The problem of obtaining the proper modes and phases at the aperture of the feed becomes more and more difficult and narrowband as the number of modes increases. The method is also applied to match the fields of a spherical reflector.

A second method of obtaining the coefficients of the hybrid modes is given by Thomas (Theoretical Performance of Prime Focus Paraboloids Using Cylindrical Hybrid Modes, Proc. IEE, vol. 118, pp. 1539-1549, Nov. 1971). In this case the radiation field of each hybrid mode is found. He optimizes the feed by adding the feed patterns of each hybrid mode to approximate the pattern: $\text{Sec}^2 \psi/2$ between $\pm \psi_0$ and zero elsewhere. This will compensate for the $\text{Cos}^2 \psi/2$ natural distribution from an isotropic feed due to the radial distance to the reflector. The ratio of the modes is found by optimizing the product of the spillover and amplitude taper efficiencies. The amplitudes of the modes become the variables of a computer optimization routine.

Thomas also uses the figure of merit as a parameter to optimize. This factor takes into account the noise temperature of the system.

$$\text{F.M.} = \frac{T_r \eta_a}{T}$$

T_r = receiver noise temperature including the blackbody noise in the main beam of the antenna.

T = Total system noise temperature = $T_r + (1 - \eta_s)T_s$

T_s = Effective noise temperature of the spillover region. Many times T is taken as 150 K; the average between the ground (300 K) and sky (0 K).

η_a = Amplitude taper efficiency

η_s = Spillover efficiency

Using this parameter, the overall system will be optimized and not just the antenna efficiency.

A third method of improving the efficiency is match fields by using a spherical wave expansion method. In this case the feed and reflector fields are expanded in a series of spherical harmonics which are the product of associated Legendre functions and spherical Bessel function. The fields can be approximated very well by just a few terms in the expansion. Not only can prime focus reflectors, but dual reflector and offset reflector systems can be handled by this method. Similiar to the cylindrical hybrid mode expansion, the coefficients of the different expansions are matched at some boundary. This method is expanded in some detail in a book by P. J. Wood, Reflector Antenna Analysis and Design.

REFLECTOR TOLERANCES

All reflectors will have anomalies which will reduce the gain that is predicted from the feed analysis. If the reflector is spun, then there will be tool marks or if made from petals, there will be seams. Large reflectors will deform under their own weight. There are also thermal problems when the sun shines on one part of the reflector and produces thermal gradients across the reflector. This is especially severe in space borne reflectors. In general the reflector will only approximate a paraboloid because of machining and fabrication tolerances. It is important to minimize the cost of the reflector by specifying as loose a tolerance as possible for the manufacturing. As the frequency is raised, the tolerance required on the reflector will decrease by the square of frequency. The possible gain of the reflector increases by the square of frequency provided an optimum feed antenna is made for each frequency. The maximum possible gain will approach a limit because of the surface tolerance of the reflector. We will only consider small surface anomalies and assume that the reflector retains its basic parabolic shape or deforms in a predictable fashion.

If the reflector retains its general shape, then surface anomalies will cause phase errors in the aperture. That is, the curvature of the reflector has not changed appreciably due to surface errors to cause large amplitude variations in the aperture plane field. Small random amplitude variations have little effect on gain. The effect of these surface imperfections is to cause a change in the distance along the ray path from the feed to the aperture plane. These imperfections can be caused equally by the subreflector of a dual reflector system and have equal effect. We can handle both reflectors by the same theory. If the anomalies are random, then they are indistinguishable from random errors in the feed pattern phase. Some of these effects are given on page 601 and 603. For now we will assume that the feed antenna has no random phase errors and no phase center phase error losses. We can express the phase error loss efficiency due to the reflector surface errors in the aperture from the development on page 570.

$$PEL = \frac{\left| \int_0^a \int_0^{2\pi} E(r, \phi) e^{j\delta(r, \phi)} r dr d\phi \right|^2}{\left(\int_0^a \int_0^{2\pi} |E(r, \phi)| r dr d\phi \right)^2}$$

$\delta(r, \phi)$ is the ray path deviation along the ray path. As expressed this includes the feed phase error. We cannot separate the two terms, but we can approximate the losses as being separable. Because the phase error term, $\delta(r, \phi)$, is small, the exponential can be expanded in a Taylor series. D.K. Cheng (Effect of Arbitrary Phase Errors on the Gain and Beamwidth Characteristics of Radiation Pattern, IRE Trans. on Antennas and Propagation, vol. AP-3, pp. 145-147, July 1955) has found an upper bound on the phase error due to random errors by using a limit on the integrals. If the peak of the phase error is m (radians), then the change in gain (phase error) will be bounded.

$$\frac{G}{G_0} \geq \left(1 - \frac{m^2}{2}\right)^2$$

G_0 is the gain without phase error. This bound has been plotted on page 603. Using this gain estimate is too conservative but it is useful as an upper bound.

The phase error can be found more accurately by assuming that the errors are Gaussian distributed and the errors are correlated over regions. This has been expanded by John Ruze (Antenna Tolerance Theory - A Review, Proc. IEEE, vol. 54, pp. 633-640, April 1966). To be correlated over a region means that there are dents in the surface and that the errors at one point depend on points nearby (the correlation area) or it may mean that the antenna is made from segments.

$$PEL = e^{-\bar{\delta}^2} + \frac{1}{\eta} \left(\frac{2c}{D} \right)^2 e^{-\bar{\delta}^2} \sum_{n=1}^{\infty} \frac{\bar{\delta}^{2n}}{n \cdot n!}$$

c is the distance over which the errors are correlated and D is the diameter. $\bar{\delta}^2$ is the mean square of the phase errors.

$$\bar{\delta}^2 = \frac{\int_0^{2\pi} \int_0^a |E(r, \phi)| \delta^2(r, \phi) r dr d\phi}{\int_0^{2\pi} \int_0^a |E(r, \phi)| r dr d\phi}$$

η is the aperture efficiency. The infinite series converges rapidly. When the surface deviations are correlated, then the phase error loss efficiency is not as large as when the correlation is ignored.

If the correlation distance, c , is small compared to the diameter, then the second term can be ignored. The phase error loss efficiency can be expressed:

$$PEL = e^{-(4\pi\epsilon_0/\lambda)^2} = e^{-\bar{\delta}^2}$$

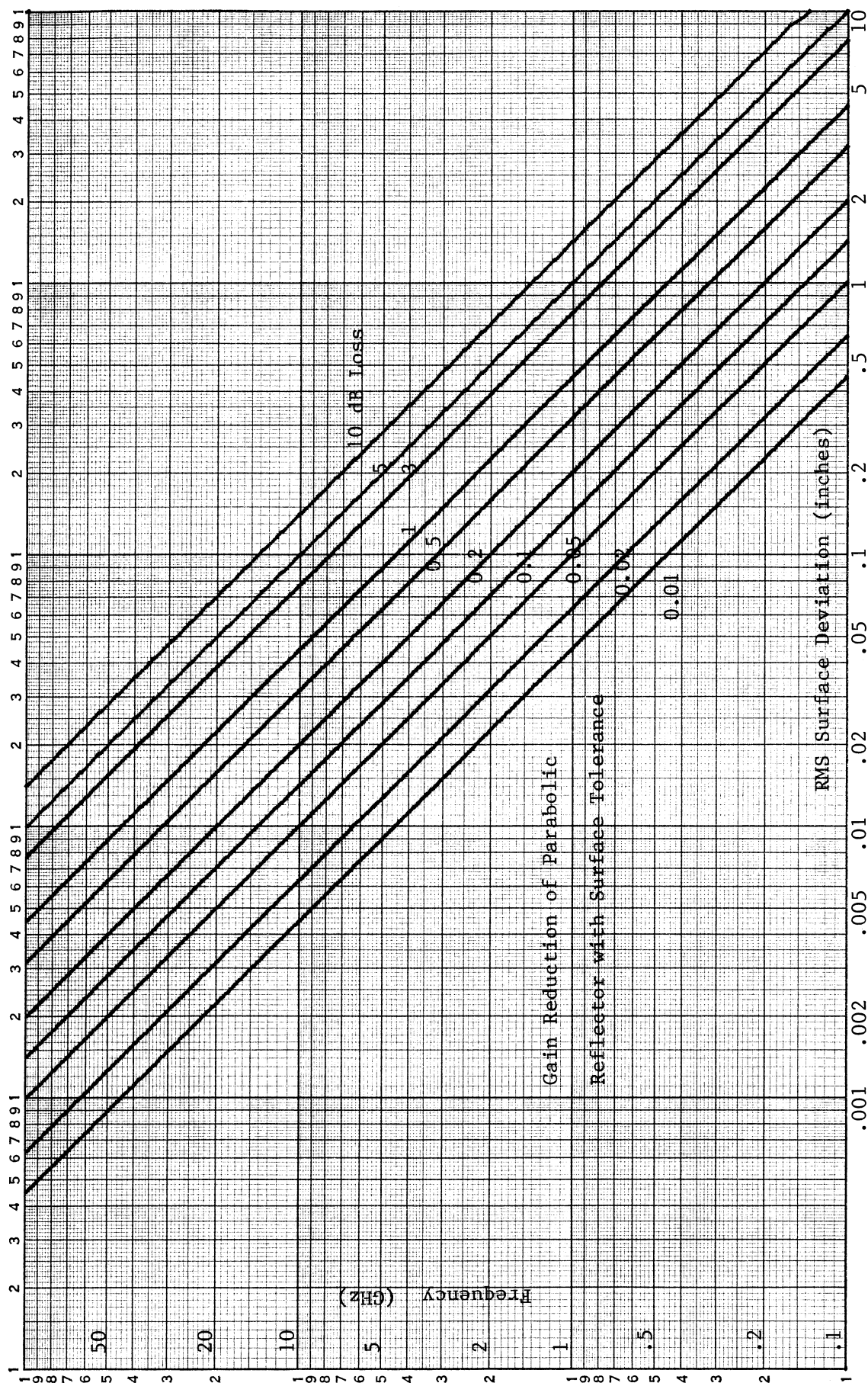
ϵ_0 is the effective RMS reflector tolerance. The factor is 4π instead of 2π because the wave has twice the distance to travel since the wave travels further to the reflector and after reflection travels further to the aperture plane. From the equation of $\bar{\delta}^2$ we can find ϵ_0^2 .

$$\epsilon_0^2 = \frac{\int_0^{2\pi} \int_0^a |E(r, \phi)| \epsilon^2(r, \phi) r dr d\phi}{\int_0^{2\pi} \int_0^a |E(r, \phi)| r dr d\phi}$$

Ruze gives the following expressions for the distance, ϵ , in terms of the deviation measured along the Z axis, ΔZ , and along the surface normal, Δn .

$$\epsilon = \frac{\Delta Z}{1 + (r/2f)^2} \quad \epsilon = \frac{\Delta n}{\sqrt{1 + (r/2f)^2}}$$

A plot of the RMS reflector error for various phase error losses is given on page 656. For example the required RMS tolerance at 10 GHz to give less than



0.5 dB loss is 0.032 inches or about 1/35th wavelengths. This chart can be used to specify the reflector tolerance once the surface tolerance loss has been assigned.

The effective RMS reflector tolerance is a function of the amplitude distribution in the aperture. Because ϵ_0 is derived from the phase error loss, we can relate this to the feed pattern by using the formula on page 592.

$$\epsilon_0^2 = \frac{\int_0^{2\pi} \int_0^{\psi_0} |E_f(\psi, \phi)| \tan \frac{\psi}{2} \epsilon^2(\psi, \phi) d\psi d\phi}{\int_0^{2\pi} \int_0^{\psi_0} |E_f(\psi, \phi)| \tan \frac{\psi}{2} d\psi d\phi}$$

Most of the time the aperture pattern is taken as uniform since the reflector tolerance is specified independent of the feed.

The tolerance theory has been extended by M. S. Zarghamee (On Antenna Tolerance Theory, IEEE Trans. on Antennas and Propagation, vol. AP-15, pp. 777-781, Nov. 1967) to include effects of the distribution of the errors. Many times the reflector surface is more accurate in some regions than in others due to better structural support or construction. The second variation of surface deviations is defined.

$$\eta_0^4 = \frac{\iint |E(r, \phi)| (\epsilon^2(r, \phi) - \epsilon_0^2) r dr d\phi}{\iint |E(r, \phi)| r dr d\phi}$$

The phase error loss due to the surface deviations becomes

$$PEL = e^{-(4\pi\epsilon_0/\lambda)^2} e^{(\pi\eta_0/\lambda)^4}$$

The systematic errors of the reflector can be determined by mechanical measurements. These systematic errors are correlated over the diameter of the reflector. The most common distortion is astigmatism: the focal point is different in different planes. When we take a pattern through the axis of the reflector, we can detect two types of errors. One of the errors is coma lobes; that is, the first sidelobes are unequal. This indicates that the phase center of the feed is not on the axis of the reflector. Because the larger lobe occurs on the side toward the axis, we must move the feed away from the larger sidelobe (the wave is reflected) to eliminate coma. See the plot on page 621. We can encounter cases where the equivalent axis is different in different planes: lateral astigmatism (also called coma). More common is axial astigmatism. We can detect this by looking at patterns through the axis. If there is axial displacement, then the pattern will appear as on page 628. The feed is moved along the axis of the reflector. When the pattern sidelobes and nulls become more distinct, the focal point is aligned with the phase center of the feed in that plane. Of course, we will have to separate out the possible astigmatism of the feed antenna. By doing a series of measurements in different ϕ planes, a compromise axial position can be found or the dish adjusted to remove the various sources of astigmatism.

If the focus is unclear (indistinct), we can have a case of spherical aberration. The wave focal point is at different points along the axis for different radial distances on the reflector. This error is difficult to detect by microwave measurements.

Another important pattern degradation due to errors in the reflector surface is raised sidelobes. In general, it is difficult to achieve low sidelobes because of the effects of blockage and feed support diffraction. When dealing with a general aperture which is approximated by an array, the effects of random errors on the gain is secondary to the effects on the sidelobes. The sidelobe level caused by random errors is dependent on the correlation interval and the size of the aperture. Larger apertures are less effected and apertures with more taper have larger sidelobe levels due to random errors. This topic is covered in some detail in R. C. Hansen Microwave Scanning Antennas, vol I, pp. 74f.

FEED MISMATCH DUE TO REFLECTOR

The feed antenna is usually matched outside the reflector, but when placed in the paraboloid, some of the reflected energy will be received by the feed. This received energy will change the effective voltage reflection coefficient seen at the terminals. We can approach the problem by using physical optics to calculate the field at the feed. The reflection coefficient will be given in terms of an integral over the currents of the reflector. This integral will be reduced to a single algebraic expression by using the principle of stationary phase.

Let us assume that the feed is a Huygens source. This will simplify the expressions of the analysis, but will retain its validity for a general source because any source can be expanded into two orthogonal Huygens sources. When we combine the current on the bottom of page 631 with the results on page 636 and ignore the Z component, we obtain the surface current on the reflector.

$$\bar{K}_s = \frac{2\bar{a}_x}{\eta} \cos \frac{\psi}{2} \frac{e^{-jk\rho}}{\rho} \left[\frac{P_t \eta}{4\pi} G_f(\psi, \phi) \right]^{1/2}$$

G_f is the gain of the feed antenna in the direction (ψ, ϕ) . P_t is the input power which is proportional to some reference voltage.

$$P_T = \frac{|V|^2}{Z_0}$$

The radiation of each differential current element is found from the magnetic vector potential. At the feed aperture the potential becomes

$$d\bar{A} = \frac{2\bar{a}_x}{4\pi\eta} \cos \frac{\psi}{2} \frac{e^{-j2k\rho}}{\rho^2} |V| \left[\frac{\eta}{4\pi Z_0} G_f(\psi, \phi) \right]^{1/2} dS$$

The field associated with this is easily found because the feed is in the far field of the reflector.

$$\bar{E} = -j\omega\mu\bar{A}$$

Using this electric field, we can find the Poynting vector magnitude.

$$S_r = \frac{|E|^2}{\eta}$$

The power received by the feed antenna is the Poynting vector magnitude times the effective area of the feed.

$$P_r = |S_r| A_e = \frac{|E|^2}{\eta} \frac{G_f(\psi, \phi) \lambda^2}{4\pi}$$

We are interested in the voltage reflection coefficient which means we must find the voltage on the transmission line.

$$V_r = (Z_o P_r)^{\frac{1}{2}} = |E| \lambda \sqrt{\frac{G_f(\psi, \phi) Z_o}{4\pi \eta}}$$

When we substitute this back up through the equations, we obtain the differential voltage reflection coefficient.

$$dV_r = \frac{2\omega\mu\lambda}{(4\pi)^2\eta} \cos \frac{\psi}{2} \frac{e^{-j2k\rho}}{\rho^2} |V| G_f(\psi, \phi) dS$$

The reflection coefficient is the integral of this differential voltage over the surface of the reflector. Making a few substitutions for the constants, we obtain the following integral.

$$|\Gamma| = \frac{V_r}{|V|} = \iint \cos \frac{\psi}{2} \frac{G_f(\psi, \phi)}{4\pi} \frac{e^{-j2k\rho}}{\rho^2} dS$$

This can be generalized to any reflector by replacing $\cos \psi/2$ by $\cos i$, where i is the angle of incidence from the feed to the reflector.

We are left with an integral over the surface of the reflector. We will solve this by the method of stationary phase. If the reflector is large in terms of wavelengths, then the contributions from areas nearly an angle will cancel each other. The amplitudes will be approximately the same, but the phase, $2k\rho$, will vary rapidly for small changes in ψ . The summation of these phasors in the complex plane will be zero. The only place that there will be any net contribution to the integral will be at those points where the phase varies slowly. These will occur where the first derivatives of the surface are zero relative to the axis toward the feed. Most of the contribution to the integral occurs from those areas near normal incidence.

We will pick a Z axis along the normal incident ray and expand the reflector surface in a Taylor series about this axis as was done one page 582. The integral is approximately the value of the amplitude at the point of normal incidence times an integral of the phase function over a small region about the point.

$$|\Gamma| \simeq \frac{G_f(\rho_0)}{4\pi \rho_0^2} \iint_S e^{-j2k\Phi(x, y)} dx dy$$

$$\Phi(x, y) = \rho - \rho_0 = \sqrt{x^2 + y^2 + (\rho_0 - z_0)^2} - \rho_0$$

The distance $z = -\frac{1}{2} \left(\frac{x^2}{\rho_1} + \frac{y^2}{\rho_2} \right)$, ρ_1 & ρ_2 are the principle radii of curvature of the surface about the Z axis. When we substitute this into $\Phi(x, y)$ and retain terms of second order, we get the approximation

$$\Phi(x, y) \simeq \frac{1}{2} \left(\frac{\rho_1 + \rho_0}{\rho_1 \rho_0} \right) x^2 + \frac{1}{2} \left(\frac{\rho_2 + \rho_0}{\rho_2 \rho_0} \right) y^2$$

The integral is separable and each part becomes the form

$$\int_{\delta} e^{-2k\alpha x^2} dx$$

If we increase the limits of the integral to infinity, then we can find a solution. The portion of the integral beyond the small region around the normal will not contribute because the phase moves rapidly and cancels

$$\int_{-\infty}^{\infty} e^{-j^2 k \alpha x^2} dx = \sqrt{\frac{\pi}{2\alpha k}} e^{-j(\frac{\pi}{4})}$$

Since we are not interested in the phase, we can ignore that factor. When take the product of the two approximations and reduce common factors, we obtain and approximate expression for the reflection coefficient.

$$|\Gamma| \simeq \frac{G_f(\rho_0) \lambda}{8\pi \rho_0} \sqrt{\frac{\rho_1 \rho_2}{(\rho_1 + \rho_0)(\rho_2 + \rho_0)}}$$

Consider the parabola. The radius of curvature is $-2f$ and $\rho_0 = f$.

$$|\Gamma| \simeq \frac{G_f(0) \lambda}{4\pi f}$$

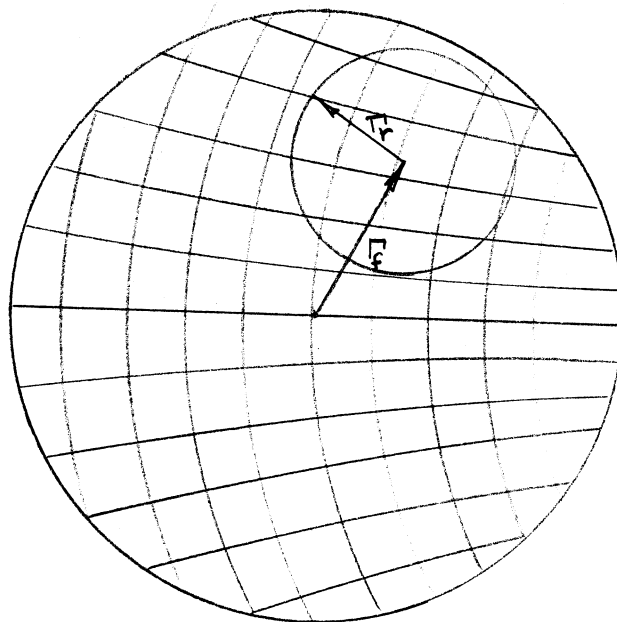
The reflection coefficient is proportional to the reciprocal of the focal length in wavelengths times the feed bore sight gain divided by 4π . For a constant F/D, larger reflectors will have smaller reactions on the feed.

Suppose we have a reflector with F/D = 0.5. The beamwidth of the source should be 60° from the graph on page 597 for minimum feed losses. The bore-sight gain (directivity) is 10.4 dB from page 39. If the reflector is 10 ft. in diameter, then the above equation reduces to

$$|\Gamma| = 0.171/\text{Freq. (GHz)}$$

Frequency	$ \Gamma $	VSWR	RTN LS
0.5	0.343	2.045	9.3 dB
1.0	0.172	1.414	15.3
2.0	0.086	1.188	21.3
4.0	0.043	1.090	27.3
8.0	0.021	1.044	33.4

The reaction of the reflector only becomes significant when the reflector is only a few wavelengths across. At that point the stationary phase approximation is no longer valid. If the feed can be moved along the axis of the reflector, then the component due to the reflector can be separated from the mismatch of the feed itself. When the feed is moved along the axis, the following Smith chart response is seen at a single frequency.



The reflection coefficient of the feed, Γ_f , remains constant but the phase of the reflector reaction, Γ_r , will change and trace a circle on the Smith chart. As shown above, the vector from the center of the chart to the center of the circle traced when the feed is moved along the axis is the feed free space reflection coefficient. The radius of the circle is the magnitude of the reflector reaction on the feed antenna. In those cases where the feed antenna is not matched well in free space, the effect of the reflector will not be seen.

There are two methods of reducing the reaction of the reflector. In the first method a flat plate is placed at the vertex of the reflector. This plate which may be as much as 1/6 th of the diameter will reflect energy out of phase with the energy from the rest of the reflector and cancel the total reaction of the reflector. Silver, Microwave Antennas, gives a technique for designing these, but it is usually a cut and try design. The bandwidth of the vertex plate is quite narrow and difficult to predict. A physical optics approximation of the vertex plate will fail because it is too small in wavelengths for it to be valid. In the second methods the reflector or subreflector is modified. If the reflector can be shaped so that there is a null in the direction of the feed, then the reflection coefficient will be reduced. But when this is done, the effective blockage of the feed increases since a sharp null cannot be produced. This method will give large bandwidths. A small raised cosine annulus can be put into the reflector to redirect energy into the feed and cancel energy from other regions. This has the advantage that it can be analyzed by geometric optics although like the vertex plate, it is narrow band. By adding more rings the feed can be matched at more than one band. Of course, these techniques can be used to remove the mismatch of the total feed system.

OFFSET REFLECTOR

A reflector which has its feed out of the aperture eliminates many of the problems of the center fed reflector. Of course, there is no aperture blockage. This blockage raises the sidelobes (pp. 612) and will increase the cross polarization due to edge diffractions from the feed or subreflector and support struts. Second, by using an offset fed reflector, there is no restriction on the size of the feed structure. The transmitter or receiver can be located with the feed antenna.

The geometry of the offset fed reflector is shown on page 663. The reflector is circular as seen from the Z axis but instead of being centered on the axis of the paraboloid, it is offset. The center is at some angle, ψ_o , from the axis of the paraboloid and the reflector subtends an angle $2\psi_e$ from the focus. The focus is still located as for the full parabola. Each part of the parabola retains its focussing property. It will convert a spherical wave from the feed into a plane wave in the aperture plane defined by the axis. In order to eliminate excessive spillover loss, the feed boresight is pointed at the center of the reflector. The phase center of the feed is still located at the focus of the paraboloid.

The offset reflector can be analyzed with the same tools as the centered antenna. The aperture field method as well as the physical optics approximation can be used. Without going through that again, we can state some of the results. Along the X axis (pp. 663) there will be an amplitude taper because of the natural tapering of the parabola. For a symmetrical feed pattern the energy in the aperture will be higher at the bottom than the top. Of course, reflectors with higher F/D will have less of this effect.

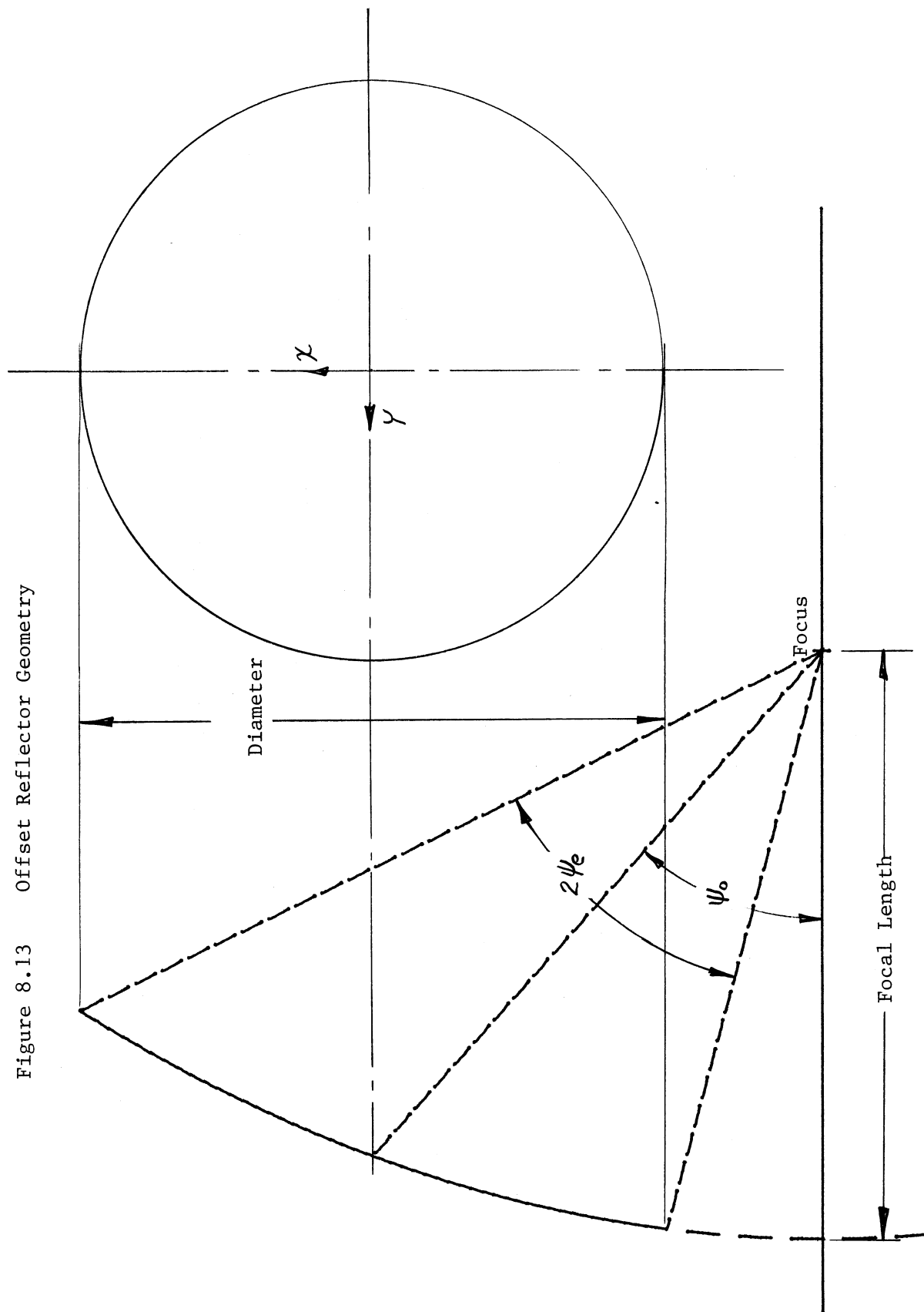
In the symmetric reflector the cross polarization component can be eliminated by using a Huygens source feed. If there are cross polarization lobes, they occur in the diagonal planes (Condon lobes). This is not the case with the offset fed reflector. Because the feed horn is tilted up to point at the center, there will be cross polarization in the plane along the Y axis. The symmetry is destroyed. There is no cross polarization in the plane along the X axis because symmetry is maintained. The results of the central feed antenna given on page 632 also hold in general form here. As the F/D is increased, the cross polarization decreases. This is due in part to the decreased tilt of the feed antenna. When the offset angle, ψ_o , decreases, then the cross polarization also decreases as it approaches the central feed case. Another polarization effect which has been observed is beam squint when the feed is circularly polarized. There will be a slight difference between the RHC and LHC beam pointing angle. Again, this effect is less for larger F/D.

The F/D of the offset fed reflector is given by the expression

$$F/D = \frac{\cos \psi_e + \cos \psi_o}{4 \sin \psi_e}$$

The easiest way of obtaining large F/D is to use a dual reflector. Both the Cassegrain and Gregorian reflector systems carry over. The subreflector

Figure 8.13 Offset Reflector Geometry



should be kept out of the aperture to eliminate all blockage. With these systems it is possible to get very low cross polarization which enables frequency reuse with orthogonal polarizations.

The offset fed reflector can be scanned by moving the feed laterally along the axis perpendicular to the boresight of the feed (the line defined by ψ_o). The beam deviation factor is modified from the value given on page 624.

$$(\text{BDF})_{\text{offset}} = (\text{BDF})_{\text{center fed}} \frac{(\text{F/D})_{\text{offset}}}{(\text{F/D})_{\text{center fed}}}$$

Example: Given an offset fed reflector with $\psi_o = 45^\circ$ and $\psi_e = 40^\circ$, find the beam deviation factor.

$$(\text{F/D})_{\text{center fed}} = \frac{\cos(40^\circ) + 1}{4 \sin(40^\circ)} = 0.687$$

$$(\text{F/D})_{\text{offset fed}} = \frac{\cos(40^\circ) + \cos(45^\circ)}{4 \sin(40^\circ)} = 0.573$$

From the graph on page 624, $(\text{BDF})_{\text{center}} = 0.928$. The formula above gives the beam deviation factor.

$$(\text{BDF})_{\text{offset}} = 0.774$$

The feed must be laterally offset further to get the same scanning.

One proposed use for offset fed reflectors is communication satellites where a dual reflector system is combined with an array feed. If there is a cluster of separate feeds around the focus, then each feed will give a separate beam on the earth. Each beam will come from a lateral offset scanned feed. The beams can be centered on large cities and provide channels between them. Since the reflector can have low sidelobes without the blockage, there will be little crosstalk from signals entering the sidelobes.

A corrugated horn feed is essential to keep the sidelobes low because it provides a good illumination of the reflector. In order to be able to scan the beam far off axis, it is necessary to increase the size of the subreflector. The corrugated horn is able to more accurately approximate the Huygens source than the regular horn and will give less cross polarization.

The effective F/D of the reflector will be from 2 to 3 which will provide low cross polarization and the possibility of frequency reuse. The large F/D also greatly reduces the amplitude taper in the aperture. The area efficiency of the reflector should be able to approach 80% because of the large F/D. Only the subreflector must be increased to accommodate the off axis beams. When off axis plane waves are incident on the main reflector, the beam is focussed off axis on the subreflector which has been increased. The subreflector then focusses the wave into the off axis feed horn.

In other schemes the cluster of feeds is formed into an array. The beam can be continuously scanned instead of being fixed. The reflector system is unique because not only can it be scanned by phase shifting in the array, but by amplitude tapering. If the effective center of the aperture is moved off center, then the beam will scan.

SPHERICAL REFLECTOR

The biggest advantage of the spherical reflector is its ability to be scanned by a large amount without degrading its performance. In order to correct for its spherical aberration it must be feed with a line source feed or have a corrector subreflector. The feed is rotated about the center of the sphere and illuminates the portion of the sphere centered on the radial line. The portion of the sphere illuminated depends on the length of the feed.

On page 666 is a diagram of the ray tracing through the spherical reflector when a plane wave is incident. Because the reflector has circular symmetry all rays will intersect the axis (the radial line in the direction of the plane wave). We can see from the diagram that the rays which strike the outer portions of the sphere are reflected closer to the vertex. The focus has become a line. Consider the single ray shown with dimensions. It is incident on the reflector at some distance, H , from the axis. A radial line is drawn from the center to the point of incidence. The radial line is, of course, a normal to the surface is at an angle, ψ , from the axis. This angle is also the angles of incidence and reflection. An isosceles triangle is formed from the reflected ray, the axis and the radial line. From this and the geometry of the sphere we can find the distance Z , the location on the axis of the intersection of the reflected ray.

$$Z = \frac{R}{2 \cos \psi} \quad H = R \sin \psi$$

Using the trigonometric identity $\sin^2 \theta + \cos^2 \theta = 1$, we can eliminate ψ from the equations.

$$\begin{aligned} \frac{H^2}{R^2} + \frac{R^2}{4 Z^2} &= 1 \\ H^2 &= R^2 \left(1 - \frac{R^2}{4 Z^2} \right) \end{aligned}$$

We can use this equation to find the distribution of power along the axis. Using the conservation of energy, we can say that the power in a differential area of the plane wave is reflected into a differential length on the axis. If we take the ratio of the differential area to the differential length, then we will get the amplitude distribution.

$$dA = 2\pi H dH$$

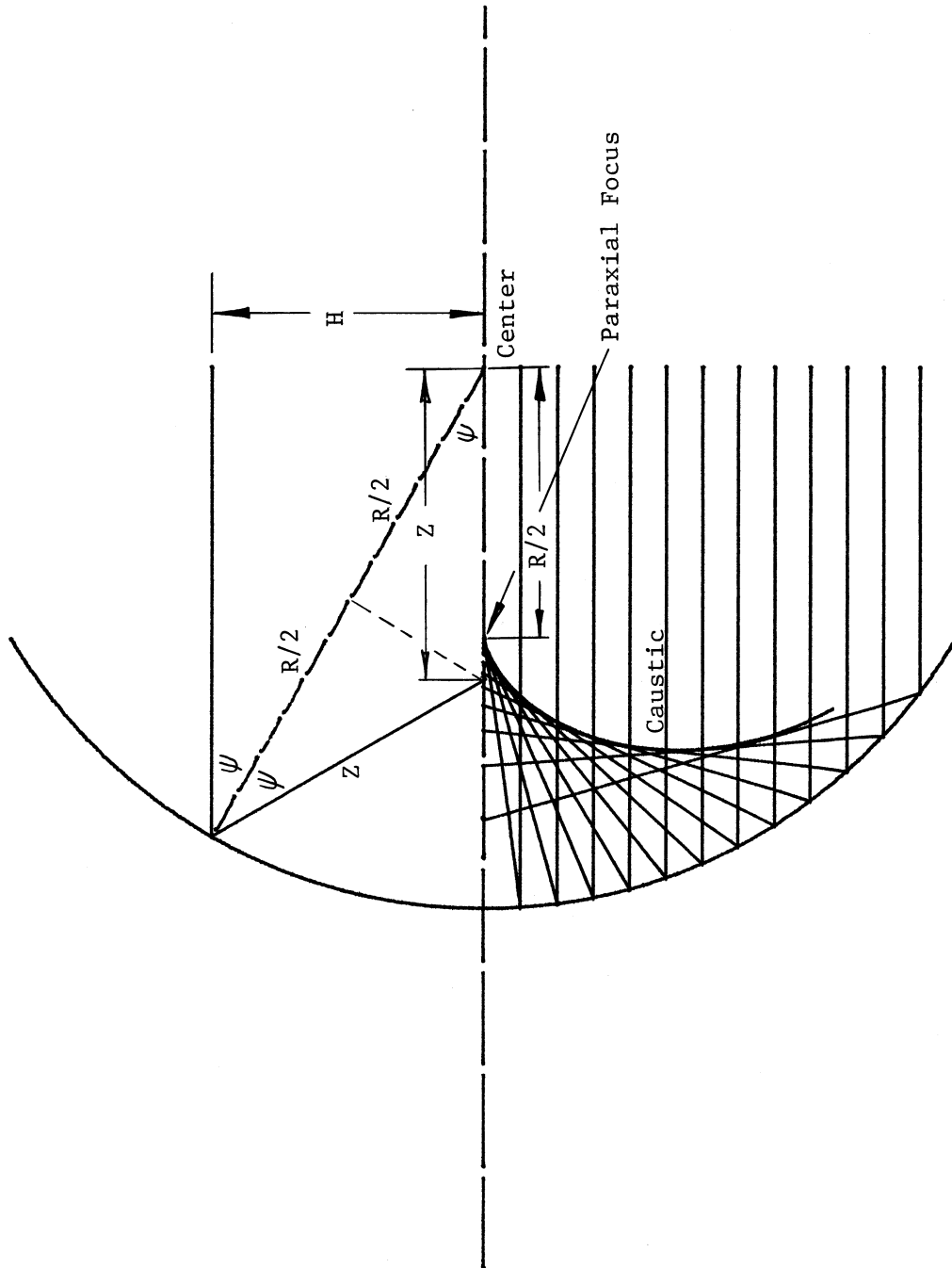
The equation above for the reflected wave can be differentiated implicitly.

$$2 H dH = \frac{R^2}{2 Z^3} dZ$$

The power distribution on the axis is given by $P_z = \frac{\pi B R^2}{2 Z^3}$ where B is a constant.

If we take the limit as H approaches zero, then we find the location of the focus for waves near the axis. This is called the paraxial focus.

Ray Tracing in Spherical Reflector



$$\text{Paraxial Focus} = R/2$$

We can normalize the amplitude to the value at the paraxial focus.

$$P_z = \frac{P_o R^3}{8 Z^3}$$

A plot of this distribution in dB is given on page 668. The required length of the feed is determined by the subtended angle of the reflector. We find this by ray tracing the furthestmost ray and finding the intersection with the axis.

$$\text{Feed Length} = R (1/\cos \psi - 1)/2$$

This function is plotted on the bottom of page 668. For example, if the half subtended angle is 35° , then the feed must be 0.092 radius long and the amplitude will be tapered by 2.2 dB.

Not only does the amplitude along the feed have to be varied, but the phase as well to match the wave intersecting the axis. We need the path length along the ray to the aperture plane as a function of Z . The distance is found from the diagram on page 666.

$$\text{Path Length} = R \cos \psi + Z$$

We can solve for $\cos \psi$ in terms of Z from the equation on the top of page 665.

$$\text{Path Length} = R^2/(2Z) + Z$$

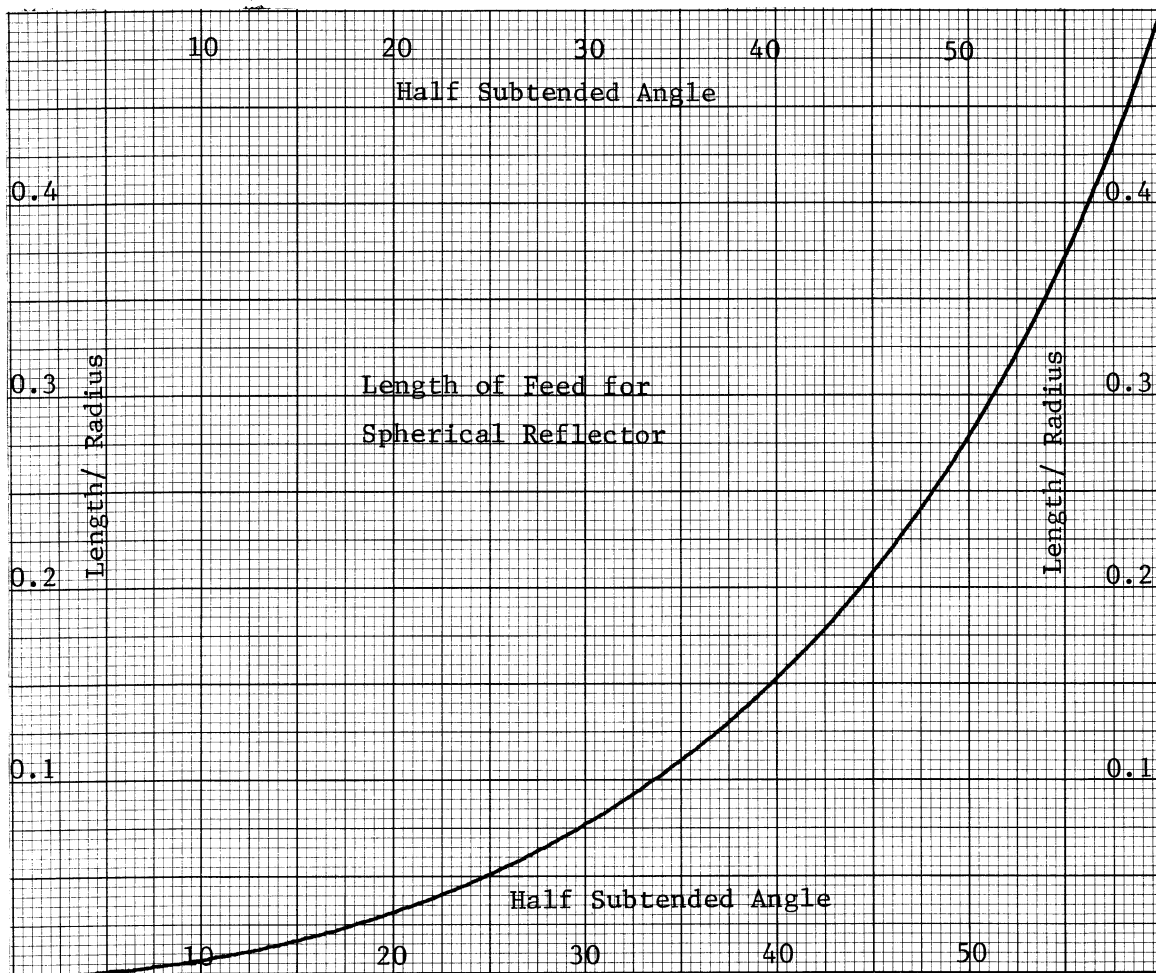
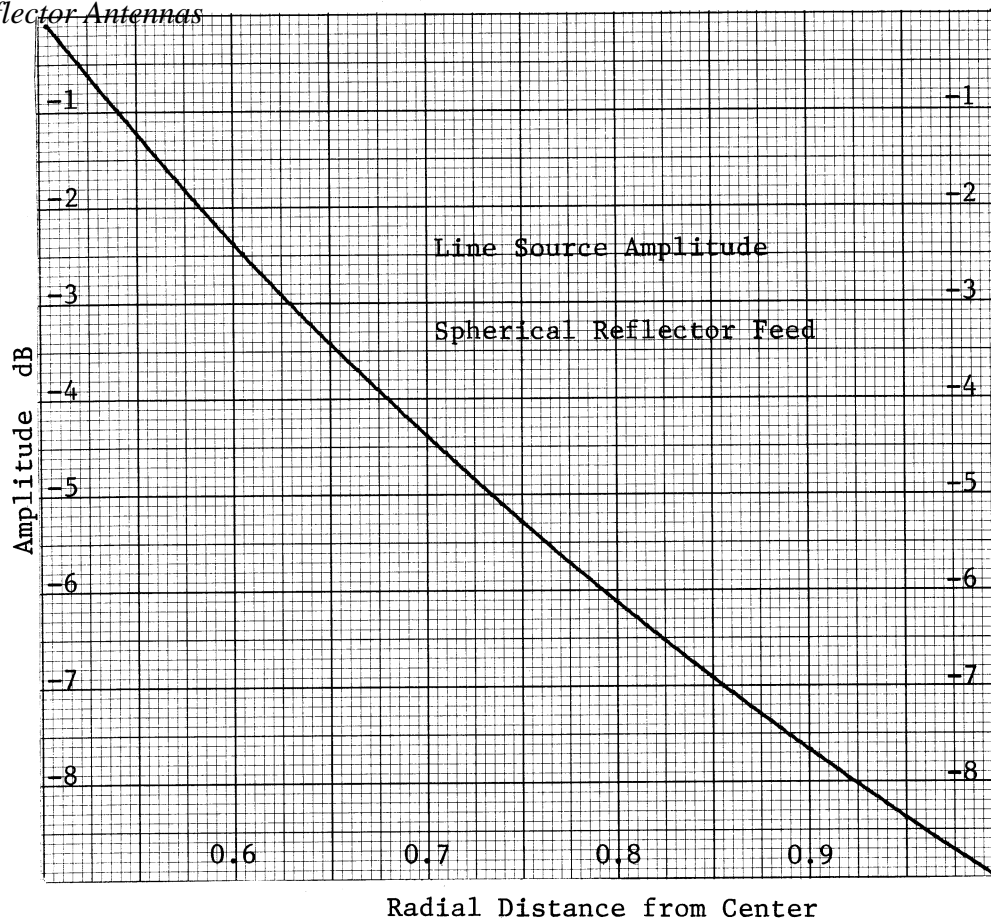
This function is plotted on page 669 relative to the path length at the paraxial focus. For reflectors whose subtended angle is small, the phase along the feed can be approximated by a linear function. The distance changes 0.063 radius in the example above with $\psi_o = 35^\circ$. The phase change along the feed is

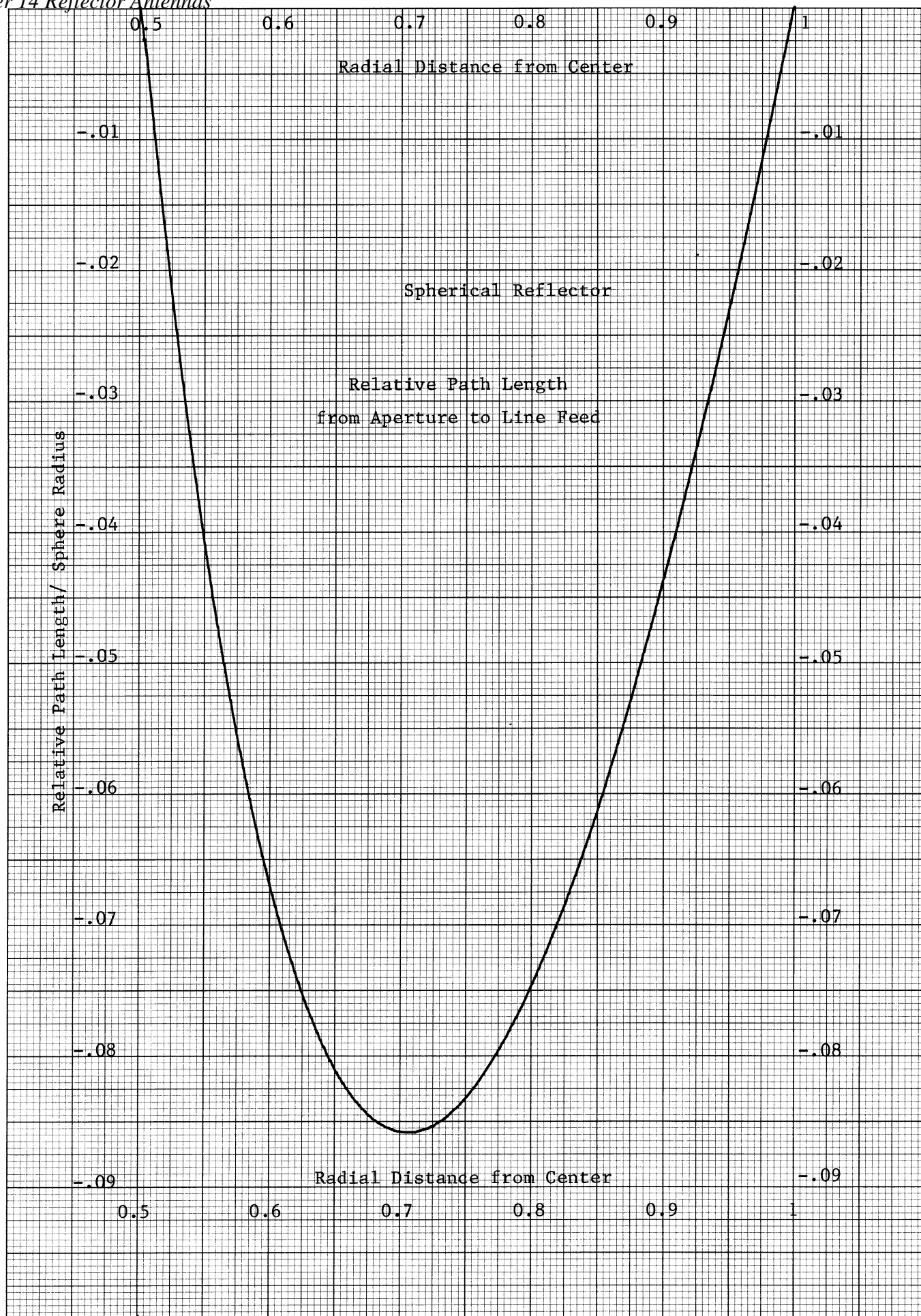
$$\text{Phase change} = \frac{2\pi}{\lambda} R 0.063$$

If the reflector is 10 feet in diameter and operating at 3.9 GHz, the phase change would be 450° . The feed length is 5.52 inches or 1.82 wavelengths. If the feed is a leaky wave antenna, then the relative velocity in the structure should be 1.46. This velocity could be provided by a waveguide structure operating at a frequency = 1.37 (Cutoff Frequency).

CORRECTOR SUBREFLECTOR FOR SPHERICAL REFLECTOR

It is possible to design a subreflector which corrects for the spherical aberration and focuses the rays into a single point. A spherical wave radiated from the focus will be transformed into a plane wave in the aperture. This means that all the ray paths must be equal, since both the sphere around the feed and the aperture plane are eikonals (pp. 580). When we find the surface which gives equal path lengths, then Snell's law of reflection will be automatically satisfied from Fermat's Principle. The ray paths are stationary.





The figure on page 671 shows the geometry of the corrector subreflector. The problem can be treated in 2 dimensions because there is circular symmetry. The focus is located at position (F,0) where F is the distance from the center of the sphere. The corrector crosses the axis at (C,0). Suppose the curve of the corrector is given by W(Z,r). Let us find the path length of the ray. The central ray has the length

$$2R - C + (F - C)$$

This ray is blocked by the corrector but we will pick it to be the length of all the rays. The length of the general ray is

$$\begin{aligned} \overline{PQ} + \overline{QS} + \overline{SF} \\ \overline{PQ} = R \cos \psi \quad \overline{QS} = (Z - R \cos \psi)^2 + (r - R \sin \psi)^2 \\ \overline{SF} = (F - Z)^2 + r^2 \end{aligned}$$

We can equate these path lengths.

$$\begin{aligned} R \cos \psi + (Z - R \cos \psi)^2 + (r - R \sin \psi)^2 + (F - Z)^2 + r^2 \\ = 2(R - C) + F \end{aligned}$$

From the angle, 2ψ , we can find a second relationship.

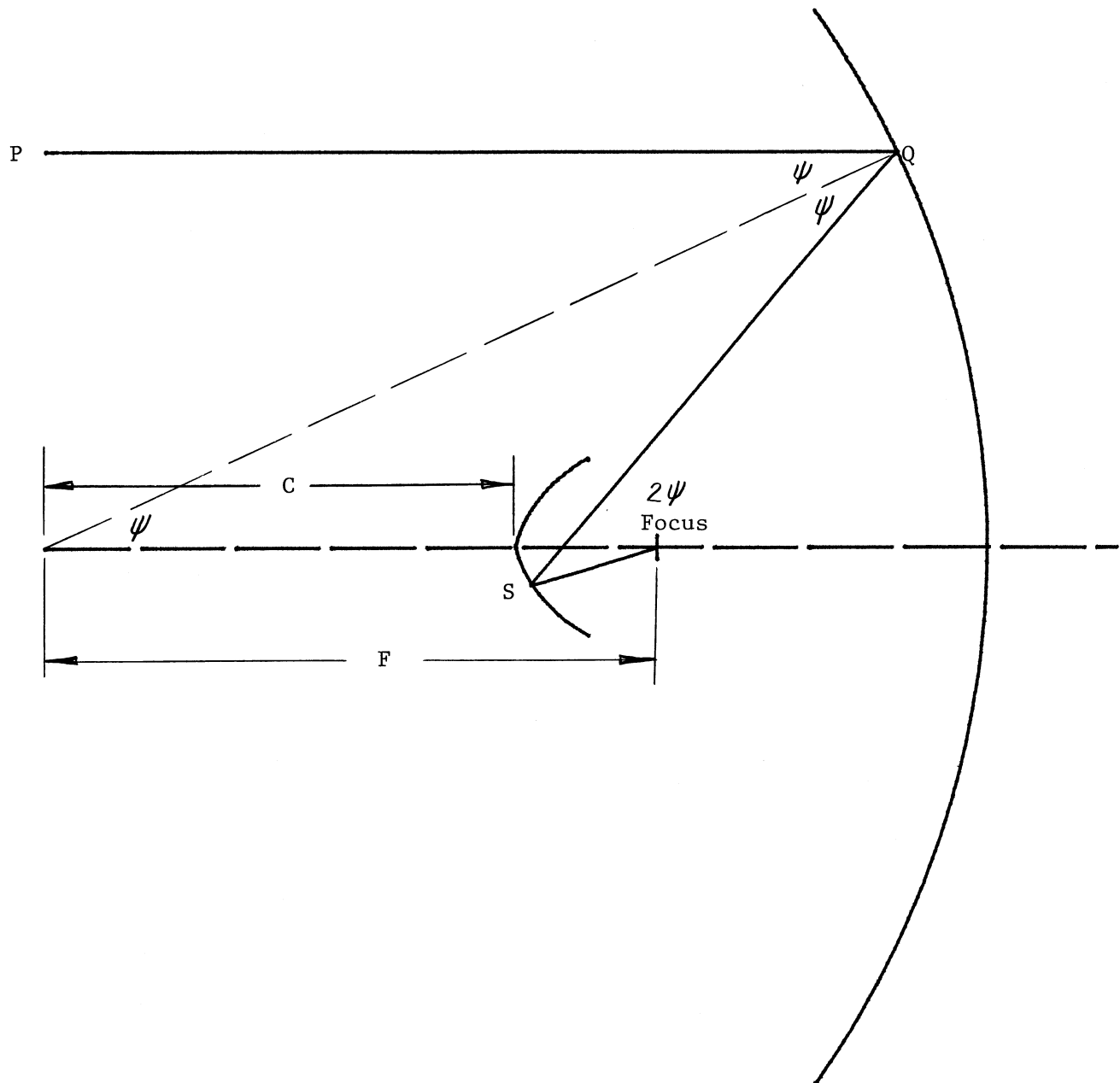
$$(r - R \sin \psi) = (Z - R \cos \psi) \tan 2\psi$$

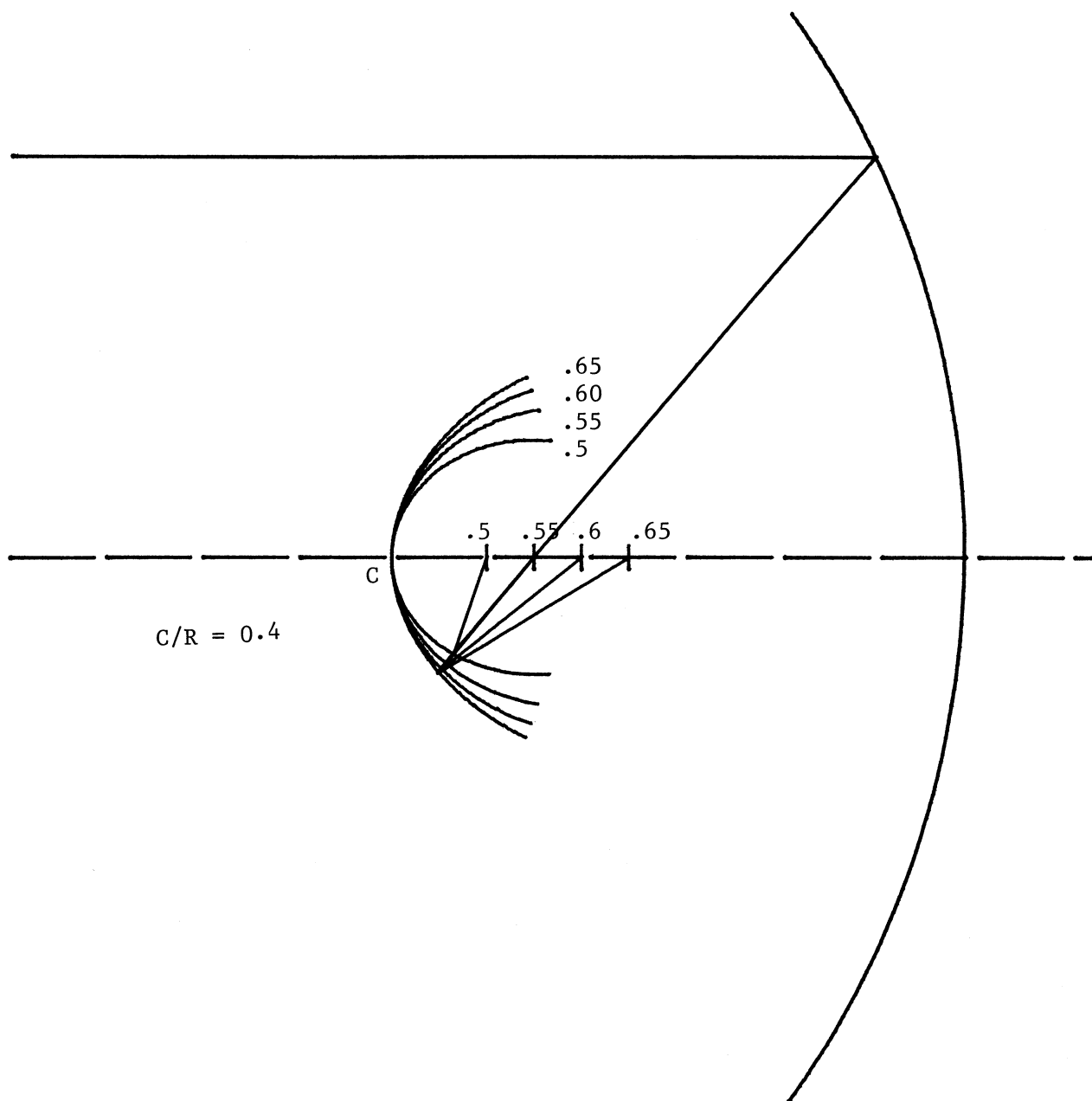
The two equations can be solved for r and Z and normalized to R, the radius of the sphere.

$$\begin{aligned} Z/R &= \cos \psi - (\cos^2 \psi - 4(1 - C/R) \cos \psi - (1 + (F/R)^2) + \\ &\quad (2 + (F/R) - 2(C/R))^2) \cos 2\psi / (4 (F/R \cos^2 \psi - \cos \psi - C/F + 1)) \\ r/R &= (2 Z/R \cos \psi - 1) \sin \psi / \cos 2\psi \end{aligned}$$

The equations have arbitrary parameters: C/R and F/R, which means there is a two space continuum of solutions. Not all designs are practical. C/R can be no larger than 0.5 or the rays from the central portion will strike the subreflector before crossing the axis. If F/R becomes too large compared to C/R, then the subtended angle of the subreflector seen from the feed becomes small and a feed antenna with a small beamwidth will be required which will have a large aperture. There is a trade-off similar to the Cassegrain or Gregorian reflector to be considered. The figure on page 672 points out another potential problem. This figure shows a number of possible subreflectors for C/R = 0.4. When we trace the rays, we find for designs with F/R less than 0.61 that the rays will strike the feed before reaching the subreflector for the portions of the reflector near the edge. Since the feed antenna will have some size, the minimum F/R is 0.65.

Corrector for Spherical Reflector





We can relate the feed pattern of the feed antenna to the aperture distribution by using conservation of energy and differential areas.

$$F(\psi) \sin \psi \, d\psi \, d\phi = A(H) \, H \, dH \, d\phi$$

$F(\psi)$ is the feed pattern, H is the radial distance in the aperture, and $A(H)$ is the aperture distribution (power). The aperture field can be found

$$E(H) = \sqrt{\frac{F(\psi) \sin \psi}{H} \frac{d\psi}{dH}}$$

Consider the paraboloid reflector. $H = 2 F \tan^2 \psi/2$ F is the focal length.

$$dH = F \sec^2 \psi/2 \, d\psi = \rho \, d\psi$$

$$H = \rho \sin \psi$$

If the feed voltage pattern is E_f , we take it out of the radical and get the result:

$$E(H) = E_f(\psi) \sqrt{\frac{\sin \psi}{\rho \sin \psi} \frac{1}{\rho}} = E_f(\psi) / \rho$$

This is the same result we get on page 589 assuming a spherical source.

We can use this result to find the aperture field distribution for the spherical reflector with a corrector. On page 674 is plot showing the aperture distribution for an isotropic feed and ones tapered toward the edge of the subreflector for $C/R = 0.4$ and $F/R = 0.65$. These plots show the central blockage. The losses can be found by integrating the feed pattern and aperture distribution.

	10 dB Taper	20 dB Taper
Amplitude Taper Loss	0.05 dB	0.38
Spillover Loss	0.64	0.56

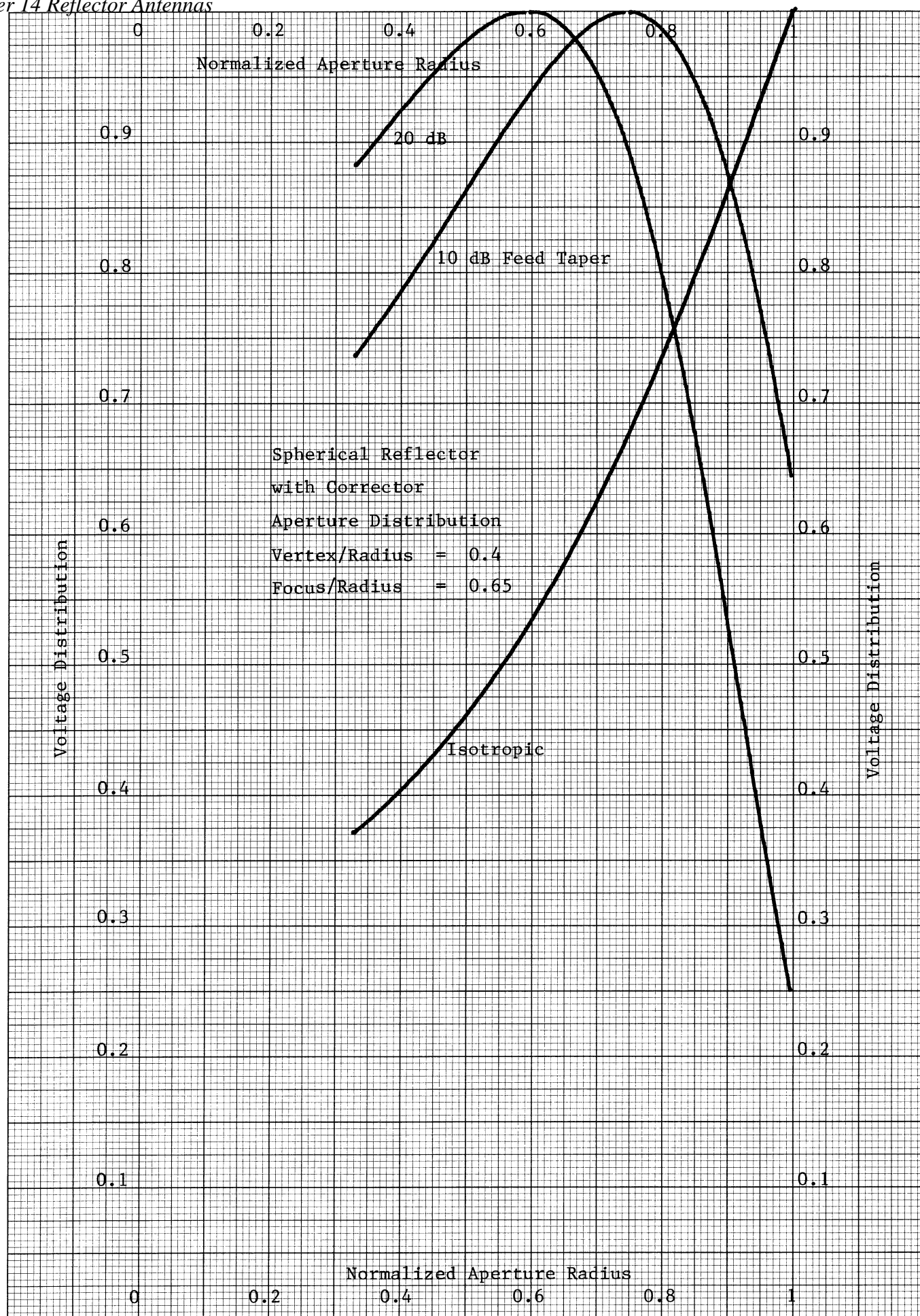
These were found using the formulas on pages 608 and 609 for blocked apertures. There is also a blockage loss if we want to compare to the full diameter of the possible aperture.

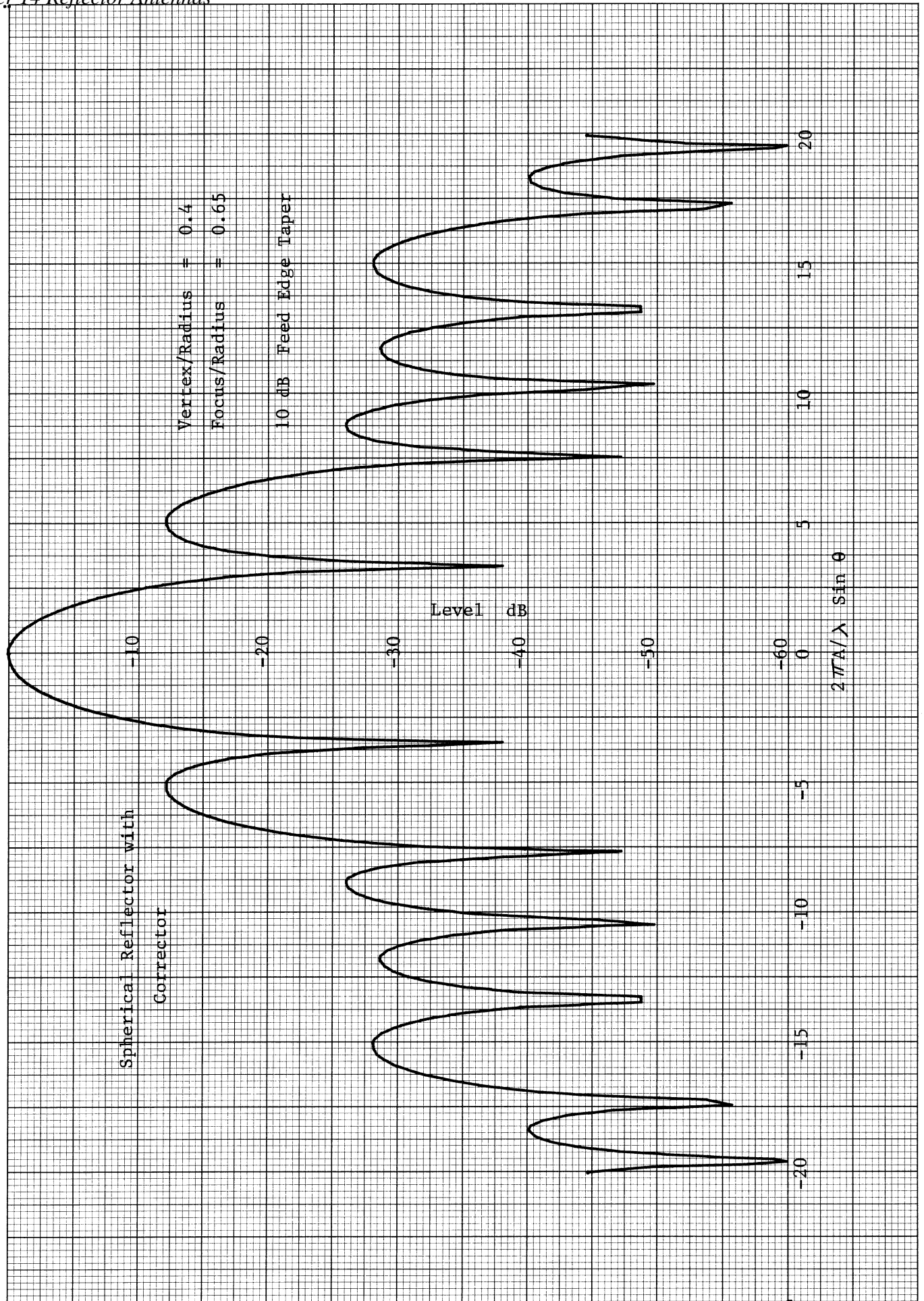
$$\text{Blockage Loss} = 10 \log(1 - (H_{\min}/H_{\max})^2)$$

The corrector subreflector blocks about 33% of the radius of the projected sphere.

$$\text{Blockage Loss} = 0.5 \text{ dB}$$

The spillover loss includes the energy which is blocked by the corrector. A parabolic reflector with similar feed taper and central blockage would have losses of about 2.1 dB. The 10 dB taper case above only has 1.2 dB of loss. It is less because the subreflector has reflected the energy out to the edges of the aperture.



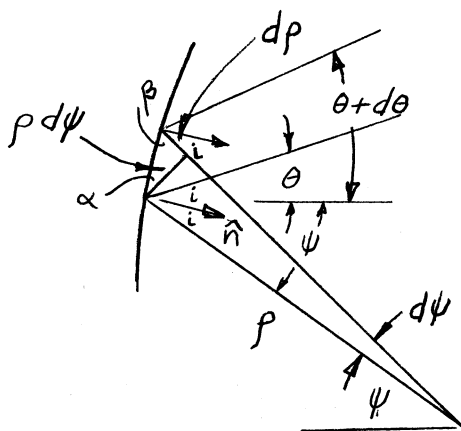


More details of the spherical reflector corrector can be found in the original paper: F. S. Bolt and E. L. Bouche, "A Gregorian Corrector for Spherical Reflectors", IEEE Trans. on Antennas and Propagation, vol. AP-12, pp. 44-47, Jan. 1964 and in the book: Antenna Theory, Part II edited by R. E. Collin and F. J. Zucker.

SHAPED REFLECTORS

We have used a geometric optics method to relate the field from a spherical source to a second eikonal surface, the aperture plane of the corrected spherical reflector. At this point the far field pattern is found from the aperture distribution. Only by using diffraction theory is a pattern found. Geometric optics predicts a pencil beam only in the projection of the aperture. We will use geometric optics to find the shapes of reflectors which spread the energy in defined patterns. But because of diffraction effects, the final pattern must be found by considering the field distribution on an aperture, the currents induced on the reflector, or by including diffracted fields from the edges of the reflector (GTD) with the geometric optics field.

Two principles are used to design shaped reflectors. The first is the geometric optics reflection. The second is the conservation of energy in ray tubes. The reflection is expressed as a differential. Conservation of energy can be expressed either in terms of differential areas or integrals. Consider a ray in the plane of incidence on a reflector and the corresponding differential angles about the incident and reflected rays. We will assume that the ray is emitted from some point source which could be either spherical or cylindrical.



The sum of the angles θ and ψ is twice the incident angle, i .

$$\theta + \psi = 2i$$

If we consider the differential triangle at the surface, we find the slope of the reflector.

$$\tan \alpha = \frac{dp}{\rho d\psi}$$

The angle ψ has only changed by a differential amount, so the angle of incidence at $\psi + d\psi$ along the reflector is still i in the limit. The sum of the angle β of the differential triangle and the angle of incidence is normal to the surface.

$$\beta + i = \pi/2$$

The length $\rho d\psi$ is normal to the line defined by $\psi + d\psi$, therefore

$$\alpha + \beta = \pi/2 \quad \beta = \pi/2 - \alpha$$

$$i + \pi/2 - \alpha = \pi/2 \quad \text{or} \quad \alpha = i$$

Combining these equations gives us the differential relationship of the geometric reflection.

$$\tan((\theta + \psi)/2) = \frac{d\rho}{\rho d\psi}$$

We can integrate this differential equation for a solution.

$$\ln \frac{\rho(\psi)}{\rho_0(\psi_1)} = \int_{\psi_1}^{\psi} \tan \frac{\theta(\psi) + \psi}{2} d\psi$$

ψ_1 is some initial angle of the feed to some point on the reflector. θ is a function of ψ . $\rho_0(\psi_1)$ is some arbitrary constant which defines the initial radius. Geometric optics is a zero wavelength approximation and is consistent at any size. This is the same with the parabolic reflector. All parabolic reflectors collimate the beam, but size is arbitrary from geometric optics. Only by considering diffraction or currents induced on the reflector can we find the gain and beamwidth of the antenna.

Take the case $\theta(\psi) = 0$.

$$\ln \frac{\rho(\psi)}{\rho(\psi_1)} = \int_{\psi_1}^{\psi} \tan \psi/2 d\psi = -2(\ln \cos(\psi/2) - \ln \cos(\psi_1/2))$$

Using the properties of the natural logarithm, this becomes

$$\ln \frac{\rho(\psi)}{\rho(\psi_1)} = \ln \left(\frac{\cos^2(\psi_1/2)}{\cos^2(\psi/2)} \right)$$

Taking the exponential of each side we get the polar equation of the reflector.

$$\rho(\psi) = \rho(\psi_1) \frac{\cos^2(\psi_1/2)}{\cos^2(\psi/2)}$$

If $\psi_1 = 0$, then we can set $\rho(\psi_1) = F$ and obtain the equation for the parabola given on page 585. This is a known result because if $\theta(\psi) = 0$ then a cylindrical or spherical wave has been converted into a plane wave by the reflector.

The differential equation of the reflection only tells us the shape of the reflector for a given direction of reflection and incident waves, $\theta(\psi)$. We must still find the power density in various directions. This is found from the ratio of differential areas and the conservation of energy. If the feed power pattern is $G_f(\psi, \phi')$ and $P(\theta, \phi)$ is the reflected field, then the two are related for a given ray.

$$K P(\theta, \phi) dA(\theta, \phi) = G_f(\psi, \phi') dA_f(\psi, \phi')$$

K is a constant which is found by equating the total powers incident and reflected from the surface. This is assuming that the reflections are one to one with the feed pattern. If they are not, then the right hand side of the equation is a sum. But the sum must be over field intensity instead of powers. Each ray will have an associated phase depending on the path length and the feed pattern phase. This forms the basis for GTD where the waves are diffracted in all directions from an edge and add to the reflected waves and direct waves from the feed.

CYLINDRICAL REFLECTOR SYNTHESIS

We have concentrated on circularly symmetric reflectors, but we can also feed cylindrical reflectors with a line source antenna. The surface is generated by a curve which has been moved along a line parallel to the Z axis. Pattern multiplication establishes the total pattern. The reflector establishes the beam in one plane and the line source in the other. It also reduces the problem to a two dimensional one.

The power radiated by the feed in a particular direction is given by

$$G_f(\psi) d\psi$$

where $G_f(\psi)$ is the feed antenna power pattern. This power is reflected in the direction θ . The reflected power density is given by

$$P(\theta) d\theta$$

These are proportional $G_f(\psi) d\psi = K P(\theta) d\theta$

The limits of the reflector are ψ_1 and ψ_2 which are reflected into angles θ_1 and θ_2 , respectively. The total power incident on the reflector is equal to the total power reflected.

$$\int_{\psi_1}^{\psi_2} G_f(\psi) d\psi = K \int_{\theta_1}^{\theta_2} P(\theta) d\theta$$

This established the constant K . We can integrate the differential equation to find a formal solution.

$$\int_{\theta_1}^{\theta} P(\theta) d\theta = \frac{1}{K} \int_{\psi_1}^{\psi} G_f(\psi) d\psi$$

This equation is used with a known feed and pattern functions to find the relationship $\theta(\psi)$ which is used with the reflection differential equation

to find the reflector shape. The reflector is found only to within a scaling constant.

$$\rho(\psi) = \rho(\psi_1) e^{\int_{\psi_1}^{\psi} \tan((\theta(\psi) + \psi)/2) d\psi}$$

Only in a few cases will the feed pattern and the reflected pattern be known as analytic functions. The feed pattern maybe measured or in the case of a horn antenna found from an integration over an aperture. In these cases it is necessary to perform numerical integrations in the energy balance differential equation. A table can be generated for integral of the end point, θ , for example, and the value of the integral. This is done for each integral with the feed pattern integral values multiplied by the constant $1/K$. Using interpolation routines, θ can be related to a given ψ . This can also be done graphically. Once we have a relationship between θ and ψ , or a means of calculating it, we can use the relationship above to find the polar equation of the reflector to within a scaling constant.

TOROIDAL REFLECTOR

The cylindrical reflector can be evolved into a reflector with circular symmetry forming a toroidal reflector. A diagram of the toroidal reflector is given on page 680. A curve has been rotated about some center line to form a torus reflector. The line feed of the cylindrical reflector becomes a ring source around the reflector as shown. We will assume that the feed and reflector are symmetric about the axis so that we can reduce the problem to two dimensions. The feed pattern and the reflector pattern will be independent of ϕ . The geometry of the problem is defined on page 681. If we refer to the drawing on page 676, we can relate these angles to the old ones and determine that the differential equation of reflection is the same.

$$\frac{d\rho}{\rho d\psi} = \tan((\theta + \psi)/2)$$

This means that we can use the same integral solution to this equation once we have found the relationship between θ and ψ .

The power radiated by the feed in a particular direction must be related to the spherical coordinate system.

$$G_f(\psi) \sin \psi d\psi d\phi$$

The reflector pattern power density is also in spherical coordinates.

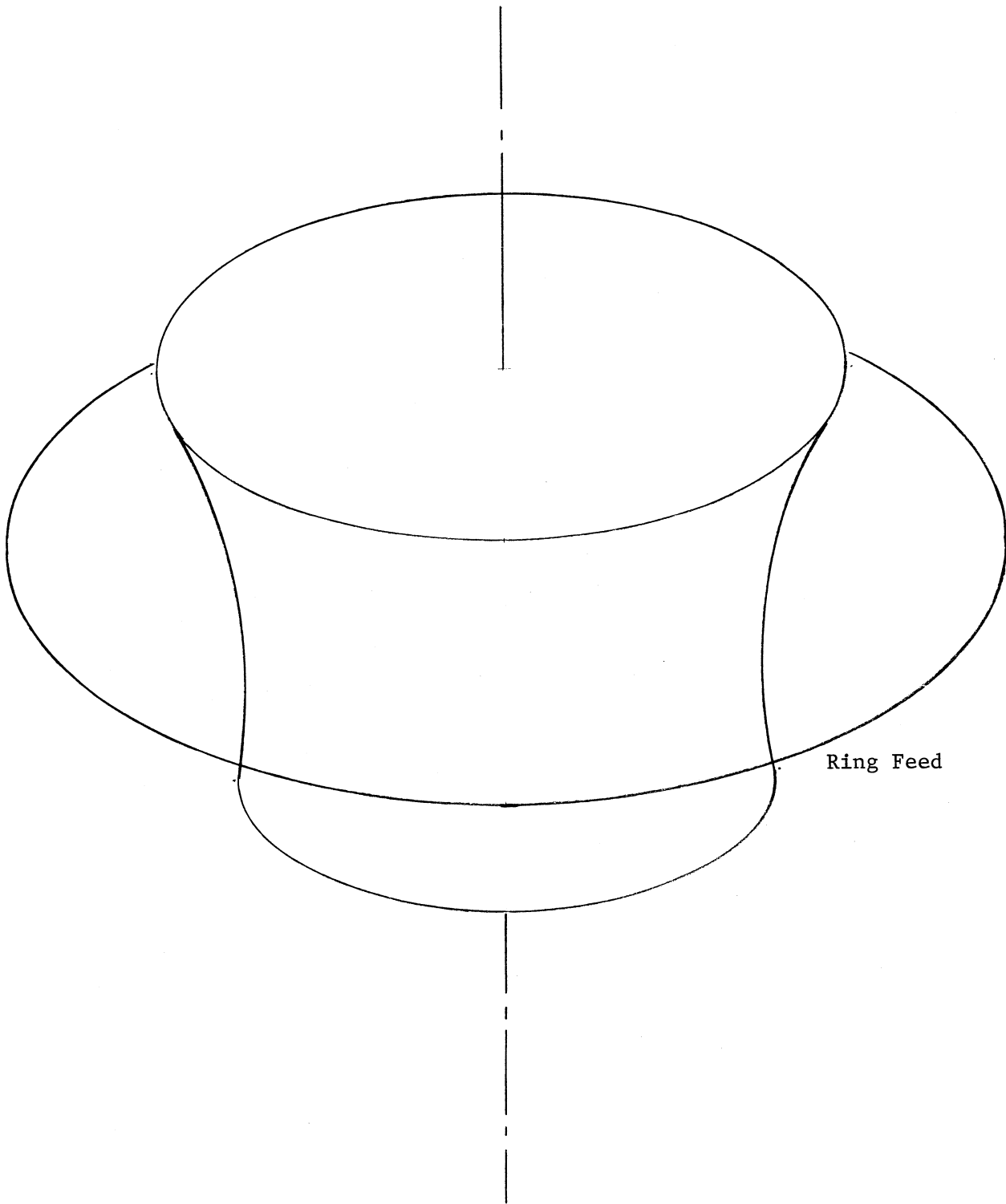
$$P(\theta) \sin \theta d\theta d\phi$$

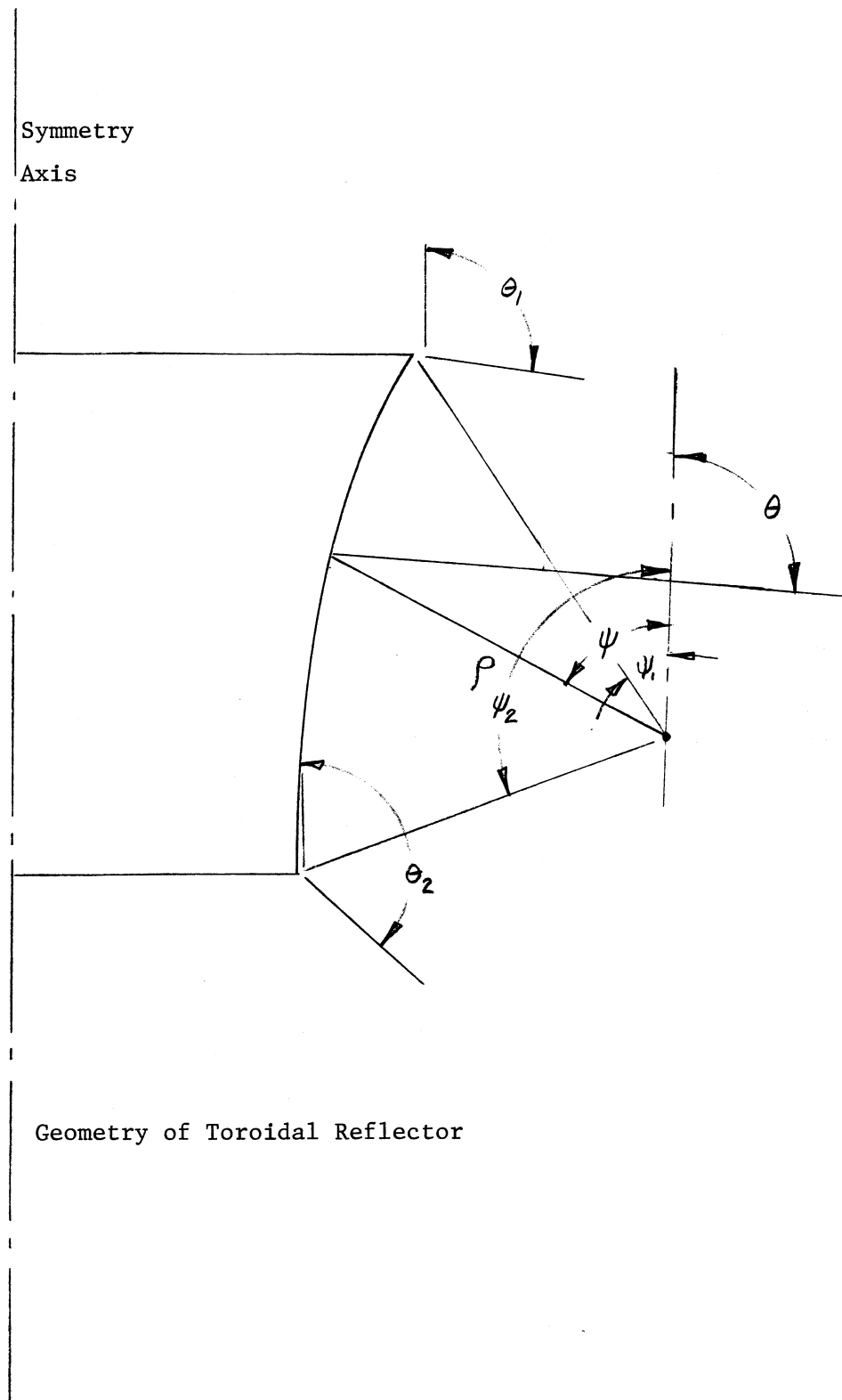
$$G_f(\psi) \sin \psi d\psi = P(\theta) \sin \theta d\theta K$$

The constant K is found by equating the total power reflected to the total power incident on the reflector.

$$K = \frac{\int_{\psi_1}^{\psi_2} G_f(\psi) \sin \psi d\psi}{\int_{\theta_1}^{\theta_2} P(\theta) \sin \theta d\theta}$$

Toroidal Reflector





The differential equation equating the power densities can be integrated to find a solution.

$$\int_{\theta_1}^{\theta} P(\theta) \sin \theta d\theta = \frac{1}{K} \int_{\psi_1}^{\psi} G_f(\psi) \sin \psi d\psi$$

With known feed pattern, $G_f(\psi)$, and known reflector pattern, $P(\theta)$, both sides of this equation can be integrated to find a relationship between θ and ψ . At this point we have the same problem as on page 678 only the integrals have changed. The relationship is established by equating values of the integrals which must be done graphically or by numerical interpolation from tables of values.

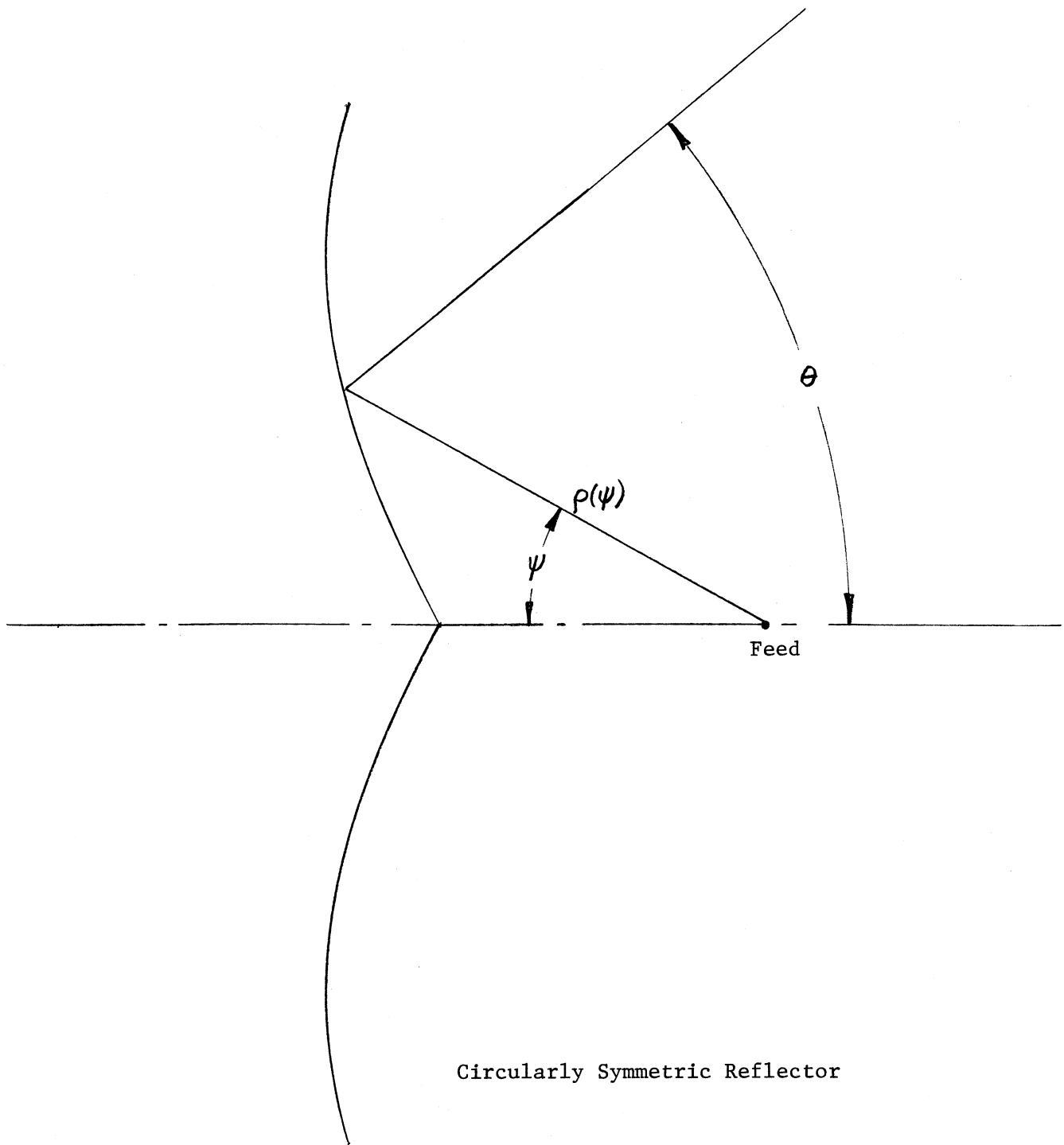
CIRCULARLY SYMMETRIC REFLECTOR

The toroidal reflector can be evolved into a circularly symmetric reflector by rotating the ring feed up until it is on the Z axis. The ring shrinks to a point feed. A diagram showing the geometry of the reflector is on page 683. The angles are the same as shown on page 676. The differential areas are found in spherical coordinates just like the toroidal reflector and the same set of equations apply here for the synthesis of the reflector surface.

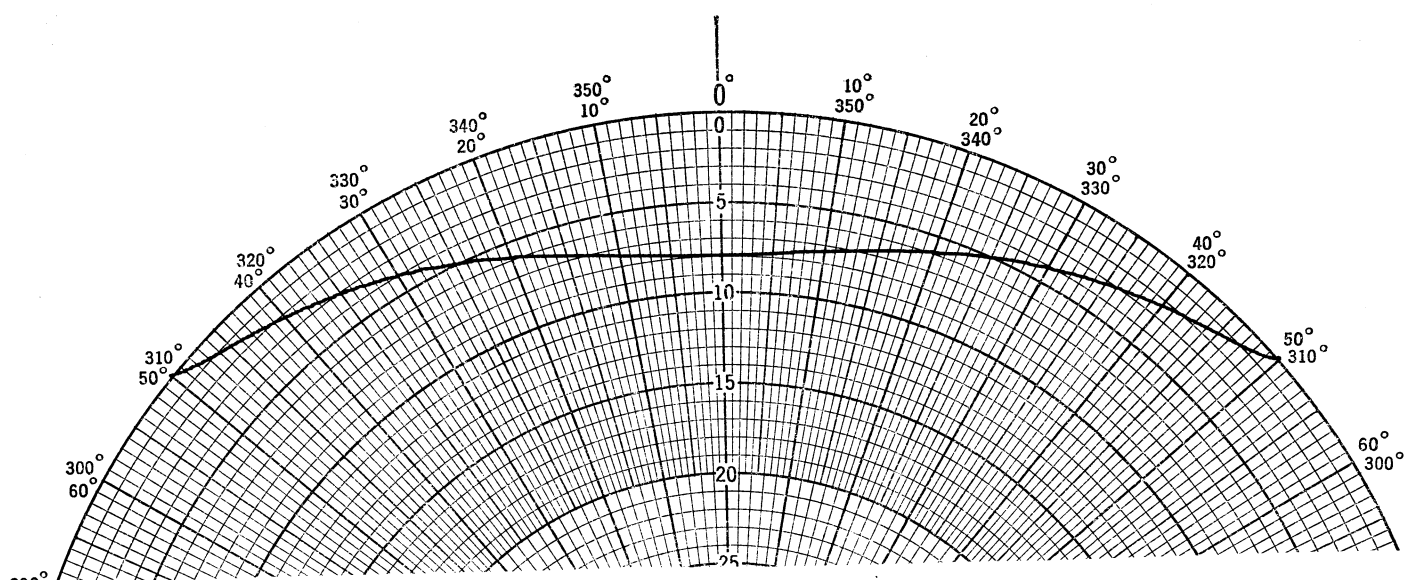
We will use this reflector for a design example to illustrate the method which is used for cylindrical, toroidal, or circularly symmetric reflectors. The integrals over the feed and reflector patterns differ only slightly in the different cases. Suppose we are designing a reflector for a spacecraft to transmit a pattern which is vertically polarized on the surface of the earth. The satellite is 1000 nautical miles high. The visible portion of the earth will extend a little more than 50° from nadir. Because the pattern must be vertically polarized, we cannot expect to transmit to a station directly below. We can shape the reflector pattern so that it compensates for the increased range to the horizon compared to inner angles. On page 684 is a plot showing a pattern which would compensate for the increased range. Our required pattern will extend from 30° to 50° where most of the visible surface is contained. This is $P(\theta)$ with $\theta_1 = 30^\circ$ and $\theta_2 = 50^\circ$.

A feed antenna which will give us vertical polarization everywhere is a circular waveguide horn excited in the TM_{01} mode. This mode has circular symmetry so we can use a symmetric reflector. We will pick a reflector which has a half subtended angle of 50° . From the feed point of view this is equivalent to an $F/D = 0.54$. A suitable feed pattern is shown on the bottom of page 684. The pattern is down by 9 dB at the edge of the reflector. We will also cut a hole in the center of the reflector at the other 9 dB point, 5° . Our feed pattern angle, ψ , extends from 5° to 50° .

We will pick the reflection from $\psi = 5^\circ$ to be $\theta = 30^\circ$ and from $\psi = 50^\circ$ to be $\theta = 50^\circ$. This is arbitrary because we can reverse the reflections. In this design there will be no caustic, a place where rays cross. We must perform the energy integrals over the feed and reflection patterns. If we normalize each of these to the total integrals between the end angles of the feed or reflection pattern, then we can equate the normalized integrals. On page 685 is a plot of the two normalized integrals versus the feed angle or the reflection angle. These have been found by numerical integration of the patterns. We use this diagram to find the relationship between θ and ψ .



Range Compensation Pattern for a Satellite @ 1000 nm



CIRCULAR WAVEGUIDE HORN IN TM-01 MODE

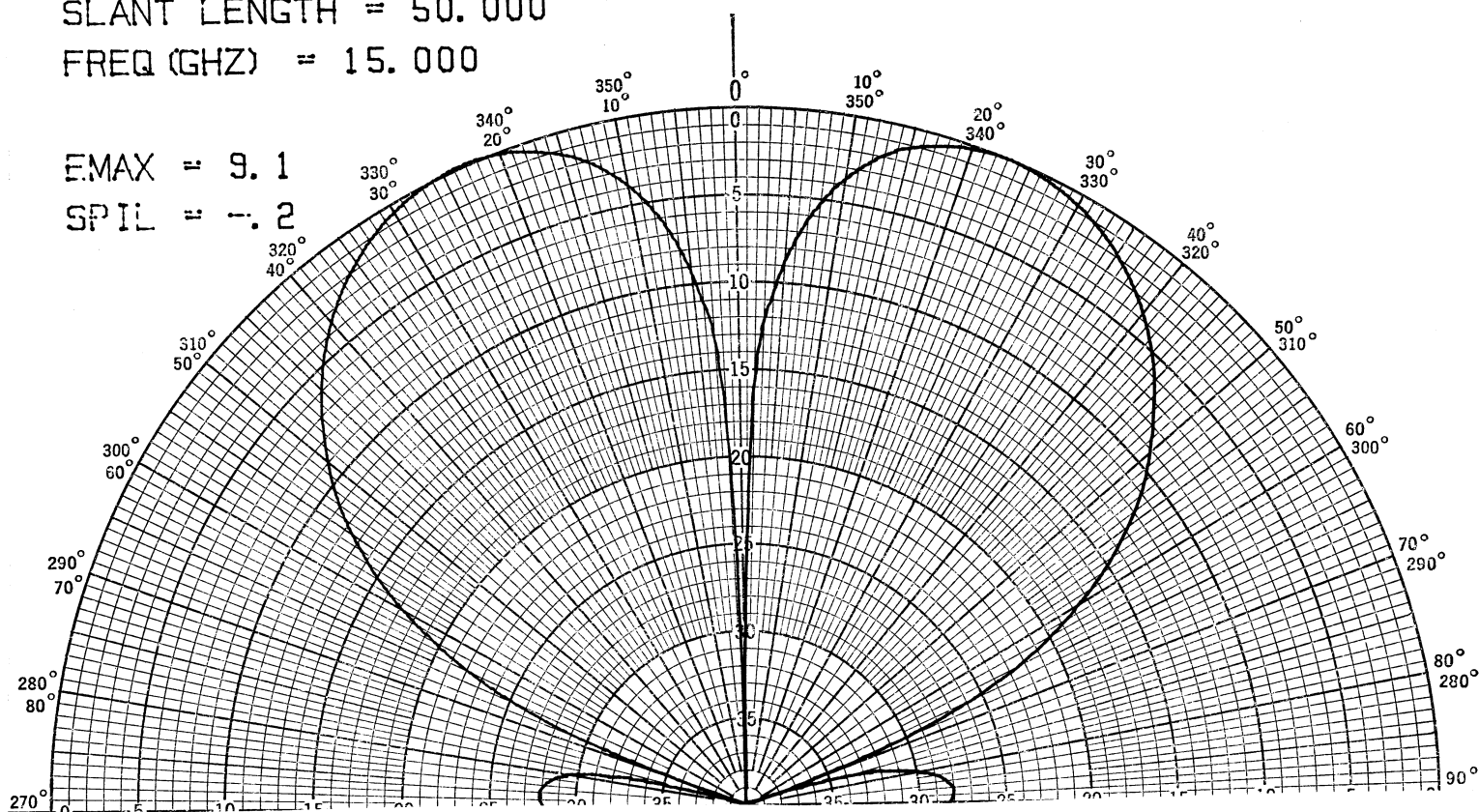
APERTURE R. = .726

SLANT LENGTH = 50.000

FREQ (GHZ) = 15.000

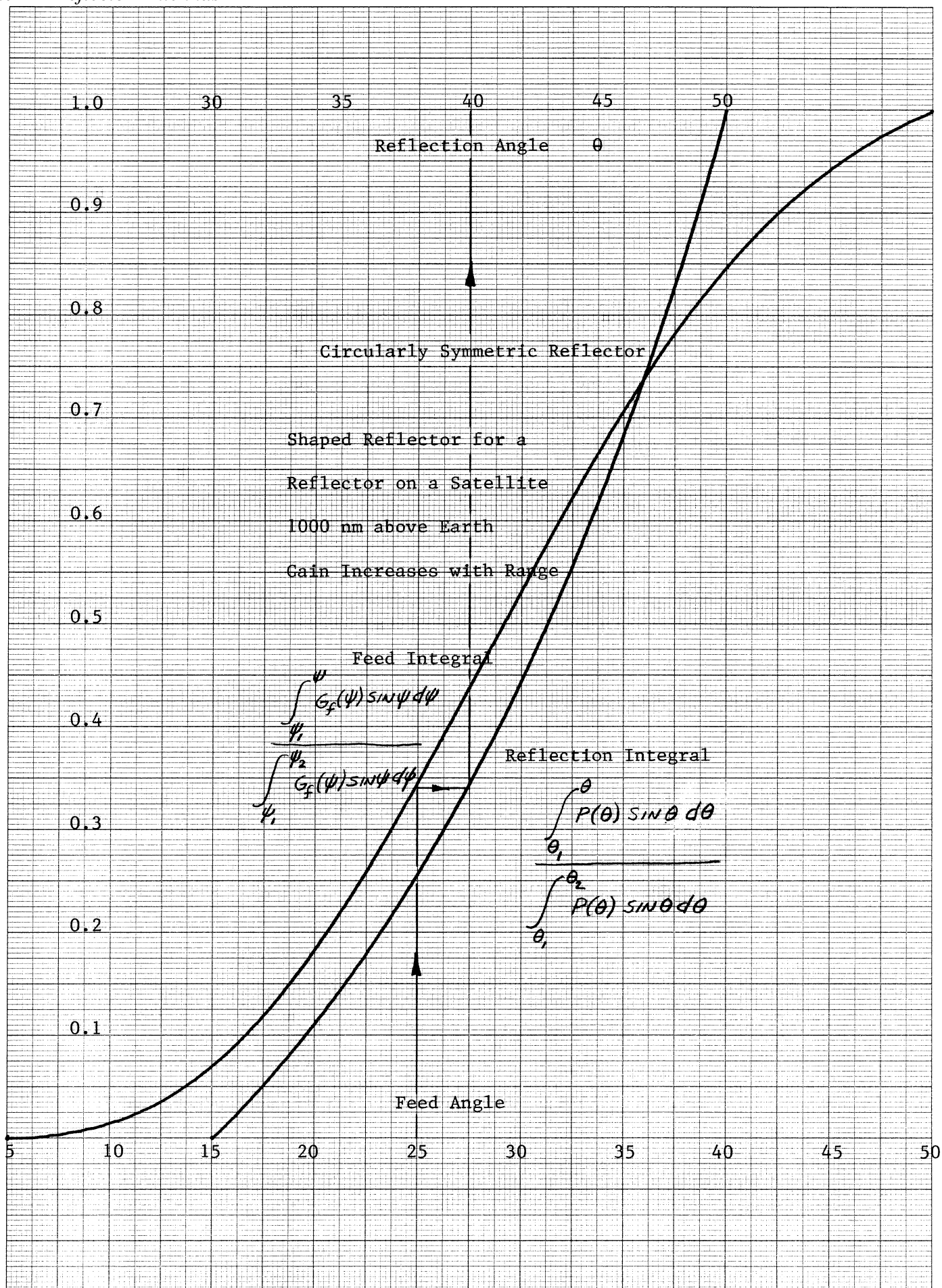
EMAX = 9.1

SPIL = -.2



46 1510

K&E 10 X 10 TO THE CENTIMETER 18 X 25 CM.
KEUFFEL & ESSER CO. MADE IN U.S.A.



These integrals over the patterns are equal when for a given feed angle, the wave is reflected in a given direction θ . Traced on the plot is the example of $\psi = 25^\circ$. From the 25° feed angle scale draw a vertical line to the normalized feed integral curve. At the intersection draw a horizontal line to the curve of the normalized reflection pattern integral. From the point of intersection of the of the horizontal, draw another vertical line to the scale on the top of the graph. This is the reflection angle, 40° . Of course, the end points are $\psi = 5^\circ$ to $\theta = 30^\circ$ and $\psi = 50^\circ$ to $\theta = 50^\circ$ which is what was picked as the end points. After we draw sufficient sets of these contructions, we can plot a curve of θ versus ψ . This has been done on page 687.

With a given relationship between θ and ψ , the differential equation of the geometric reflection can be integrated to find a normalized polar equation of the reflector. The required equation is given on the top of page 679.

$$\frac{\rho(\psi)}{\rho(\psi_0)} = e^{\int_{\psi_0}^{\psi} \tan((\theta(\psi) + \psi)/2) d\psi}$$

Like the feed and reflection pattern integrals, numerical methods can be used with this integral to find the normalized radius. Below is a table of the normalized polar equation of the reflector.

Angle	Radius	Angle	Radius	Angle	Radius
5	1.0	21	1.1241	37	1.3768
6	1.0056	22	1.1352	38	1.3989
7	1.0114	23	1.1468	39	1.4220
8	1.0175	24	1.1590	40	1.4460
9	1.0237	25	1.1717	41	1.4709
10	1.0303	26	1.1850	42	1.4969
11	1.0371	27	1.1990	43	1.5239
12	1.0441	28	1.2135	44	1.5520
13	1.0515	29	1.2288	45	1.5812
14	1.0592	30	1.2446	46	1.6116
15	1.0673	31	1.2612	47	1.6432
16	1.0757	32	1.2786	48	1.6760
17	1.0845	33	1.2966	49	1.7103
18	1.0937	34	1.3154	50	1.7459
19	1.1034	35	1.3350		
20	1.1135	36	1.3555		

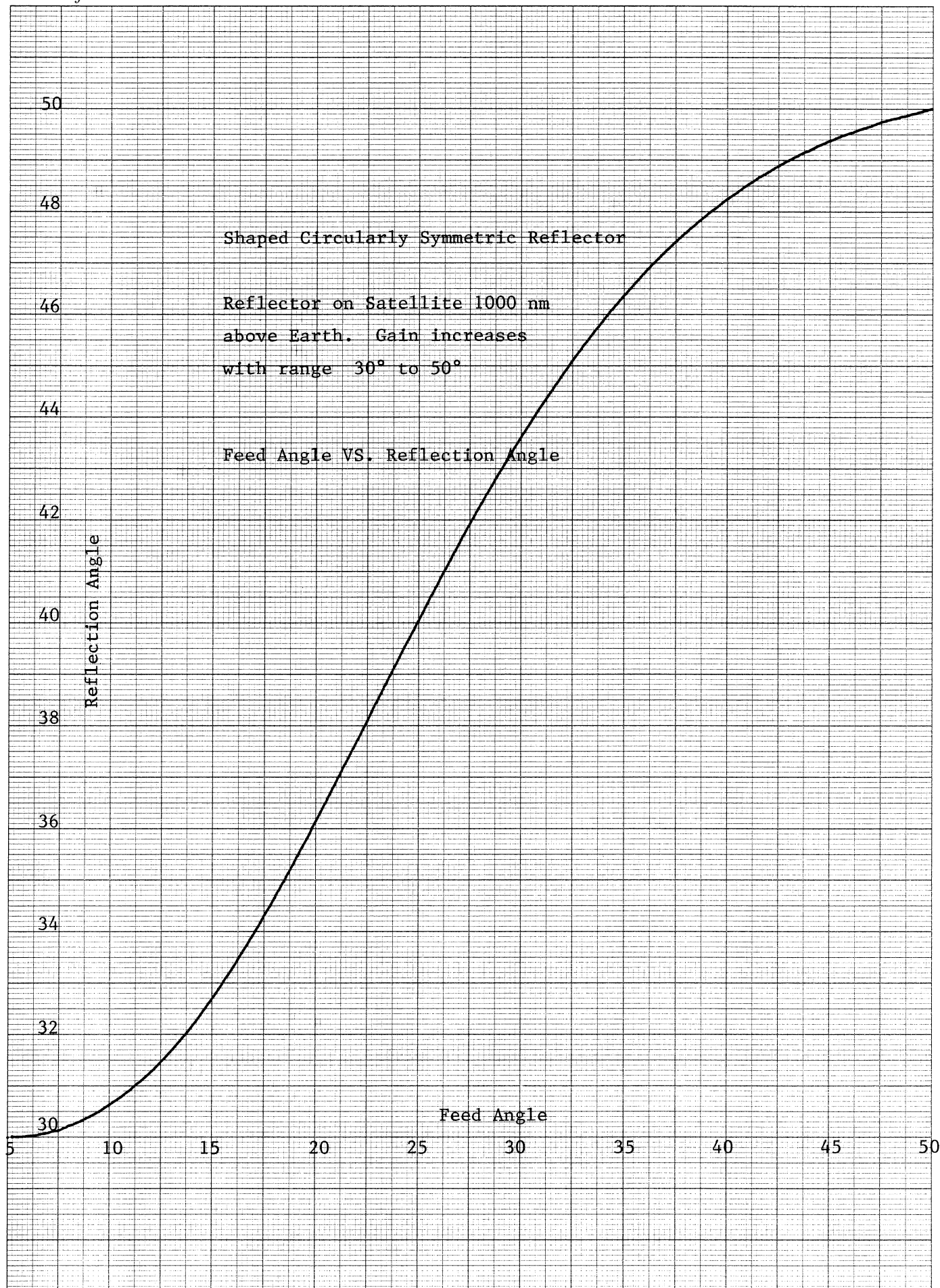
A cross sectional diagram is drawn on page 688. The reflector has a hole in the center because that portion was not specified. The feed horn has little pattern energy in that direction anyway.

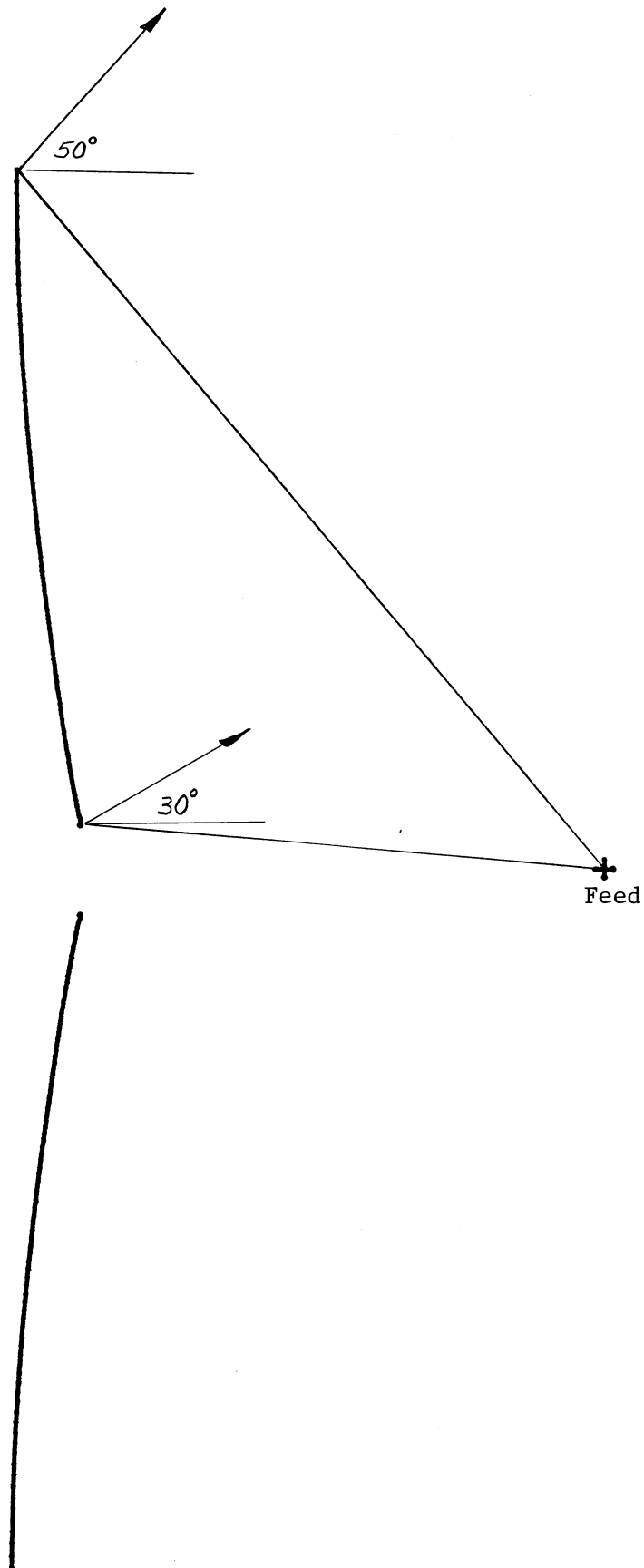
The reflector can also be designed so that the inner edge reflects the feed energy toward 50° while the outer edge reflects toward 30° . This reflector is said to have a caustic because the rays will cross in front of the reflector. Another reflector was designed using the same steps given above. A scale drawing of this reflector surface is given on page 689 along with the previous design.

We usually think of a reflector as something to decrease the beamwidth of the

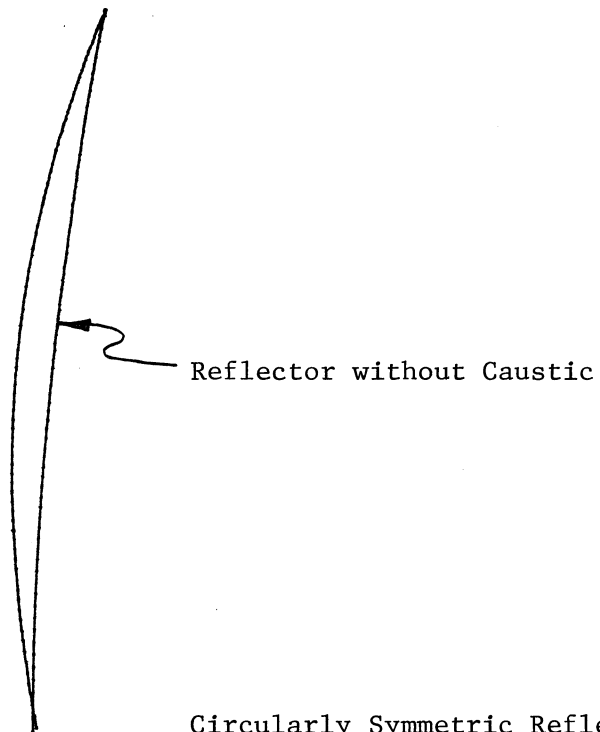
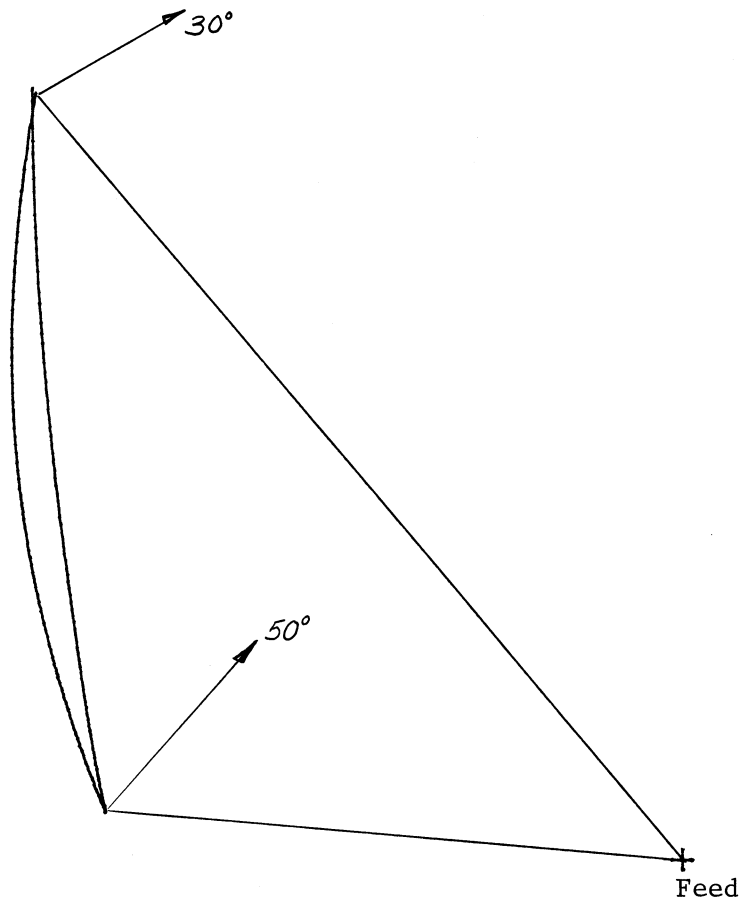
46 1510

10 X 10 TO THE CENTIMETER
KEUFFEL & ESSER CO. MADE IN U.S.A.





Circularly Symmetric Reflector
without Caustic Reflection



Circularly Symmetric Reflector
with Caustic

feed. A reflector was designed to transform the same feed pattern into the pattern on the top of page 684 from $\theta = 0^\circ$ to $\theta = 50^\circ$ for the satellite at 1000 nm. The reflector design proceeds just the same. The result is given on page 691. The reflector without a caustic is convex to spread the beam. Since we can redirect the energy with the reflector, we can fill the hole in the feed pattern. Unfortunately, the polarization effects will insert a null.

A reflector can be designed with a constant angle θ_0 for reflection. We can substitute this directly into the reflection differential equation as was done on page 677 and integrate. The result is the polar equation

$$\rho(\psi) = \rho_0 \frac{\cos^2((\psi_0 + \theta_0)/2)}{\cos^2((\psi + \theta_0)/2)}$$

This curve is sometimes called a paraconic. A curve which will give a beam at 50° is given on page 692.

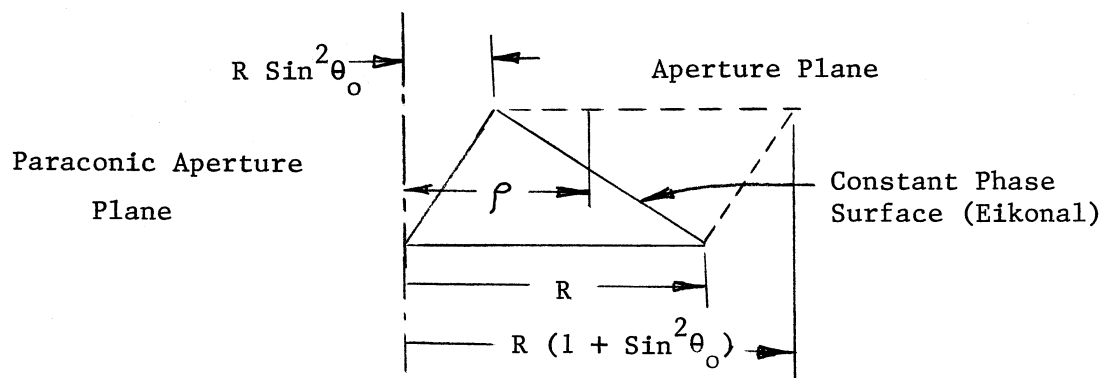
We can find the gain of the paraconic by aperture integration or physical optics. Before we do that, we will estimate the gain from a scanned aperture. Suppose we have a paraconic which is 40 wavelengths in diameter and is scanned to 50° as the reflector on page 692. The beam is formed on each side by an aperture which is only one-half the total. There is a phase taper in the aperture plane to tilt the beam to 50° .

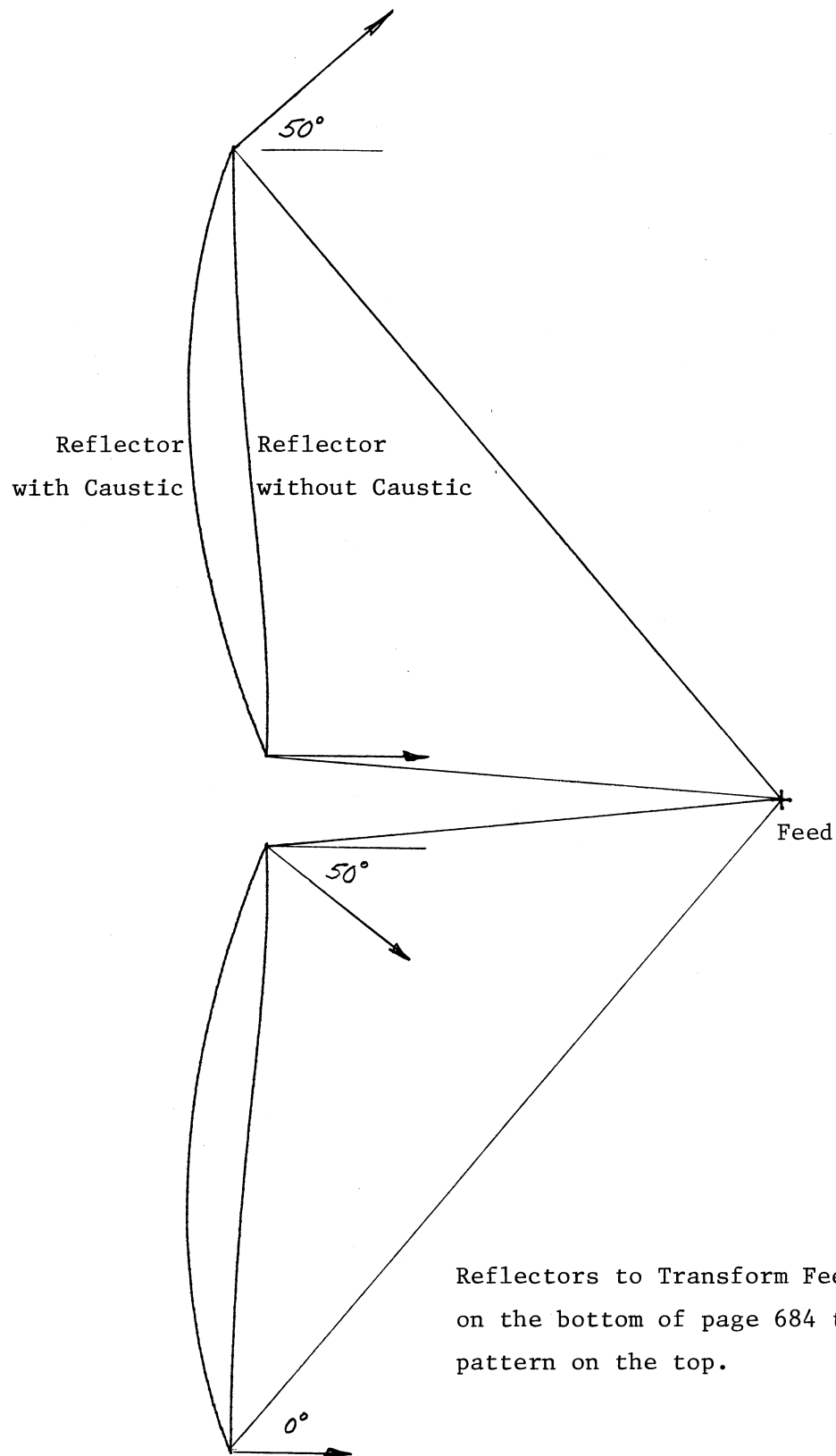
If we assume that the amplitude is uniform in the aperture, then we can find a minimum beamwidth due to one side.

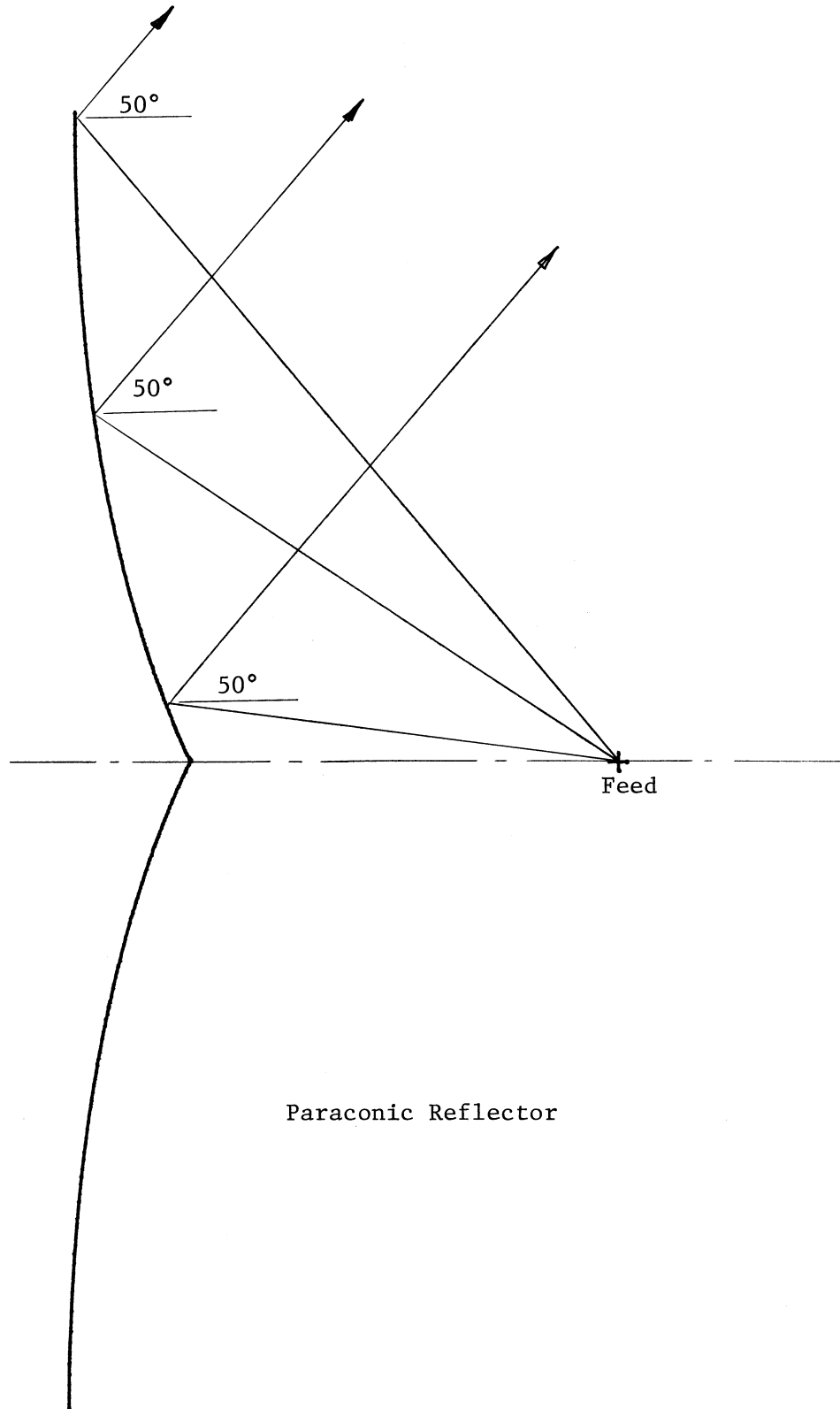
$$BW = 57.3/20 = 2.8^\circ$$

This is the beamwidth for a half aperture on boresight. We can find the effect of scanning on page 554. A beam which is scanned to 50° has 1.6 times the beamwidth. This gives us a beamwidth of about 4.5° . The reflector has a butterfly pattern which means we can estimate the directivity from the curves on page 44. The gain is about 15 dB. We will find a slightly higher gain when we integrate the aperture, but compared to 42 dB gain for a uniform aperture on boresight, this is a large reduction.

We can analyze the reflector by using an aperture plane. The following diagram shows the aperture.







Paraconic Reflector

There will be a phase taper across the aperture because of the distance from the eikonal. If we assume a uniform amplitude in the aperture plane, then we will obtain an upper bound to the gain of the paraconic reflector similar to $4\pi A/\lambda^2$. The aperture field is given by

$$e^{-jk \sin \theta_0 (\rho - R_{\min})}$$

The directivity is found from the formula on page 569.

$$\text{Directivity} = \frac{\pi (1 + \cos \theta)^2}{\lambda^2} \frac{\left| \int_0^{2\pi} \int_{R_{\min}}^{R_{\max}} e^{-jk\rho \sin \theta_0} e^{jk\rho \sin \theta \cos(\phi - \phi')} \rho d\rho d\phi \right|^2}{\int_0^{2\pi} \int_{R_{\min}}^{R_{\max}} \rho d\rho d\phi}$$

We can perform the ϕ integrations.

$$\int_0^{2\pi} e^{jk\rho \sin \theta \cos(\phi - \phi')} d\phi = 2\pi J_0(k\rho \sin \theta)$$

$$\int_0^{2\pi} \int_{R_{\min}}^{R_{\max}} \rho d\rho d\phi = \pi (R_{\max}^2 - R_{\min}^2)$$

J_0 is the zeroth order Bessel equation of the first kind. In the numerator integral we can substitute $t = \rho/\lambda$ and reduce the directivity to

$$\text{Directivity} = \frac{4\pi^2 (1 + \cos \theta)^2}{(R_{\lambda})^2 (1 + 2 \sin^2 \theta_0)} \left| \int_{\frac{R_{\lambda}}{\lambda} \sin^2 \theta_0}^{\frac{R_{\lambda}}{\lambda} (1 + \sin^2 \theta_0)} e^{-j2\pi t \sin \theta_0} J_0(2\pi t \sin \theta) t dt \right|^2$$

The directivity can be found when $\theta = \theta_0$ by performing the integration numerically. The results are plotted on page 694. Our example of a 40 wavelength diameter paraconic designed to a beam center, θ_0 , of 50° has 15.4 dB gain from the graph.

The graph is an upper bound because a uniform aperture distribution was assumed. The gain of any real paraconic reflector will be less. We can use the aperture amplitude distribution to find an amplitude taper loss. The edge taper is increased from the parabolic reflector.

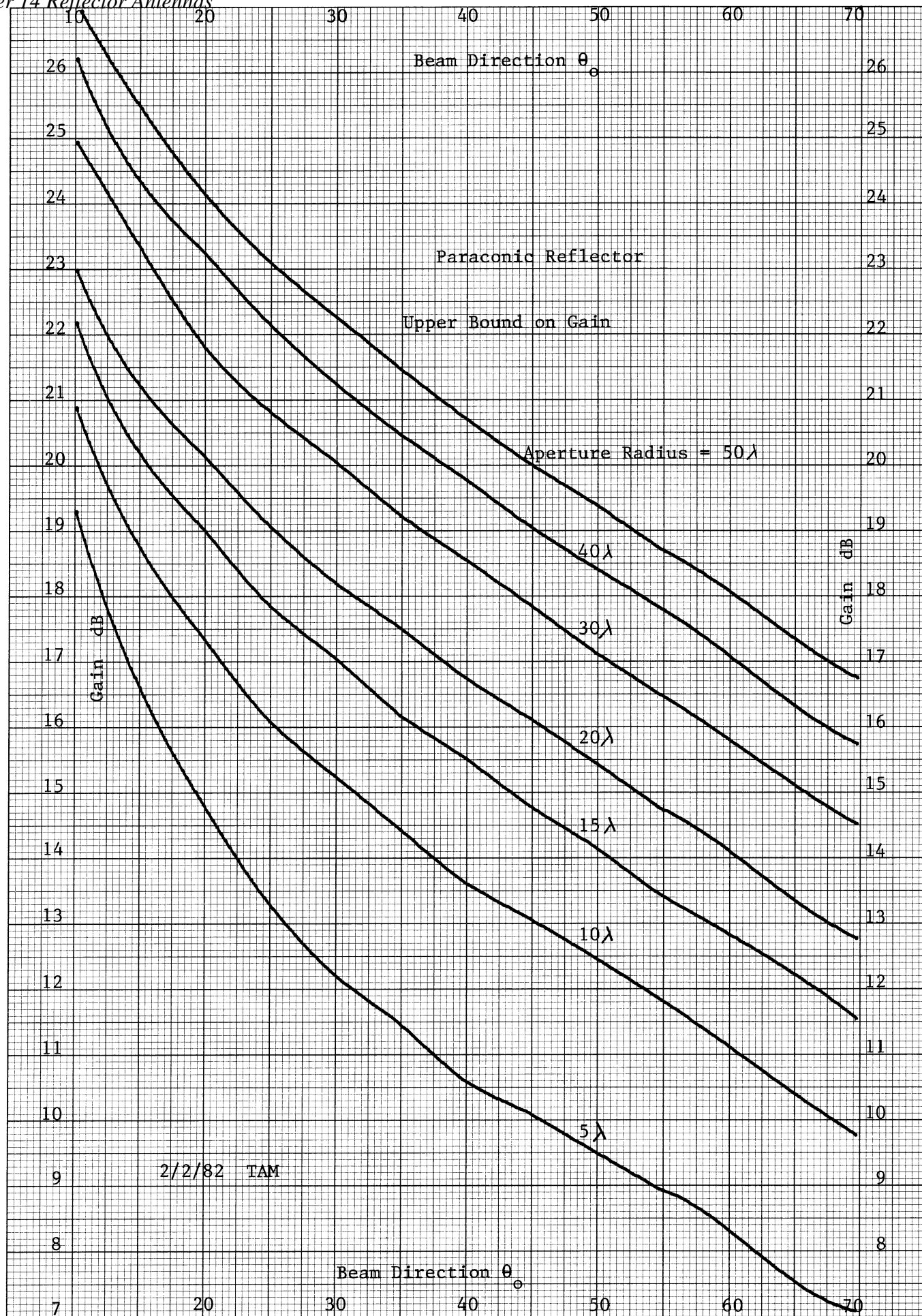
$$E_a(r) = E(\psi)/\rho$$

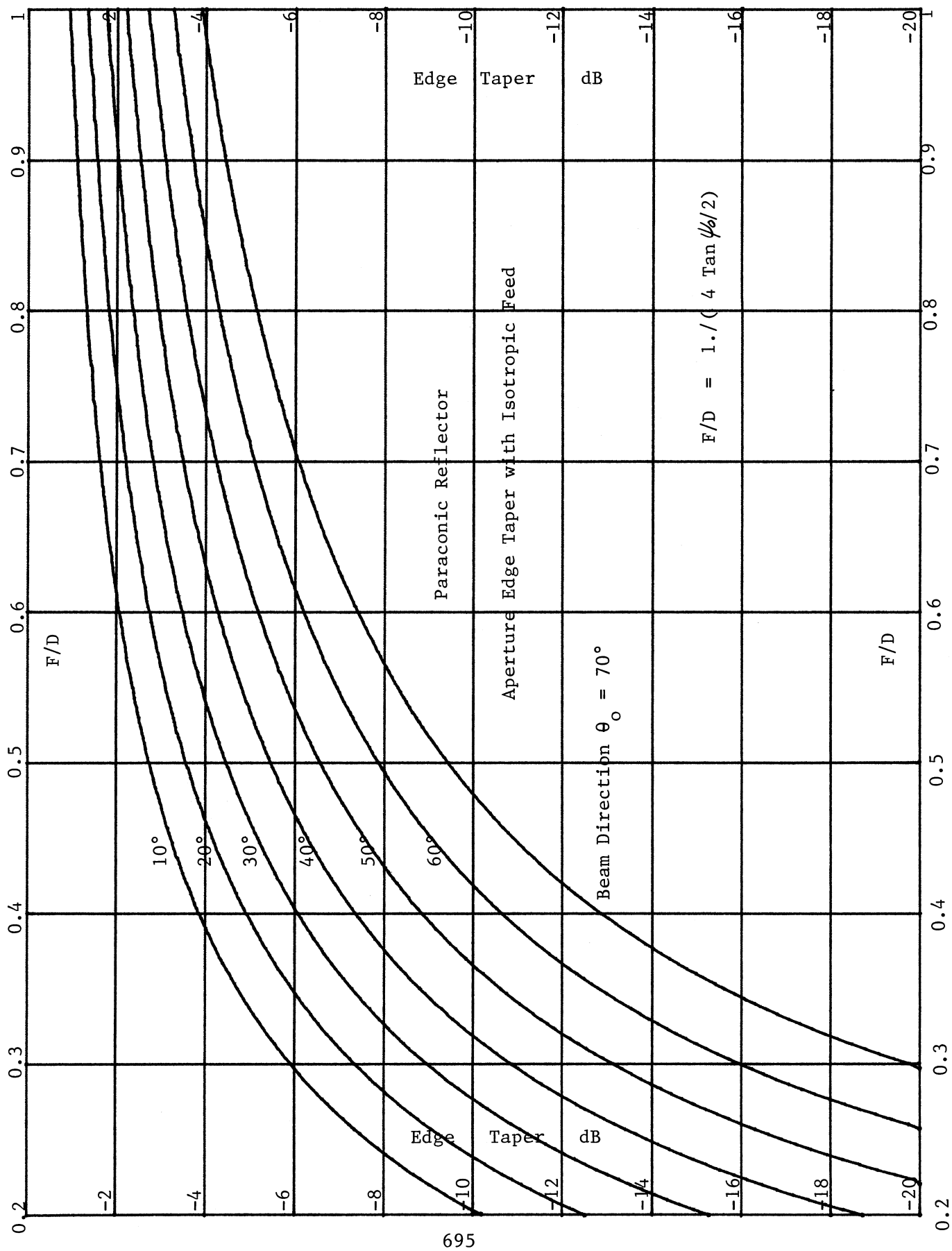
$$\rho = \frac{\rho_0 \cos^2(\theta_0/2)}{\cos^2((\theta_0 + \psi_0)/2)}$$

We can associate ψ_0 with an F/D and plot the edge taper for various beam directions similar to page 590 for an isotropic feed. The result is on page 695. Comparing with the plot on page 590, we can see that the edge

46 1320

10 X 10 TO 1/4 INCH 7 X 10 INCHES
KEUFFEL & ESSER CO. MADE IN U.S.A.





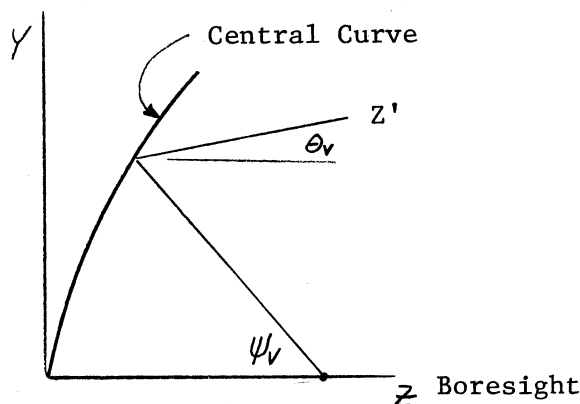
taper on the aperture has increased. It also increases with increased beam scan. Because of this the amplitude taper loss of the paraconic reflector will be greater than the equivalent parabolic reflector.

When the beam is shaped as on page 582f, the gain will be less than a paraconic reflector which directs all the energy in one direction. The actual pattern of the shaped reflector will be determined by diffraction just like the paraconic.

DOUBLY CURVED REFLECTORS FOR SHAPED BEAMS

It is a common radar requirement to have a narrow beam in one plane and a shaped beam in the other plane. The required pattern is usually a cosecant squared pattern in the vertical plane so that up to a given altitude the return will be independent of range. The beam can be obtained with a cylindrical antenna, but it is simpler to feed from a single feed antenna instead of a line source.

We will only specify the pattern in the principle planes denoted, θ_V , the shaped pattern, and θ_H , the pencil beam. Similarly, we will specify the feed antenna in terms of ψ_V and ψ_H . For a given angle ψ_V from the feed the wave will be reflected in a direction θ_V . The only allowed θ_H is zero; that is, the wave is collimated in the horizontal plane. There is symmetry about the vertical central curve and the problem reduces to designing this curve.



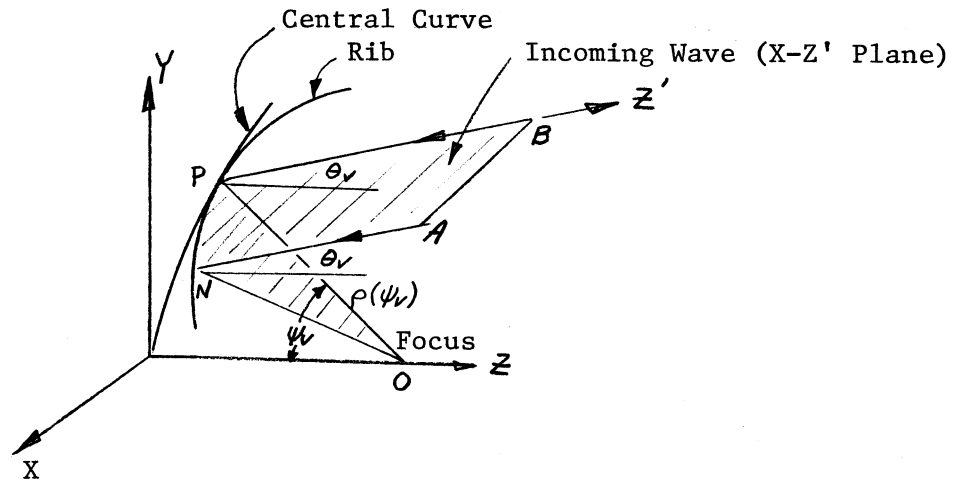
For a given ψ_V , all incoming waves at an angle θ_V must be reflected into the feed; that is, for varying ψ_H . These incoming rays form a plane which is seen on edge in the diagram above. The central curve lies in the Y-Z plane while the collimated wave lies in the X-Z' plane (X is out of the paper). Z' is in the direction of the incoming wave. A rib will be designed which lies in the X-Z' plane to reflect the wave coming from the direction θ_V into the feed.

A. S. Dunbar, "Calculation of Doubly Curved Reflectors for Shaped Beams", Proc. IRE, vol. 36, pp. 1289-96, October 1948.

S. Silver, Microwave Antenna Theory and Design, Section 13.8, pp. 502, McGraw Hill, New York, 1948.

T. F. Carberry, "Analysis Theory for the Shaped Beam Doubly Curved Reflector Antenna", IEEE Trans. on Antenna and Propag., vol. AP-17, March 1969.

Consider the rib which is drawn below.



The curve from P to N lies in the X-Z' plane and is called a rib of the reflector. An incoming wave from direction θ_v will have a constant phase line (eikonal) from A to B in the figure above which is parallel to the X axis. To focus the beam the phase distances along the ray paths must be the same (see page 667).

$$\overline{BP} + \overline{PO} = \overline{AN} + \overline{NO}$$

This is used to derive the equation of the rib in the X-Z' plane which is a parabola with a focal length given by

$$F = \rho_c(\psi_v) \cos^2((\theta_v(\psi_v) + \psi_v)/2)$$

The focus is located on the Z' axis.

The problem is reduced to designing the central curve $\rho_c(\psi_v)$. The reflected energy density is given by

$$P(\theta_v) d\theta_v \rho_c(\psi_v) d\psi_v$$

This is similar to the energy density given on page 673 for the spherical reflector corrector. The feed energy density is

$$G_f(\psi_v) d\psi_v d\psi_H$$

These energy densities are proportional.

$$K G_f(\psi_v) d\psi_v = P(\theta_v) \rho_c(\psi_v) d\theta_v$$

If the limits of the central curve are ψ_1 and ψ_2 which correspond to reflections in directions θ_1 and θ_2 , then the integrals of the feed and reflection patterns can be normalized and equated.

R. S. Elliott, Antenna Theory and Design, Section 10.6, pp. 504, Prentice Hall, 1981.

$$\frac{\int_{\psi_1}^{\psi_2} \frac{G_f(\psi_v)}{\rho_c(\psi_v)} d\psi_v}{\int_{\psi_1}^{\psi_2} \frac{G_f(\psi_v)}{\rho_c(\psi_v)} d\psi_v} = \frac{\int_{\theta_1}^{\theta_2} P(\theta_v) d\theta_v}{\int_{\theta_1}^{\theta_2} P(\theta_v) d\theta_v}$$

This is similar to the circularly symmetric reflector example except that the feed pattern integral depends on the radial distance to the central rib. We must know $\rho_c(\psi_v)$ before we can determine $\theta_v(\psi_v)$ which will be required to find $\rho_c(\psi_v)$ using the reflection differential equation.

$$\rho_c(\psi_v) = \rho_c(\psi_1) e^{\int_{\psi_1}^{\psi_v} \tan((\psi_v + \theta_v(\psi_v))/2) d\psi_v}$$

The solution can only be found by an iterative process. We must assume some $\rho_c(\psi_v)$, solve for $\theta_v(\psi_v)$ and use this to find a new $\rho_c(\psi_v)$. After a few iterations, $\rho_c(\psi_v)$ will converge. We can use normalized ρ_c with the above ratio of integrals. A good starting function of ρ_c is a parabola.

$$\frac{\rho_c(\psi_v)}{\rho_c(\psi_1)} = \frac{\cos^2(\psi_1/2)}{\cos^2(\psi_v/2)}$$

One problem is that this method may produce a surface which is not uniquely defined. The reflector is picked to have a constant width in the horizontal plane. The surface is defined by ribs which are parabolas in the plane X-Z'. Z' is defined by the reflection angle θ_v and changes direction along the reflector. It is necessary to plot the curve of the vertical coordinate of the edge versus ψ_v to see that it is monotonic. If there are loops in the curve, then the surface is not uniquely defined. Given a width, X, we can find the vertical coordinate of the edge by the following development. The location of the rib on the central curve is given by

$$\rho_c(\psi_v) \sin \psi_v$$

The rib is a parabola in the X-Z' plane with focus given on page 697. The Z' coordinate at the edge is

$$Z' = \frac{X^2}{4 F(\psi_v)}$$

The vertical dimension is given by the projection of this on the Y axis.

$$Y = \rho_c(\psi_v) \sin \psi_v + Z' \sin \theta_v$$

Elliot points out that this method is approximate and that not all points on the reflector will have the proper slope for reflection. Provided that the beam is approximately a pencil beam with small deviations in beam shape, then the surface will give the desired pattern. The surface can be designed with or without a caustic depending on the reflection angles at the edges, but there will be less chance of an ununique surface with the caustic design.

Carberry presents a method of analyzing the reflector using physical optics. The currents are found on the reflector by matching boundary conditions. These currents are integrated to find the far field through the magnetic vector potential. It has been found that when applying these methods that it is necessary to subdivide the reflector into many intervals because the phase of the currents move rapidly with distance. The analysis must be repeated with finer and finer intervals until the result converges.

OTHER BEAM SHAPING REFLECTORS

A dual reflector antenna (Cassegrain or Gregorian) can be designed to produce an arbitrary phase and amplitude in the aperture plane by shaping both the subreflector and main reflector. Using conservation of energy and the differential equations of reflections, Galindo derives a pair of differential equations in terms of the aperture radius. Instead of integrating the energy differential equation, both differential equations are solved simultaneously using Runge-Kutta or other suitable numerical methods for differential equations. Williams finds solutions with the restriction of equal amplitude and phase in the aperture plane by integrating the energy equation. All these dual reflectors are circularly symmetric reflectors. Usually a circular corrugated horn is used for a feed because its pattern is independent of ϕ .

Collin considers using a parabolic reflector for the main reflector instead of the shaped main reflector. In many cases the difference between the shaped reflector and a parabola is small. The field in the aperture plane will have approximately the same amplitude but a quadratic phase error. We can build the shaped subreflector and feed, and measure the pattern: phase and amplitude. These can be referenced to a phase center to give minimum phase error loss on the main reflector by using optimization routines. This is a real advantage when retrofitting an existing large main reflector.

Another technique of beam shaping in one plane is to use a linear array of feeds with all but at most one feed laterally offset from the axis of the parabolic reflector. The offset feeds will give patterns as shown on pages 621, 622, and 626. These patterns are added to the main central beam to shape the main lobe. Many times these feeds are fed as a resonant array which will require empirical adjustment to achieve the proper amplitudes and phasings. Further details are in Silver, Microwave Antenna Theory and Design, Section 13.3.

The reflector can remain a paraboloid but with the outside rim shape an ellipse. The beamwidth in each plane is the Fourier transform of the aperture size and distribution in that plane. Wide dimensions give narrow beams. A feed is needed with a wider beamwidth in one plane than the other to illuminate the reflector. One problem with such feeds is astigmatism; for example rectangular horns. For long flare angles the phase center will be near the aperture and for short flare angles it will be further in the throat. A pillbox antenna will help some of these problems.

Galindo, V., "Design of Dual Reflector Antennas with Arbitrary Phase and Amplitude Distributions", IEEE Trans., AP-12, pp. 403-408, July 1964.

Williams, W. F., "High Efficiency Antenna Reflector", Microwave Journal, vol. 8, pp. 79-82, July 1965.

Collins, G., "Shaping of Subreflectors in Cassegrainian Antennas", IEEE Trans. AP-21, pp. 309-313, May 1973.